DIFFRACTION BY A SLIT IN A THICK CONDUCTING SCREEN

A Dissertation

Presented to

The Faculty of Graduate Studies

University of Manitoba

In Partial Fulfillment

of the Requirements for the Degree

Doctor of Philosophy

---

by

Satish Chander Kashyap

June 1971

TO TERESA

AND

TO MY PARENTS

WITH DEEP GRATITUDE AND AFFECTION

ABSTRACT

The diffraction of a plane electromagnetic wave by a slit in a thick conducting screen is investigated using the Wiener-Hopf and the generalized scattering matrix techniques. For purposes of the analysis, the diffraction by two identical semi-infinite parallel plate waveguides forming a tandem slit configuration is treated first in order to determine the interaction between the open ends of the waveguides. This interaction is then utilized in solving for the thick slit geometry which is obtained by filling the parallel plate regions with a dielectric whose permittivity is allowed to approach infinity. For an E-polarized incident plane wave, the solution is expressed in ray-optical terms and the diffraction by each thick edge is viewed as that due to a thin edge centred at the middle of the thick edge and modified by an appropriate diffraction coefficient. The thick edge-edge interaction term, on the other hand, is also modified such that each thick edge is viewed by the other as the combination of an inhomogeneous line source as well as a line dipole. It is shown that, in general, the effective width of a slit becomes smaller with increasing screen thickness. The far field scattering properties of a thick slit thus obtained are employed to determine the scattering coefficients of symmetric and asymmetric waveguide diaphragms of finite thickness. This application, though best suited to the high frequency range far from modal cutoffs, is shown to lead to accurate results even in the dominant mode range.

ACKNOWLEDGEMENTS

The author expresses his sincere appreciation to Professor M. A. K. Hamid who suggested the problem and took an active interest in the work throughout.

Sincere thanks are due to many faculty members and colleagues for their comments and discussions. The author wishes to thank Messers. H. Unger and N. J. Mostowy for their help in carrying out the experiments. The author also wishes to thank Mrs. Lena McAlinden for the excellent typing of the manuscript and Miss Teresa Delbaere for proofreading it.

The financial assistance of the National Research Council, under Grant A3326, and the Defence Research Board, under Grants 3801-42 and 6801-37, is also acknowledged.

TABLE OF CONTENTS

LIST OF FIGURES

LIST OF TABLES

CHAPTER I

INTRODUCTION

Numerous microwave structures dealing with diffraction and waveguide propagation employ slits or slots of various sizes for coupling purposes. Although these structures are simple to construct in principle, they normally present serious mechanical difficulties unless the screen thickness is finite. Since the thickness also affects the electrical performance of these structures, it should be incorporated as a design parameter. As most of the available analysis applies to apertures in infinitesimally thin screens, any attempt to study this parameter should therefore be of interest to those engaged in design or application of such structures.

This thesis is concerned with the diffraction of a plane electromagnetic wave by a slit in a thick conducting screen. It also deals with the application of these results to finding the effect of finite thickness on reflection and transmission properties of asymmetric and symmetric waveguide diaphragms. Although the study is specifically confined to slits in free space or waveguides, some of the results may be also extended to deal with thick slots in free space or waveguides. The extension to the design of multicavity waveguide filters using thick diaphragms is another interesting application which is omitted here but reported elsewhere [1].

The diffraction of a plane electromagnetic wave by a slit (or strip) in a thin conducting screen has received wide attention due to its

importance in microwave and optical instrumentation [2-6]. Considerable literature is available on the subject and is briefly reviewed here as background to the thick slit problem. It is well known that an exact solution for the thin slit can be found in terms of eigenfunction series of Mathieu functions [7,8], but its usefulness is limited to $ka < 10$ (where k is the wave number and a is the half aperture width) because of the difficulty in tabulating the Mathieu functions and poor convergence of the series. Power series solutions in ka, also restricted to small slit widths, have been reported by Groschwitz and Hönl [9], Hönl and Zimmer [10], Müller and Westpfahl [11], and Bouwkamp [12]. For large slit widths Clemmow [13] used the concept of edge currents, while Millar [14] presented an asymptotic solution of the integral equations by successive iteration. A Wiener-Hopf treatment of the integral equation approach was given by Levine [15].

In 1953, Keller [16] proposed a more promising approach called the geometrical theory of diffraction for a large class of diffraction problems. The proposed ray-optical method provides physical insight into the mechanism of diffraction since the geometrical parameters dictate the paths of the propagating rays. Another basic advantage of this method lies in its simplicity since it employs elementary (trigonometric) functions for the far field on a ray and the resulting asymptotic series is comparable in accuracy, though more rapidly convergent, than the infinite series resulting from the boundary value solution for large aperture dimensions. The theory, as proposed or modified, has been very successful in solving many problems in

diffraction by apertures [2,17,18], by smooth objects [19,20], in antenna structures [21,22] and waveguides [23]. In the application to waveguides, special mention should be made to the work of Yee and Felsen [24-27] who proposed a novel approach to the scattering by discontinuities in a waveguide using the free space scattering properties of the scattering centres constituting the discontinuity. It was found that while the ray-optical technique is best suited to the high frequency (multimode) regime far from the modal cutoffs, it is capable of providing satisfactory results even in the range of propagation of only the dominant mode. More recent work on the problem of diffraction by a slit (or a strip) has been due to Khaskind and Vainshteyn [28], Popov [29], Yu and Rudduck [4], Tan [5] and Ufimtsev [6]. An assumption common to all these investigations is that the slit (or the strip) is infinitesimally thin. The difficulty in considering a finite screen thickness arises from the fact that no convenient extension of the conventional methods of approach can be readily found.

Very few investigations have dealt with the subject of slits or slots in thick screens. Nomura and Inawashiro [30] proposed a boundary value solution using Weber-Shafheitlin's integrals and Jacobi's polynomials for the problem of transmission of acoustic waves through a circular channel of a thick wall. Wilson and Soroka [31] obtained an approximate solution for acoustic incidence which coincided with the complicated exact solution of Nomura and Inawashiro [30] over a wide range of frequencies. Budach [32] presented an approximate solution for acoustic incidence on a thick slit of dimensions very small compared

to the wavelength λ. More recently, Lehman, using the analytic properties of finite Fourier transforms, showed that the electromagnetic field distributions for a thick slit can be obtained by solving a single variable Fredholm equation of the second kind [33]. His numerical approach, though restricted to a symmetrical excitation (i.e. two plane waves illuminating the slit symmetrically at angles θ and $-\theta$), spans the Rayleigh to geometrical optics range. However, since the approach is numerical, there is a lack of physical insight into the mechanism of diffraction leading to a very limited application of the results obtained.

Since the ray-optical method has been successful in a large number of free space and waveguide problems, it presents a promising approach to the analysis of the thick slit problem. However, the conventional ray method is inconvenient to apply because of the four scattering centres and the large number of edge-edge interactions involved. Moreover, it is restricted to the case of sufficiently large screen thickness. Thus an appropriate diffraction coefficient, associated with an equivalent thin edge situated at the centre of the thick half plane, would be of great use in the elimination of these restrictions.

Hanson [34] apparently was the first to consider the thick half plane problem. Under the assumption that $kb \ll 1$ (where $2b$ is the thickness of the half plane) he obtained a solution correct to the zeroth order of kb. Such a solution bears strong similarity to that of diffraction by a semi-infinite parallel plate waveguide, which is

also solvable by the Wiener-Hopf method. Sometime later Jones [35] formulated the thick half plane problem in terms of two equations of the Wiener-Hopf type and obtained an approximate solution under the assumption that $kb << 1$. Harden [36] has reported extensive near field experimental data on the field intensity and phase characteristics of the diffraction pattern of a thick half plane whose thickness is of the order of the wavelength. The most recent work on this topic is due to Lee and Mittra [37] who obtained a solution to the diffraction of a plane wave by a parallel plate waveguide, loaded with a dielectric recessed by an arbitrary distance δ from the aperture, in terms of a highly convergent Neumann series involving scattering matrices. The scattering matrices were obtained from the well-known solution to the problem of diffraction and radiation by a semi-infinite parallel plate waveguide [38]. The solution of the thick half plane problem for an incident H-polarized plane electromagnetic wave was obtained by letting $\delta \to 0$ and allowing the permittivity of the dielectric to approach infinity.

Since one of the novel applications of the thick slit solution is to the scattering by a thick waveguide diaphragm, it would be relevant to discuss some of the approaches that have been employed in the past to deal with this problem. Mumford [39] proposed an approximate formula deduced from experimental results to account for the finite thickness of waveguide irises. Akhiezer [40] extended Bethe's [41] theory for small holes to include the effect of the finite screen thickness. In investigating the properties of narrow slots, Oliner [42]

viewed the thick slot as a composite structure consisting of a length of waveguide equal to the slot wall thickness and of cross-sectional dimensions equal to those of the slot. Cohn [43] using a conformal mapping technique suggested by Davy [44], obtained an approximate formula for capacitance between two infinite plates of finite thickness. The thickness of a capacitive iris was accounted for by considering a line section of certain length and the formulae obtained were applicable only for $2b/\ell >> 1$ (where $2b$ is the thickness and ℓ the width of the aperture). Garb et al. [45] made an integral equation formulation for the fields on the two sides of a thick slot connecting two cavities. Though their solution is applicable for any ratio of $2b$ to ℓ, it is valid only for both $2b$ and $\ell << \lambda$. Thus, most of these investigations are restricted to slit or slot dimensions small compared to the wavelength.

This thesis is concerned with a ray-optical solution of the thick slit problem for a plane electromagnetic wave incident at an oblique angle. The solution, expressed in terms of simple diffraction coefficients assigned to each thick half plane is shown to be applicable to a large number of related problems. For the purposes of the analysis, we first find the solution to the problem of diffraction by a tandem slit configuration. This forms the basis of Chapter II. The tandem slit problem is basic to the problem of a thick slit similar to the manner in which the solution of the parallel plate waveguide problem led to the solution of the thick half plane [37]. Numerical computations are performed for various values of slit width (ℓ) and slit separation

(2b) and the results compared with variational and experimental results of Alldredge [46]. It is shown that as the tandem slit separation increases, the first peak in the scattered cross-section decreases and moves towards values corresponding to larger slit widths.

In Chapter III we first obtain the solution to the thick half plane problem for an incident E-polarized electromagnetic plane wave. Diffraction patterns for various values of screen thickness (2b) and angle of incidence θ_o are obtained, and it is shown that the peak in the diffraction patterns moves gradually towards $\theta = -\theta_o$ with the increase of kb. In the latter part of Chapter III the results for the thick half plane and the tandem slit configuration are combined to form the solution to the thick slit problem. Computations of the diffraction patterns are performed for various values of slit width and screen thickness and compared with experimental data. It is found that the effective width of a slit decreases with increasing screen thickness.

In Chapter IV the solution for the far field diffraction by a thick slit is utilized to find the scattering coefficients of thick asymmetric and symmetric diaphragms. The results obtained are compared with experimental and/or available numerical data [47]. Chapter V summarizes the general conclusions of this thesis. Finally, most of the material in Chapters II to IV has already been reported elsewhere [1,48-51].

CHAPTER II

FORMULATION OF THE BOUNDARY VALUE PROBLEM OF A TANDEM SLIT

In this chapter, the diffraction of a plane electromagnetic wave by two slits in a tandem configuration (see Fig. 2.1) is investigated by the Wiener-Hopf technique. The solution of this problem is employed in the next chapter to solve for the thick slit by filling the space in between the parallel plate waveguides with a dielectric whose permittivity is allowed to approach infinity.

The diffraction of a plane electromagnetic wave by a slit in a conducting screen has received wide attention due to its importance in microwave and optical instrumentation [2-6]. Although an exact solution is available in terms of Mathieu functions for the thin screen case, the problem is of sufficient interest for testing asymptotic diffraction theories where edge-edge interaction is only known for large slit widths. However, when there are two slits in tandem, the problem becomes complicated since conventional methods cannot be readily extended. The geometrical theory of diffraction is inconvenient to apply because of the four scattering centres and large number of edge-edge interactions involved, unless a reduction in the number of scattering centres is achieved. Furthermore, the ray method is restricted to the case of large plate-plate separation and it has been shown [52] that, for the case of a single parallel plate waveguide, it yields results which are not in complete agreement with the asymptotic form of the exact solution. These difficulties may be overcome by using an

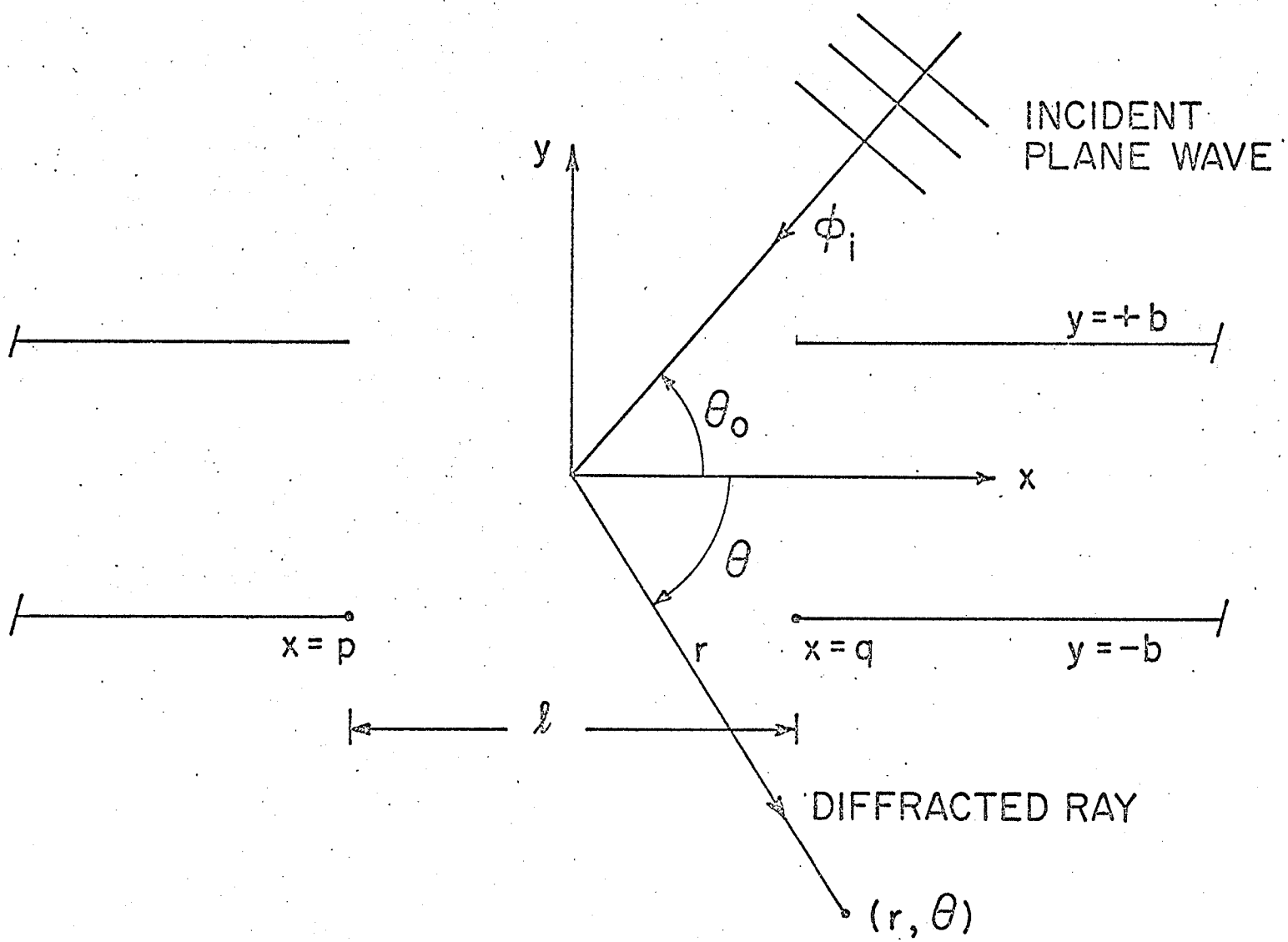

Figure 2.1 Tandem slit configuration.

equivalent edge concept and viewing the diffraction by each parallel plate waveguide as that due to a thin edge centred at the middle of the parallel plate waveguide modified by a multiplication factor, as shown later.

The problem has been solved in the past by Alldredge [46] using the variational principle. Though his analytical results are only valid for very small plate separation ($2kb < 0.985$, where k is the free space wave number and $2b$ is the plate separation), his experimental data for various values of slit width and plate separation is found to be very useful for comparing with our approximate solution.

Our approach is based on the boundary value method which leads to a Wiener-Hopf equation similar to that obtained by Jones [53] and Williams [54] for the complementary strip problem. This equation is solved in a manner similar to these authors and the results are used to extend the generalized scattering matrix solution of Lee and Mittra [37] to the thick slit problem. The final solution is obtained in the ray-optical form and expressed in terms of ray diffraction coefficients assigned to each parallel plate waveguide. Thus for small slit widths, we replace the Whittaker functions by Fresnel integrals and the resulting solution may be shown to be similar to that obtained by Yu and Rudduck [4] for the complementary strip problem. For large slit widths, the asymptotic evaluation of the Whittaker functions yields a solution similar to those of Keller [2] and Karp and Russek [3] for the case of a wide slit in a thin screen. This is shown to be possible using an equivalent edge concept where the diffraction by a parallel plate

waveguide is attributed to a thin edge with an appropriate multiplication factor.

2.1 Derivation of the Integral Equation

Consider the parallel plate tandem slit configuration shown in Fig. 2.1. Let an E-polarized plane wave

$$\phi_i = \exp(-ikx\cos\theta_o - iky\sin\theta_o)e^{-i\omega t} \tag{2.1}$$

be incident on the plates. The time dependence $e^{-i\omega t}$ will henceforth be omitted. Let ϕ be the field scattered by the tandem slit and ϕ_t be the total field. Set

$$\phi_t = \begin{cases} \phi + e^{-ikx\cos\theta_o - iky\sin\theta_o} - e^{-ikx\cos\theta_o + ik(y-2b)\sin\theta_o} & ; \; y \geq b \\ \phi \; ; \; -b \leq y \leq b \; , \; -\infty < x < \infty \\ \qquad y \leq -b \; , \; -\infty < x < \infty \end{cases} \tag{2.2}$$

Let Φ be the Fourier transform of the scattered field ϕ with respect to the x direction. Thus

$$\Phi = \frac{1}{(2\pi)^{\frac{1}{2}}} \int_{-\infty}^{\infty} \phi \, e^{i\alpha x} \, dx \tag{2.3}$$

where α is a complex variable given by (see Fig. 2.2)

$$\alpha = \sigma + i\tau$$

The two-dimensional steady-state wave equation for ϕ can be written as

$$\frac{\partial^2\phi}{\partial x^2} + \frac{\partial^2\phi}{\partial y^2} + k^2\phi = 0 \tag{2.4}$$

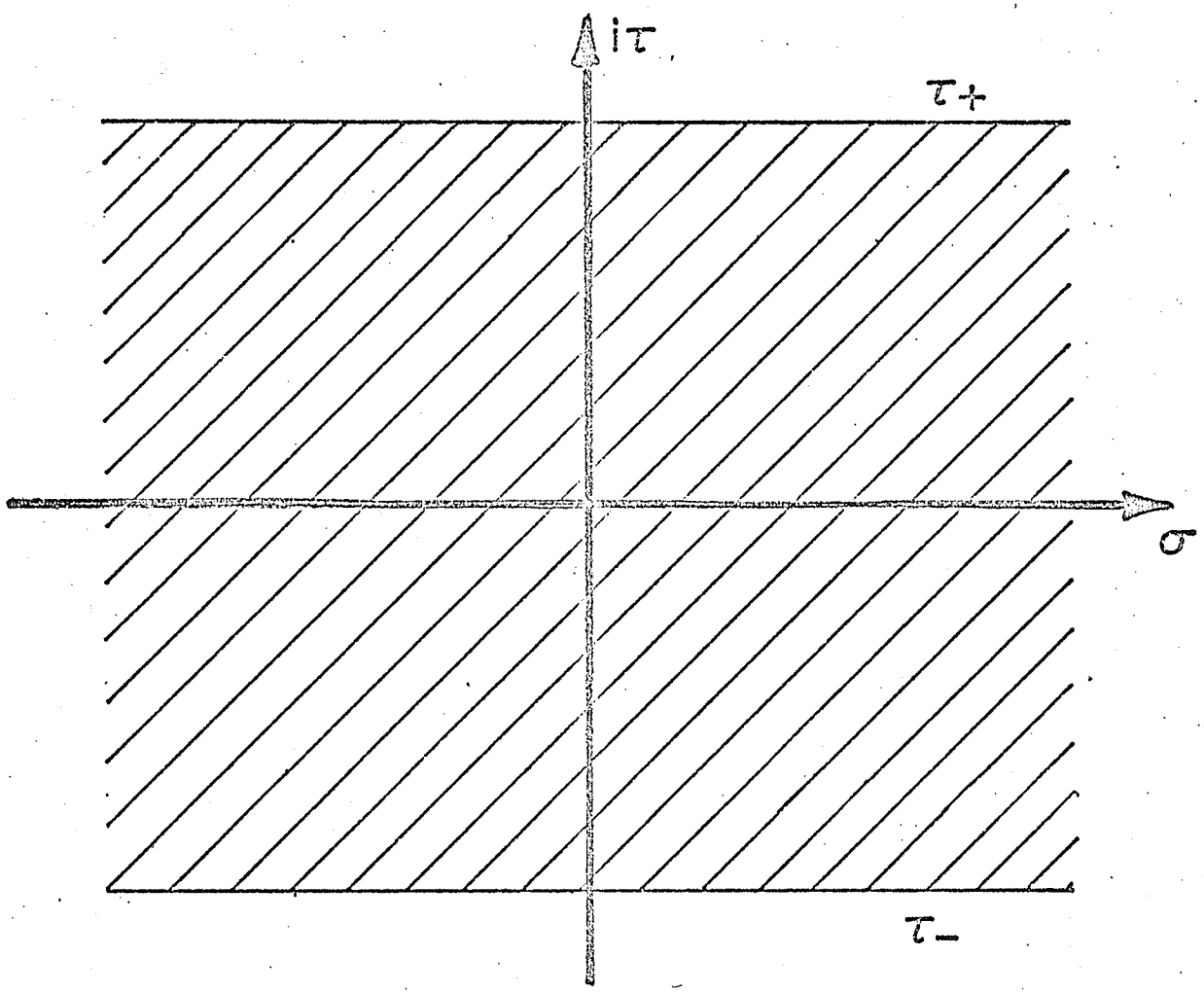

Complex α plane

Figure 2.2

Multiplying (2.4) by $(2\pi)^{-\frac{1}{2}} e^{i\alpha x}$ and integrating with respect to x from $-\infty$ to $+\infty$, we obtain

$$\frac{1}{(2\pi)^{\frac{1}{2}}} \int_{-\infty}^{\infty} \frac{\partial^2 \phi}{\partial x^2} e^{i\alpha x} \, dx + \frac{\partial^2 \Phi}{\partial y^2} + k^2 \Phi = 0 \tag{2.5}$$

which reduces to

$$\left[\frac{\partial \phi}{\partial x} e^{i\alpha x}\right]_{-\infty}^{\infty} - i\alpha \left[\phi \, e^{i\alpha x}\right]_{-\infty}^{\infty} + \frac{\partial^2 \Phi}{\partial y^2} - \gamma^2 \Phi = 0 \tag{2.6}$$

where

$$\gamma^2 = \alpha^2 - k^2 \tag{2.7}$$

and k is temporarily assumed to be complex i.e. $k = k_1 + ik_2$ ($k_1 > 0$, $k_2 > 0$). Physically when $k_2 > 0$, ϕ behaves exponentially at infinity because of the finite damping—outgoing waves must decrease exponentially as we go to infinity. Since ϕ is an outgoing wave, contributions from the bracketed terms vanish. Thus

$$\frac{\partial^2 \Phi}{\partial y^2} - \gamma^2 \Phi = 0 \tag{2.8}$$

and the solution of this equation is of the form

$$\Phi = \begin{cases} Ae^{-\gamma y} & , \; y \geq b \qquad (2.9a) \\ De^{\gamma y} & , \; y \leq -b \qquad (2.9b) \\ Be^{\gamma y} + Ce^{-\gamma y} & , \; -b \leq y \leq b \qquad (2.9c) \end{cases}$$

In this solution there are branch points at $\alpha = \pm k$. The associated branch cuts have to be arranged in such a way that (2.9) represents a solution of (2.8) which can be inverted to give ϕ. This may be done by cutting the α-plane from $+k$ to $+\infty$ in the upper half plane and

$-k$ to $-\infty$ in the lower half plane and choosing the branch such that $\gamma \to \sigma$ if $\alpha = \sigma \to +\infty$. By analytic continuation we have $\gamma = -ik$ when $\alpha = 0$ and $\gamma \to |\sigma|$ when $\alpha = \sigma \to -\infty$ (Noble [38], p. 10). It is to be noted that (2.9a) and (2.9b) should also have terms of the type $A_1 e^{\gamma y}$ and $D_1 e^{-\gamma y}$, respectively. However, these terms vanish because $\Phi(\alpha, y)$ is bounded as $|y| \to \infty$ for all α in the strip $-k_2 < \tau < k_2$.

The boundary conditions for the various quantities are:

i) $\phi_t = 0$ on $y = \pm b$, $-\infty < x < p$, $q < x < \infty$

ii) ϕ_t and Φ_t are continuous on $y = +b$, $-\infty < x < \infty$

iii) ϕ and Φ are continuous on $y = -b$, $-\infty < x < \infty$

iv) $\frac{\partial \phi_t}{\partial y}$ $\left(\text{not } \frac{\partial \phi}{\partial y}\right)$ and $\frac{\partial \Phi_t}{\partial y}$ $\left(\text{not } \frac{\partial \Phi}{\partial y}\right)$ are continuous on $y = +b$, $p < x < q$

v) $\frac{\partial \phi}{\partial y}$ and $\frac{\partial \Phi}{\partial y}$ are continuous on $y = -b$, $p < x < q$

vi) $\phi = 0(r^{\frac{1}{2}})$ and $\frac{\partial \phi}{\partial y} = 0(r^{-\frac{1}{2}})$ as $r \to 0$, where r is the distance from any of the edges [55].

The subscript "t" in the above conditions denotes total quantities.

Differentiating (2.9a) with respect to y, eliminating A and letting y tend to $(b + 0)$, we have (with $\Phi' = \frac{\partial \Phi}{\partial y}$, etc.)

$$\Phi'(b + 0) = -\gamma \Phi(b + 0) \tag{2.10}$$

which can be rewritten in the form

$$e^{i\alpha q}\Phi_+'(b + 0) + \Phi_1'(b + 0) + e^{i\alpha p}\Phi_-'(b + 0)$$

$$= -\gamma\left[e^{i\alpha q}\Phi_+(b + 0) + \Phi_1(b + 0) + e^{i\alpha p}\Phi_-(b + 0)\right] \tag{2.11}$$

where

$$\Phi_+ = \frac{1}{(2\pi)^{\frac{1}{2}}} \int_q^\infty \phi\, e^{i\alpha(x-q)}\, dx \tag{2.12a}$$

$$\Phi_- = \frac{1}{(2\pi)^{\frac{1}{2}}} \int_{-\infty}^p \phi\, e^{i\alpha(x-p)}\, dx \tag{2.12b}$$

$$\Phi_1 = \frac{1}{(2\pi)^{\frac{1}{2}}} \int_p^q \phi\, e^{i\alpha x}\, dx \tag{2.12c}$$

$$\Phi_+' = \frac{\partial \Phi_+}{\partial y}\ ,\ \Phi_-' = \frac{\partial \Phi_-}{\partial y}\ ,\ \Phi_1' = \frac{\partial \Phi_1}{\partial y} \tag{2.12d}$$

It is necessary to determine the behaviour of these transforms for large $|\xi|$. Since ϕ varies exponentially for large x as $\exp(-k_2|x|)$, it tends to zero as $|x| \to \infty$ and the transform Φ is therefore regular in the strip $-k_2 < \tau < k_2$ in the α-plane. Next consider $\Phi_-(\alpha)$ which is clearly regular in the lower half plane $\tau < k_2$. By a change of variable $z = x - p$, we have

$$\Phi_- = \frac{1}{(2\pi)^{\frac{1}{2}}} \int_{-\infty}^0 \phi(z + p) e^{i\alpha z}\, dz \tag{2.13}$$

Now the edge condition (vi, p. 14) gives $\phi(z + p) = O(z^{\frac{1}{2}})$ as $z \to 0$, so that

$$\Phi_-(\alpha) = O(|\alpha|^{-3/2}) \tag{2.14}$$

as $|\alpha| \to \infty$ in the lower half plane. Similarly $\Phi_+(\alpha)$ which is regular in the upper half plane $\tau > -k_2$, is $O(|\alpha|^{-3/2})$ as $|\alpha| \to \infty$

in the upper half plane. Also

$$e^{-i\alpha q}\Phi_1(\alpha) = \frac{1}{(2\pi)^{\frac{1}{2}}}\int_p^q \phi(x)e^{i\alpha(x-q)}\,dx = \frac{1}{(2\pi)^{\frac{1}{2}}}\int_{p-q}^0 \phi(u+q)e^{i\alpha u}\,du \tag{2.15}$$

so that the left hand side is regular in the lower half plane and is $0(|\alpha|^{-3/2})$ as $|\alpha| \to \infty$ in the lower half plane. Similarly $e^{-i\alpha p}\Phi_1(\alpha)$ is regular in the upper half plane and is $0(|\alpha|^{-3/2})$ as $|\alpha| \to \infty$ in the upper half plane.

Differentiating (2.9b) with respect to y, eliminating D and letting y tend to $(-b - 0)$, we have

$$\Phi'(-b - 0) = \gamma\Phi(-b - 0) \tag{2.16}$$

which, using (2.12), can be rewritten in the form

$$e^{i\alpha q}\,\Phi_+'(-b - 0) + \Phi_1'(-b - 0) + e^{i\alpha p}\,\Phi_-'(-b - 0) = \gamma\left[e^{i\alpha q}\,\Phi_+(-b - 0) + \Phi_1(-b - 0) + e^{i\alpha p}\,\Phi_-(-b - 0)\right] \tag{2.17}$$

Define

$$S_+'^{(o)} = \Phi_+'(b + 0) + \Phi_+'(-b - 0) \tag{2.18a}$$

$$S_+'^{(i)} = \Phi_+'(b - 0) + \Phi_+'(-b + 0) \tag{2.18b}$$

$$D_+'^{(o)} = \Phi_+'(b + 0) - \Phi_+'(-b - 0) \tag{2.18c}$$

$$D_+'^{(i)} = \Phi_+'(b - 0) - \Phi_+'(-b + 0) \tag{2.18d}$$

where the superscripts "o" and "i" refer to the outer and inner sides of the half planes, respectively. Adding and subtracting (2.11)

and (2.17) and using (2.18), we obtain

$$S_+'^{(o)}e^{i\alpha q} + S_1'^{(o)} + S_-'^{(o)}e^{i\alpha p} = -\gamma\left[D_1^{(o)} + D_+^{(o)}e^{i\alpha q} + D_-^{(o)}e^{i\alpha p}\right] \tag{2.19}$$

and

$$D_+'^{(o)}e^{i\alpha q} + D_1'^{(o)} + D_-'^{(o)}e^{i\alpha p} = -\gamma\left[S_1^{(o)} + S_+^{(o)}e^{i\alpha q} + S_-^{(o)}e^{i\alpha p}\right] \tag{2.20}$$

where $S_1'^{(o)}$, $S_-'^{(o)}$, $D_1^{(o)}$, $D_+^{(o)}$ are analogous to the corresponding quantities in (2.18).

For eliminating the constants B and C, we proceed by setting $y = b - 0$ and $y = -b + 0$ in (2.9c). Using (2.12), we have

$$e^{i\alpha q}\Phi_+(b - 0) + \Phi_1(b - 0) + e^{i\alpha p}\Phi_-(b - 0) = Be^{\gamma b} + Ce^{-\gamma b} \tag{2.21a}$$

$$e^{i\alpha q}\Phi_+(-b + 0) + \Phi_1(-b + 0) + e^{i\alpha p}\Phi_-(-b + 0) = Be^{-\gamma b} + Ce^{\gamma b} \tag{2.21b}$$

Differentiating (2.9c) with respect to y and setting $y = b - 0$ and $y = -b + 0$, we have

$$e^{i\alpha q}\Phi_+'(b - 0) + \Phi_1'(b - 0) + e^{i\alpha p}\Phi_-'(b - 0) = \gamma Be^{\gamma b} - \gamma Ce^{-\gamma b} \tag{2.22a}$$

$$e^{i\alpha q}\Phi_+'(-b + 0) + \Phi_1'(-b + 0) + e^{i\alpha p}\Phi_-'(-b + 0) = \gamma Be^{-\gamma b} - \gamma Ce^{\gamma b} \tag{2.22b}$$

Eliminating B and C from (2.21), (2.22) and using (2.18), we have

$$e^{i\alpha q}\,S_+'^{(i)} + S_1'^{(i)} + e^{i\alpha p}\,S_-'^{(i)} = \gamma\coth\gamma b\left(D_1^{(i)} + D_+^{(i)}e^{i\alpha q} + D_-^{(i)}e^{i\alpha p}\right) \tag{2.23}$$

and

$$e^{i\alpha q}\,D_+'^{(i)} + D_1'^{(i)} + e^{i\alpha p}\,D_-'^{(i)} = \gamma\tanh\gamma b\left(S_1^{(i)} + S_+^{(i)}e^{i\alpha q} + S_-^{(i)}e^{i\alpha p}\right) \tag{2.24}$$

The condition of zero tangential electric field on the plates leads to

$$D_+ = D_- = S_+ = S_- = 0$$

where the superscripts have been omitted, since from the continuity of ϕ on $y = \pm b$, $S_+^{(o)} = S_+^{(i)} = S_+$. Similarly $D_1^{(o)}$, $D_1^{(i)}$ are written as D_1 and $S_1^{(o)}$, $S_1^{(i)}$ are written as S_1.

Now from (2.18a) and (2.18b), we have

$$S_1'^{(o)} - S_1'^{(i)} = \Phi_1'(b + 0) + \Phi_1'(-b - 0) - \Phi_1'(b - 0) - \Phi_1'(-b + 0)$$

where the second and fourth terms on the right hand side cancel out because of the boundary condition (v, p. 14). Thus we have

$$S_1'^{(o)} - S_1'^{(i)} = \Phi_1'(b + 0) - \Phi_1'(b - 0)$$

$$= \frac{1}{(2\pi)^{\frac{1}{2}}} \int_p^q (2ik \sin\theta_o) e^{-ikx \cos\theta_o - ikb \sin\theta_o} e^{i\alpha x} dx$$

$$= \frac{2k \sin\theta_o \, e^{-ikb \sin\theta_o}}{(2\pi)^{\frac{1}{2}}(\alpha - k \cos\theta_o)} \left[e^{i(\alpha - k\cos\theta_o)q} - e^{i(\alpha - k\cos\theta_o)p} \right] \quad (2.25)$$

Subtracting (2.23) from (2.19), using (2.25) and recognizing that $D_1^{(o)} = D_1^{(i)} = D_1$, we have

$$e^{i\alpha q} \psi_{s_+} + A'G(\alpha) + e^{i\alpha p} \psi_{s_-} = - D_1/[L(\alpha)b] \quad (2.26)$$

where

$$A' = 2k \sin\theta_o \, e^{-ikb \sin\theta_o} \quad (2.27)$$

$$G(\alpha) = \frac{e^{i(\alpha - k\cos\theta_o)q} - e^{i(\alpha - k\cos\theta_o)p}}{(2\pi)^{\frac{1}{2}}(\alpha - k \cos\theta_o)} \quad (2.28)$$

$$\psi_{s_+} = S_+'^{(o)} - S_+'^{(i)}$$
$$\psi_{s_-} = S_-'^{(o)} - S_-'^{(i)} \tag{2.29}$$

and

$$L(\alpha) = L_+(\alpha)\, L_-(\alpha) = \frac{e^{-\gamma b} \sinh \gamma b}{\gamma b} \tag{2.30}$$

Here $L_+(\alpha)$, $L_-(\alpha)$ are regular in the upper $(\tau > -k_2)$ and lower $(\tau < k_2)$ half planes, respectively, and are asymptotic to $|\alpha|^{-\frac{1}{2}}$ as α tends to ∞ in the appropriate half planes (Noble [38], p. 102).

Similar manipulation of (2.20) and (2.24) yields

$$e^{i\alpha q}\, \psi_{D_+} + A'G(\alpha) + e^{i\alpha p}\, \psi_{D_-} = -\gamma\, S_1/K(\alpha) \tag{2.31}$$

where we have used the fact that $S_1^{(o)} = S_1^{(i)} = S_1$. Here ψ_{D_+}, ψ_{D_-} are defined analogous to those in (2.29) and

$$K(\alpha) = K_+(\alpha)\, K_-(\alpha) = e^{-\gamma b} \cosh \gamma b \tag{2.32}$$

$K_+(\alpha)$, $K_-(\alpha)$ are regular in upper $(\tau > -k_2)$ and lower $(\tau < k_2)$ half plane, respectively, and are asymptotic to constants as $|\alpha| \to \infty$ in the appropriate half planes. Both $K_\pm(\alpha)$ and $L_\pm(\alpha)$ are defined and evaluated in Appendix A.

It should be noted that (2.26) and (2.31) hold in the common strip of regularity $(-k_2 < \tau < k_2)$ of all the functions and provide the complete solution of the tandem slit configuration. They are of the same type as discussed by a number of authors [53,54,56] and are solved in the following section.

2.2 Solution of the Integral Equations

In this section we split the non-regular functions in (2.26) and (2.31) into functions which are regular in the upper and lower half planes in the α-plane and apply the usual Wiener-Hopf technique to solve for the unknown, ψ_{s_+}, ψ_{s_-}, ψ_{D_+}, ψ_{D_-}, D_1 and S_1. Thus multiplying (2.31) by $e^{-i\alpha q}$ and simplifying, we obtain

$$\psi_{D_+} K'_+(\alpha) + \frac{S_1 e^{-i\alpha q}}{K'_-(\alpha)} + e^{i\alpha(p-q)} \psi_{D_-} K'_+(\alpha) = - A'G(\alpha) K'_+(\alpha) e^{-i\alpha q} \tag{2.33}$$

where

$$K'(\alpha) = \frac{K(\alpha)}{(\alpha^2 - k^2)^{\frac{1}{2}}} = \frac{K_+(\alpha)\, K_-(\alpha)}{(\alpha + k)^{\frac{1}{2}}\, e^{-i\pi/4} (\alpha - k)^{\frac{1}{2}}\, e^{i\pi/4}} = K'_+(\alpha)\, K'_-(\alpha) \tag{2.34}$$

For applying the Wiener-Hopf technique, it is necessary to determine the behaviour of the terms in (2.33) for large $|\alpha|$. Thus rewriting (2.29) for ψ_{D_+}, we have

$$\psi_{D_+} = D'^{(o)}_+ - D'^{(i)}_+$$

Also from (2.18), we have

$$D'^{(o)}_+ = \Phi'_+(b + 0) - \Phi'_+(-b - 0) \quad , \text{etc.}$$

Following steps similar to (2.13), (2.14) and using the condition that $\frac{\partial \phi}{\partial y}(r) = 0(r^{-\frac{1}{2}})$ as $r \to 0$, it can be shown that ψ_{D_+} is regular in the upper half plane $(\tau > - k_2)$ and is $0(|\alpha|^{-\frac{1}{2}})$ as $|\alpha| \to \infty$ in the upper half plane. Thus the first term in (2.33) is regular in the upper half plane and is $0(|\alpha|^{-1})$ as $|\alpha| \to \infty$ in the upper half plane.

Similarly, the second term is regular in the lower half plane $(\tau < k_2)$ and is $O(|\alpha|^{-1})$ as $|\alpha| \to \infty$ in the lower half plane. The third and fourth terms are, however, regular in neither half plane but can be written as the sum of regular functions using Cauchy's formula

$$f(\alpha) = \frac{1}{2\pi i}\int_{ic-\infty}^{ic+\infty} \frac{f(\xi)}{\xi - \alpha}\, d\xi - \frac{1}{2\pi i}\int_{id-\infty}^{id+\infty} \frac{f(\xi)}{\xi - \alpha}\, d\xi = f_+(\alpha) + f_-(\alpha) \tag{2.35}$$

where $f(\alpha)$ is a function regular in the strip containing c and d (see Fig. 2.3). The integral along c is regular in the upper half plane and the integral along d is regular in the lower half plane.

Introducing the expression for $G(\alpha)$ (2.28) in (2.33) and using (2.35), we have

$$\psi_{D_+} K_+'(\alpha) + \frac{A'}{(2\pi)^{\frac{1}{2}}} \frac{e^{-ikq\cos\theta_o}}{\alpha - k\cos\theta_o} \left\{ K_+'(\alpha) - K_+'(k\cos\theta_o) \right\} + M_+(\alpha) + N_+(\alpha)$$

$$= -\frac{e^{-i\alpha q_{S_1}}}{K_-'(\alpha)} - M_-(\alpha) - N_-(\alpha) - \frac{A'}{(2\pi)^{\frac{1}{2}}} \frac{e^{-ikq\cos\theta_o}}{(\alpha - k\cos\theta_o)} K_+'(k\cos\theta_o) \tag{2.36}$$

where

$$M_+(\alpha) + M_-(\alpha) = e^{i\alpha(p-q)}\, \psi_{D_-}(\alpha)\, K_+'(\alpha) \tag{2.37}$$

$$N_+(\alpha) + N_-(\alpha) = -\frac{A'}{(2\pi)^{\frac{1}{2}}} \frac{e^{i\alpha(p-q)-ikp\cos\theta_o}}{(\alpha - k\cos\theta_o)} K_+'(\alpha) \tag{2.38}$$

Here we have used the fact that

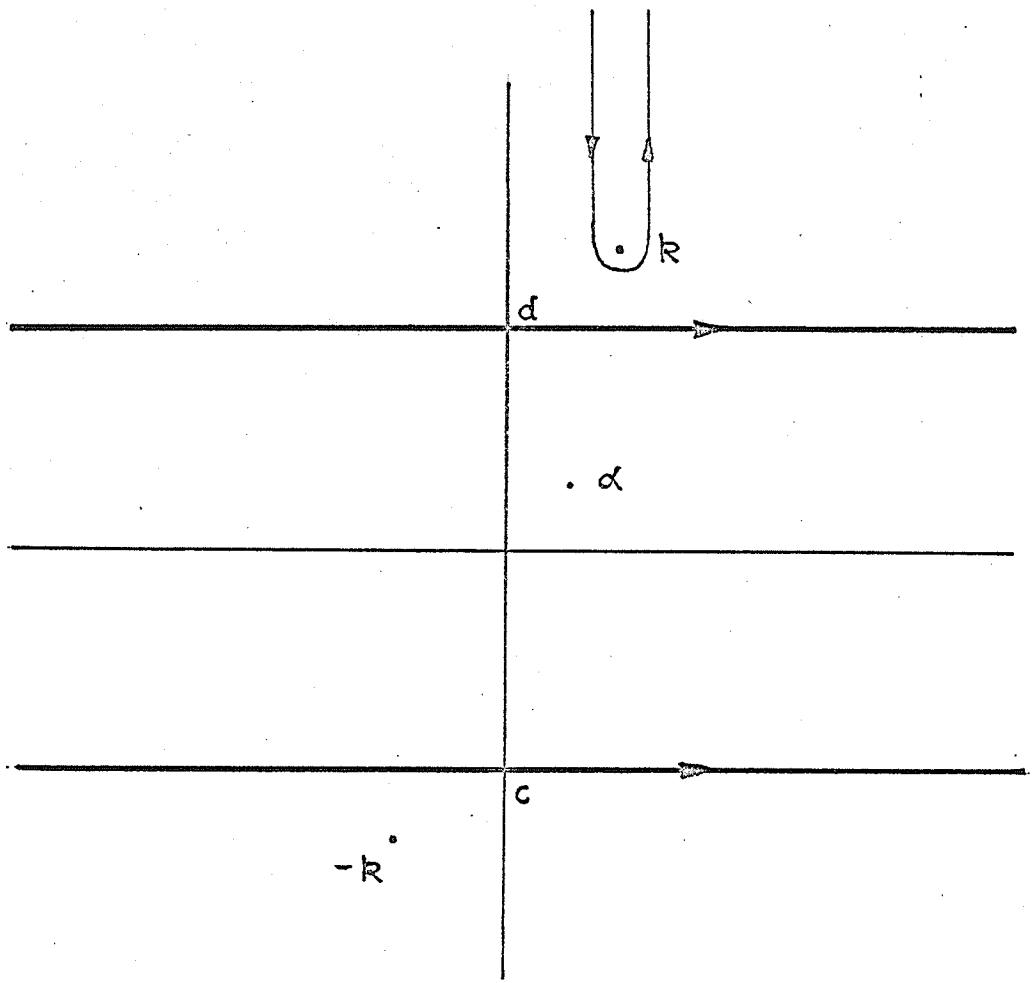

Fig. 2.3 The integration contours in the complex ξ-plane

$$\frac{e^{-ikq\cos\theta_o}K'_+(\alpha)}{\alpha - k\cos\theta_o} = \left[\frac{e^{-ikq\cos\theta_o}}{\alpha - k\cos\theta_o}\left\{K'_+(\alpha) - K'_+(k\cos\theta_o)\right\}\right] + \left[\frac{e^{-ikq\cos\theta_o}}{\alpha - k\cos\theta_o}K'_+(k\cos\theta_o)\right]$$

where the terms in the first and second square brackets are regular in the upper $(\tau > -k_2)$ and lower $(\tau < k_2\cos\theta_o)$ half planes, respectively, assuming that $0 < \theta_o < \pi/2$. (If $\pi/2 < \theta_o < \pi$ the Wiener-Hopf technique should be applied in the strip $k_2\cos\theta_o < \tau < k_2$ — in either case the object is to obtain relations holding in a symmetrical strip $-k_2|\cos\theta_o| < \tau < k_2|\cos\theta_o|$. The reasons for this will become clear below).

Similarly multiplying (2.31) by $e^{-i\alpha p}$, using (2.34) and rearranging, we have

$$\psi_{D_-}K'_-(\alpha) + \frac{S_1 e^{-i\alpha p}}{K'_+(\alpha)} + e^{i\alpha(q-p)}\psi_{D_+}K'_-(\alpha) = -A'G(\alpha)K'_-(\alpha)e^{-i\alpha p} \tag{2.39}$$

The first term in (2.39) is regular in the lower half plane $(\tau < k_2)$ and is $0(|\alpha|^{-1})$ as $|\alpha| \to \infty$ in the lower half plane. Also the second term is regular in the upper half plane $(\tau > -k_2)$ and is $0(|\alpha|^{-1})$ as $|\alpha| \to \infty$ in the upper half plane. The third and fourth terms are, however, regular in neither half plane but can be written as the sum of regular functions using (2.35). This leads to

$$\psi_{D_-}K'_-(\alpha) + Y_-(\alpha) - \frac{A'}{(2\pi)^{\frac{1}{2}}}\frac{e^{-ikp\cos\theta_o}K'_-(\alpha)}{(\alpha - k\cos\theta_o)} - Z_-(\alpha) = -\frac{e^{-i\alpha p}S_1(\alpha)}{K'_+(\alpha)} - Y_+(\alpha) + Z_+(\alpha) \tag{2.40}$$

where

$$Y_+(\alpha) + Y_-(\alpha) = e^{i\alpha(q-p)}\psi_{D_+} K'_-(\alpha) \tag{2.41}$$

$$Z_+(\alpha) + Z_-(\alpha) = -\frac{A'K'_-(\alpha)e^{i\alpha(q-p)-ikq\cos\theta_o}}{(2\pi)^{\frac{1}{2}}(\alpha - k\cos\theta_o)} \tag{2.42}$$

$M_+(\alpha)$, $Y_+(\alpha)$ and $M_-(\alpha)$, $Y_-(\alpha)$ are regular in the upper $(\tau > -k_2)$ and lower $(\tau < k_2)$ half planes, respectively, and are $0(|\alpha|^{-1})$ as $|\alpha| \to \infty$ in the respective half planes. $N_+(\alpha)$, $Z_+(\alpha)$ and $N_-(\alpha)$, $Z_-(\alpha)$ are regular in the upper $(\tau > -k_2)$ and lower $(\tau < k_2\cos\theta_o)$ half planes, respectively, and are $0(|\alpha|^{-3/2})$ as $|\alpha| \to \infty$ in the respective half planes. Thus the left hand side of (2.36) and right hand side of (2.40) are regular in the upper half plane $(\tau > -k_2)$. The other sides are regular in the lower half plane $(\tau < k_2\cos\theta_o)$. Their behaviour, as $|\alpha| \to \infty$ in the respective half planes indicates that the extended form of Liouville's theorem (Noble [38], p. 38) can be applied to prove that each side of each equation equals zero.

Let

$$\psi_{D_-} - \frac{A'e^{-ikp\cos\theta_o}}{(2\pi)^{\frac{1}{2}}(\alpha - k\cos\theta_o)} = H_{D_-}(\alpha) \tag{2.43a}$$

$$\psi_{D_+} + \frac{A'e^{-ikq\cos\theta_o}}{(2\pi)^{\frac{1}{2}}(\alpha - k\cos\theta_o)} = H^*_{D_+}(\alpha) \tag{2.43b}$$

where the asterisk indicates that $H^*_{D_+}(\alpha)$ has a pole at $\alpha = k\cos\theta_o$ but otherwise is regular for $\tau > -k_2$. $H_{D_-}(\alpha)$ is regular for $\tau < k_2\cos\theta_o$. On equating the left hand sides of (2.36), (2.40) to zero

and introducing explicit expressions for $M_+(\alpha)$, $N_+(\alpha)$, $Y_-(\alpha)$, $Z_-(\alpha)$ by using (2.35) and the notation in (2.43), we obtain

$$H^*_{D_+}(\alpha)K'_+(\alpha) + \frac{1}{2\pi i}\int_{ic-\infty}^{ic+\infty} \frac{e^{-i\xi(q-p)}H_{D_-}(\xi)K'_+(\xi)}{\xi - \alpha}\, d\xi$$

$$- \frac{A'e^{-ikq\cos\theta_o}}{(2\pi)^{\frac{1}{2}}(\alpha - k\cos\theta_o)} K'_+(k\cos\theta_o) = 0 \qquad (2.44)$$

and

$$H_{D_-}(\alpha)K'_-(\alpha) - \frac{1}{2\pi i}\int_{id-\infty}^{id+\infty} \frac{e^{i\xi(q-p)}}{\xi - \alpha} H^*_{D_+}(\xi)K'_-(\xi)\, d\xi = 0 \qquad (2.45)$$

In these equations $-k_2 < d < k_2\cos\theta_o$, $-k_2 < c < k_2\cos\theta_o$. In the first equation $\tau > c$; in the second $\tau < d$. From the assumption $0 < \theta_o < \frac{\pi}{2}$ we can choose 'a' so that $-k_2\cos\theta_o < a < k_2\cos\theta_o$ and take $d = -c = a$. Replacing ξ by $(-\xi)$ in (2.44) and α by $(-\alpha)$ in (2.45) and remembering that $K'_+(-\alpha) = K'_-(+\alpha)$, we have

$$H^*_{D_+}(\alpha)K'_+(\alpha) - \frac{1}{2\pi i}\int_{ia-\infty}^{ia+\infty} \frac{e^{i\xi(q-p)}H_{D_-}(-\xi)K'_-(\xi)}{\xi + \alpha}\, d\xi$$

$$- \frac{A'e^{-ikq\cos\theta_o}}{(2\pi)^{\frac{1}{2}}(\alpha - k\cos\theta_o)} K'_+(k\cos\theta_o) = 0 \qquad (2.46)$$

and

$$H_{D_-}(-\alpha)K'_+(\alpha) - \frac{1}{2\pi i}\int_{ia-\infty}^{ia+\infty} \frac{e^{i\xi(q-p)}H^*_{D_+}(\xi)K'_-(\xi)}{\xi + \alpha}\, d\xi = 0 \qquad (2.47)$$

where now $\tau > -a$ in both equations. Define

$$E^*_{D_+}(\alpha) = H^*_{D_+}(\alpha) + H_{D_-}(-\alpha) \tag{2.48a}$$

$$L^*_{D_+}(\alpha) = H^*_{D_+}(\alpha) - H_{D_-}(-\alpha) \tag{2.48b}$$

where in this case the asterisk means that expressions (2.48) are regular in $\tau > -k_2\cos\theta_o$ except for simple poles at $\alpha = k\cos\theta_o$. Adding and subtracting (2.46), (2.47) and using (2.48), we obtain

$$E^*_{D_+}(\alpha)K'_+(\alpha) - \frac{1}{2\pi i}\int_{ia-\infty}^{ia+\infty} \frac{e^{i\xi(q-p)}E^*_{D_+}(\xi)K'_-(\xi)}{\xi+\alpha}\,d\xi$$

$$= \frac{A'e^{-ikq\cos\theta_o}K'_+(k\cos\theta_o)}{(2\pi)^{\frac{1}{2}}(\alpha - k\cos\theta_o)} \tag{2.49}$$

and

$$L^*_{D_+}(\alpha)K'_+(\alpha) + \frac{1}{2\pi i}\int_{ia-\infty}^{ia+\infty} \frac{e^{i\xi(q-p)}L^*_{D_+}(\xi)K'_-(\xi)}{\xi+\alpha}\,d\xi$$

$$= \frac{A'e^{-ikq\cos\theta_o}K'_+(k\cos\theta_o)}{(2\pi)^{\frac{1}{2}}(\alpha - k\cos\theta_o)} \tag{2.50}$$

Both (2.49) and (2.50) can be solved by an approximate method due to Jones [53]. In order to apply this method, these equations are rewritten in the form

$$F^*_{D_+}(\alpha)K'_+(\alpha) + \frac{\lambda}{2\pi i}\int_{ia-\infty}^{ia+\infty} \frac{F^*_{D_+}(\xi)e^{i\xi(q-p)}K'_-(\xi)}{\xi+\alpha}\,d\xi$$

$$= \frac{A'e^{-ikq\cos\theta_o}K'_+(k\cos\theta_o)}{(2\pi)^{\frac{1}{2}}(\alpha - k\cos\theta_o)} \tag{2.51}$$

Here $F^*_{D_+}(\alpha) = E^*_{D_+}(\alpha)$ or $L^*_{D_+}(\alpha)$ as $\lambda = -1$ or $+1$, respectively, and using (2.43) and (2.48), it has the form

$$F^*_{D_+}(\alpha) = F_{D_+}(\alpha) + \frac{A'e^{-ikq\cos\theta_o}}{(2\pi)^{\frac{1}{2}}(\alpha - k\cos\theta_o)} - \frac{\lambda A'e^{-ikp\cos\theta_o}}{(2\pi)^{\frac{1}{2}}(\alpha + k\cos\theta_o)} \tag{2.52}$$

where $F_{D_+}(\alpha)$ is regular in the upper half plane $(\tau > -k_2)$ and has algebraic behaviour as $|\alpha| \to \infty$ in the upper half plane (since the terms constituting $F_{D_+}(\alpha)$ are $O(|\alpha|^{-\frac{1}{2}})$ as $|\alpha| \to \infty$ in the upper half plane). Using (2.52) in (2.51), we obtain

$$F_{D_+}(\alpha)K'_+(\alpha) + \frac{A'e^{-ikq\cos\theta_o}K'_+(\alpha)}{(2\pi)^{\frac{1}{2}}(\alpha - k\cos\theta_o)} - \frac{\lambda A'e^{-ikp\cos\theta_o}K'_+(\alpha)}{(2\pi)^{\frac{1}{2}}(\alpha + k\cos\theta_o)}$$

$$+ \frac{\lambda}{2\pi i}\int_{ia-\infty}^{ia+\infty} \frac{e^{i\xi(q-p)}F_{D_+}(\xi)K'_-(\xi)}{\xi+\alpha}\,d\xi$$

$$+ \frac{\lambda}{2\pi i}\frac{A'}{(2\pi)^{\frac{1}{2}}}\int_{ia-\infty}^{ia+\infty} \frac{e^{-ikq\cos\theta_o}e^{i\xi(q-p)}K'_-(\xi)}{(\xi - k\cos\theta_o)(\xi+\alpha)}\,d\xi$$

$$- \frac{A'}{2\pi i (2\pi)^{\frac{1}{2}}} \int_{ia-\infty}^{ia+\infty} \frac{e^{-ikp\cos\theta_o} e^{i\xi(q-p)} K'_-(\xi)}{(\xi + k\cos\theta_o)(\xi + \alpha)} d\xi$$

$$= \frac{A' e^{-ikq\cos\theta_o} K'_+(k\cos\theta_o)}{(2\pi)^{\frac{1}{2}}(\alpha - k\cos\theta_o)} \tag{2.53}$$

The first integral in (2.53) may be rewritten as

$$I = \frac{1}{2\pi i} \int_{ia-\infty}^{ia+\infty} \frac{F_{D_+}(\xi) e^{i\xi\ell} K'_-(\xi)}{\xi + \alpha} d\xi \ , \ q = -p = \frac{\ell}{2} \tag{2.54}$$

where $-(\text{Im}\ \alpha) < a < k_2$. When ℓ is large, the contributions to this integral come from the singularities of the integrand. Now

$$K'_-(\xi) = \frac{K_-(\xi)}{(\xi - k)^{\frac{1}{2}} e^{i\pi/4}}$$

$$= \frac{K(\xi)}{K_+(\xi)(\xi - k)^{\frac{1}{2}} e^{i\pi/4}}$$

$$= \frac{e^{-\gamma b} \cosh \gamma b}{K_+(\xi)(\xi - k)^{\frac{1}{2}} e^{i\pi/4}}$$

$$= \frac{1 - \gamma b + \gamma^2 b^2 \ \ldots}{K_+(\xi)(\xi - k)^{\frac{1}{2}} e^{i\pi/4}} \tag{2.55}$$

This is a power series expansion and valid only under the condition $[(kb)^2/k\ell < 1]$ as will be shown by (2.65). Using (2.55) in (2.54), we obtain

$$I = \frac{1}{2\pi i}\int_{ia-\infty}^{ia+\infty} \frac{F_{D_+}(\xi)e^{i\xi\ell}(1 - \gamma b + \gamma^2 b^2 \ldots)}{(\xi + \alpha)K_+(\xi)(\xi - k)^{\frac{1}{2}}\, e^{i\pi/4}}\, d\xi \qquad (2.56)$$

Now the quantity $(\xi + \alpha)^{-1}[K_+(\xi)]^{-1}F_{D_+}(\xi)$ is regular in the upper half plane when $-\alpha$ lies below 'a.' Thus the only contributing singularity in (2.56) is the branch point $\xi = k$. Furthermore, it is evident that only the alternate terms of the series in (2.56) contribute. Now the functions $F_{D_+}(\xi)$ and $K_+(\xi)$ are expanded about the branch point in terms of a Taylor series—both series are convergent since the functions are regular and bounded in the upper half plane. This will reduce the integral equation (2.53) to an algebraic one relating $F_{D_+}(\alpha)$ to $F_{D_+}(k)$ and $\partial^m F_{D_+}(\alpha)/\partial\alpha^m$ $(m = 0,1,2\ldots m_o)$ evaluated at the branch point $\xi = k$. These constants can be evaluated by solving a set of $m_o + 1$ linear equations. In our case this will be a complicated task for $m > 0$, because of the presence of another Taylor series for $K_+(\xi)$ and the series $1 - \gamma b + \gamma^2 b^2 \ldots$ in (2.56). Moreover, since $k\ell$ has been assumed to be large, significant contribution to the value of the integral comes from the zero order term $(m = 0)$ [53] since the higher order terms are smaller by $0(1/k\ell)$. Therefore, only the first term in the Taylor series is retained. (Such an assumption has yielded good results in a number of similar problems [38], p. 206, [57]). It is important here that $F_{D_+}(\xi)$ be slowly varying near $\xi = k$. This may be established remembering that $F_{D_+}(\xi)$ is a function of $\Phi'_+(b \pm 0)$ and $\Phi'_+(-b \pm 0)$, and that ϕ is a solution of the wave equation and may be considered

as a sum of waves emanating from four edges of the half planes (see Appendix B for details). It can also be shown that, to a first approximation $K_+(\xi)$ is a slowly varying function near $\xi = k$, except when $k \approx n\pi/2b$, where $n = 1,2,3 \ldots$ This was established numerically although the details are omitted. These values of k are associated with the modal cutoffs of the parallel plate waveguides.

Since $-(\text{Im } \alpha) < a$, the pole at $\xi = -\alpha$ lies below the contour. On the other hand α can lie close to $\xi = -k$ and this is the reason why the factor $(\xi + \alpha)^{-1}$ is kept separate from $F_{D_+}(\xi)/K_+(\xi)$; otherwise it would be sufficient to expand $(\xi + \alpha)^{-1} F_{D_+}(\xi)[K_+(\xi)]^{-1}$ as a Taylor's series. Since ℓ is assumed to be large and $\xi = k$ is the only contributing singularity, the contour can be deformed into the upper ξ-plane. Thus we cut the ξ-plane from $k = k_1 + ik_2$ to $k_1 + i\infty$ by a straight line parallel to the imaginary axis and deform the contour on to the two sides of the cut. On the right hand sides of the cut, $(\xi - k)^{\frac{1}{2}} = u^{\frac{1}{2}} e^{i\pi/4}$ where u goes from 0 to ∞. On the left hand side of the cut, $(\xi - k)^{\frac{1}{2}} = u^{\frac{1}{2}} e^{-i3\pi/4}$ and u goes from ∞ to 0 (Fig. 2.3). Thus we have

$$I = \frac{F_{D_+}(k)}{K_+(k)} T(\alpha) \tag{2.57}$$

where

$$T(\alpha) = \frac{1}{2\pi i} \int_{ia+\infty}^{ia-\infty} \frac{(1 - \gamma b + \gamma^2 b^2 \ldots) e^{i\xi\ell}}{(\xi + \alpha)(\xi - k)^{\frac{1}{2}} e^{i\pi/4}} \, d\xi \tag{2.58a}$$

$$= T_1(\alpha) + T_2(\alpha) + T_3(\alpha) + \ldots \tag{2.58b}$$

and $T_1(\alpha)$, $T_2(\alpha)$, ... correspond to the alternate terms of the series in (2.58a). After deforming the contour onto the upper half plane as described, we obtain

$$T_1(\alpha) = -\frac{e^{ik\ell}}{\pi}\,\ell^{\frac{1}{2}}\,W_{-1}[-i(\alpha + k)\ell] \tag{2.59}$$

and

$$T_{r+2}(\alpha) = \frac{e^{ik\ell}\,i^{r-1}\,(2b)^{2(1+r)}\,(2k)^{1+r}\,\ell^{-r-\frac{1}{2}}}{2(2r+2)!\,\pi}\,W_r[-i(\alpha + k)\ell]\,, \qquad r = 0,1,2\ldots \tag{2.60}$$

where

$$W_{j-\frac{1}{2}}(z) = \int_0^\infty \frac{u^j e^{-u}}{u + z}\,du = \Gamma(j+1)e^{z/2}\,z^{j/2-\frac{1}{2}}\,W_{-(j+1)/2,\,j/2}(z) \tag{2.61}$$

$W_{k,m}$ is the Whittaker function [58] and $\Gamma(\alpha)$ is the Gamma function. If W_{-1} is expressed in terms of a Fresnel integral, $T_1(\alpha)$ reduces to

$$T_1(\alpha) = -\frac{2}{h}\left(\frac{\ell}{\pi}\right)^{\frac{1}{2}}\,F(h)e^{-ih^2}\,e^{ik\ell} \tag{2.62}$$

where

$$F(v) = \int_v^\infty e^{iu^2}\,du \tag{2.63}$$

and

$$h = [(\alpha + k)\ell]^{\frac{1}{2}} \tag{2.64}$$

It is interesting to note that $(2k)^{\frac{1}{2}}\,e^{-i\pi/4}\,T_1(\alpha)$ is the same as one obtains for the interaction between the edges of a slit in a thin screen using the method of Yu and Rudduck [4]. Using the asymptotic form of

the Whittaker functions in (2.59), (2.60) for large values of $k\ell$, we obtain

$$T(\alpha) = \frac{-ie^{ik\ell}}{(\pi\ell)^{\frac{1}{2}}(\alpha + k)} \left[1 + \frac{i(kb)^2}{k\ell} - \frac{(kb)^4}{(k\ell)^2} + \ldots\right] \tag{2.65}$$

where the first term is the same as that given by Keller [2] for the E-polarization solution of a slit in a thin screen. The higher order terms, on the other hand, provide the correction due to presence of the second slit.

Now consider the second integral in (2.53)

$$\frac{1}{2\pi i}\int_{ia-\infty}^{ia+\infty} \frac{e^{i\xi(q-p)}K_-'(\xi)}{(\xi - k\cos\theta_o)(\xi + \alpha)}\, d\xi$$

$$= \frac{e^{ik\ell\cos\theta_o} K_-'(k\cos\theta_o)}{(\alpha + k\cos\theta_o)}$$

$$+ \frac{1}{(2\pi i)(\alpha + k\cos\theta_o)}\int_{ia-\infty}^{ia+\infty} \left(\frac{1}{\xi - k\cos\theta_o} - \frac{1}{\xi + \alpha}\right) K_-'(\xi)e^{i\xi(q-p)}d\xi$$

$$= \frac{e^{ik\ell\cos\theta_o} K_-'(k\cos\theta_o)}{(\alpha + k\cos\theta_o)} + R_2(\alpha) \tag{2.66}$$

where

$$R_2(\alpha) = \frac{T(-k\cos\theta_o) - T(\alpha)}{K_+(k)(\alpha + k\cos\theta_o)} \tag{2.67}$$

It should be noted that (2.66) is not valid for $\theta_o \approx 0^\circ$, since the pole $\xi = k\cos\theta_o$ in that case is near the branch point $\xi = k$. For the case

$\theta_o = 0°$, for large ℓ, the value of the integral simplifies to $2i\ell T(\alpha)$ where $T(\alpha)$ is given by (2.65).

Similarly the third integral in (2.53) can be written as

$$\frac{1}{2\pi i}\int_{ia-\infty}^{ia+\infty} \frac{e^{i\xi(q-p)}\, K_-'(\xi)}{(\xi + k\cos\theta_o)(\xi + \alpha)}\, d\xi$$

$$= \frac{1}{2\pi i(\alpha - k\cos\theta_o)} \int_{ia-\infty}^{ia+\infty} \left(\frac{1}{\xi + k\cos\theta_o} - \frac{1}{\xi + \alpha}\right) e^{i\xi(q-p)} K_-'(\xi)\, d\xi$$

$$= R_1(\alpha) \qquad (2.68)$$

where

$$R_1(\alpha) = \frac{T(+k\cos\theta_o) - T(\alpha)}{K_+(k)(\alpha - k\cos\theta_o)} \qquad (2.69)$$

Substituting for the values of the integrals in (2.53) from (2.57), (2.66) and (2.68), we obtain

$$F_{D_+}(\alpha)K_+'(\alpha) = -(2\pi)^{-\frac{1}{2}} A' e^{\mp ikq\cos\theta_o} \left\{P_1(\alpha) + \lambda R_2(\alpha)\right\}$$

$$+ (2\pi)^{-\frac{1}{2}} \lambda A' e^{-ikp\cos\theta_o} \left\{P_2(\alpha) + \lambda R_1(\alpha)\right\}$$

$$- \frac{\lambda T(\alpha) F_{D_+}(k)}{K_+(k)} \qquad (2.70)$$

where

$$P_{1,2}(\alpha) = \frac{K_+'(\alpha) - K_\pm'(k\cos\theta_o)}{\alpha \mp k\cos\theta_o} \qquad (2.71)$$

The value of $F_{D_+}(k)$ can be found by setting $\alpha = k$ in (2.70). When

this value is substituted back into (2.70), we obtain

$$F_{D_+}(\alpha)K'_+(\alpha) = -\frac{A'}{(2\pi)^{\frac{1}{2}}}\left[G_1(\alpha) - \lambda G_2(\alpha)\right] + \frac{\lambda A'T(\alpha)}{(2\pi)^{\frac{1}{2}}K_+(k)} \cdot \frac{\left[G_1(k) - \lambda G_2(k)\right]}{\left[K'_+(k) + \frac{\lambda T(k)}{K_+(k)}\right]} \tag{2.72}$$

where

$$G_1(\alpha) = e^{-ikq\cos\theta_o}P_1(\alpha) - e^{-ikp\cos\theta_o}R_1(\alpha) \tag{2.73}$$

$$G_2(\alpha) = e^{-ikp\cos\theta_o}P_2(\alpha) - e^{-ikq\cos\theta_o}R_2(\alpha) \tag{2.74}$$

Using (2.43), (2.48) and (2.52) and remembering that $F_{D_+}(\alpha)$ represents $E^*_{D_+}(\alpha)$ or $L^*_{D_+}(\alpha)$ as $\lambda = -1$ or $+1$, respectively, we have

$$F_{D_+}(\alpha) = \begin{cases} \psi_{D_+}(\alpha) + \psi_{D_-}(-\alpha) & \text{for } \lambda = -1 \\ \psi_{D_+}(\alpha) - \psi_{D_-}(-\alpha) & \text{for } \lambda = +1 \end{cases} \tag{2.75}$$

The expressions for $\psi_{D_+}(\alpha)$ and $\psi_{D_-}(\alpha)$ are thus given by

$$\psi_{D_+}(\alpha) = \frac{1}{(2\pi)^{\frac{1}{2}}K'_+(\alpha)}\left(-A'G_1(\alpha) - \frac{A'T(\alpha)\left[G_1(k)T(k) + G_2(k)K'_+(k)K_+(k)\right]}{\left[K'_+(k)K_+(k)\right]^2 - T^2(k)}\right) \tag{2.76}$$

$$\psi_{D_-}(\alpha) = \frac{1}{(2\pi)^{\frac{1}{2}}K'_-(\alpha)}\left(-A'G_2(-\alpha) - \frac{A'T(-\alpha)\left[G_2(k)T(k) + G_1(k)K'_+(k)K_+(k)\right]}{\left[K'_+(k)K_+(k)\right]^2 - T^2(k)}\right) \tag{2.77}$$

Substituting (2.76) and (2.77) into (2.31), we obtain

$$S_1 = -\frac{K'(\alpha)}{(2\pi)^{\frac{1}{2}}}\left[\frac{e^{i\alpha q}}{K'_+(\alpha)}\left(-A'G_1(\alpha)\right.\right.$$

$$\left.-\frac{A'T(\alpha)\left[G_1(k)T(k) + G_2(k)K'_+(k)K_+(k)\right]}{\left[K'_+(k)K_+(k)\right]^2 - T^2(k)}\right) + \frac{e^{i\alpha p}}{K'_-(\alpha)} \cdot$$

$$\left(-A'G_2(-\alpha) - \frac{A'T(-\alpha)\left[G_2(k)T(k) + G_1(k)K'_+(k)K_+(k)\right]}{\left[K'_+(k)K_+(k)\right]^2 - T^2(k)}\right)$$

$$\left. + A'G(\alpha)\right] \tag{2.78}$$

Similar manipulation of (2.26) yields

$$D_1 = -\frac{L(\alpha)b}{(2\pi)^{\frac{1}{2}}}\left[\frac{e^{i\alpha q}}{L_+(\alpha)}\left(-A'H_1(\alpha)\right.\right.$$

$$\left.-\frac{A'U(\alpha)\left[H_1(k)U(k) + H_2(k)L_+^2(k)\right]}{L_+^4(k) - U^2(k)}\right) + \frac{e^{i\alpha p}}{L_-(\alpha)} \cdot$$

$$\left(-A'H_2(-\alpha) - \frac{A'U(-\alpha)\left[H_2(k)U(k) + H_1(k)L_+^2(k)\right]}{L_+^4(k) - U^2(k)}\right)$$

$$\left. + A'G(\alpha)\right] \tag{2.79}$$

where

$$H_1(\alpha) = e^{-ikq\cos\theta_o}Q_1(\alpha) - e^{-ikp\cos\theta_o}V_1(\alpha) \tag{2.80}$$

$$H_2(\alpha) = e^{-ikp\cos\theta_o}Q_2(\alpha) - e^{-ikq\cos\theta_o}V_2(\alpha) \tag{2.81}$$

$$Q_{1,2}(\alpha) = \frac{L_+(\alpha) - L_\pm(k\cos\theta_o)}{\alpha \mp k\cos\theta_o} \tag{2.82}$$

$$V_{1,2}(\alpha) = \frac{U(\pm k\cos\theta_o) - U(\alpha)}{L_+(k)(\alpha \mp k\cos\theta_o)} \tag{2.83}$$

and

$$U(\alpha) = \frac{1}{(2k)^{\frac{1}{2}}\,2\pi i}\int_{ia-\infty}^{ia+\infty} \frac{e^{-\gamma b}\sinh\gamma b\; e^{i\xi\ell}}{b(\xi - k)^{\frac{1}{2}}(\xi + \alpha)}\,d\xi \tag{2.84}$$

which may be evaluated in a way similar to that for $T(\alpha)$ as shown in Appendix C.

2.3 Far Field of the Tandem Slit

Since S_1 and D_1 have been evaluated, it is now possible to determine the field ϕ in every region. Thus remembering that $S_1^{(o)} = S_1^{(i)} = S_1$ etc., we have from (2.18)

$$S_1 = \Phi_1(b) + \Phi_1(-b)$$

$$D_1 = \Phi_1(b) - \Phi_1(-b)$$

or $$\Phi_1(-b) = \frac{1}{2}(S_1 - D_1) \tag{2.85}$$

Now

$$\Phi_1(-b) = \Phi(-b) \tag{2.86}$$

since the field vanishes on the plates. Using (2.9b), (2.85) and (2.86), we obtain

$$\Phi_-(b) = \Phi_1(-b) = De^{-\gamma b} = \frac{1}{2}(S_1 - D_1) \tag{2.87}$$

and

$$\Phi(y) = \frac{e^{\gamma b}}{2}(S_1 - D_1)e^{\gamma y} \quad y \le -b \tag{2.88}$$

Thus defining regions 1, 2 and 3 to be the illumination, parallel plate and the diffraction regions, respectively, the field in region 3 is given by

$$\phi = \frac{1}{2(2\pi)^{\frac{1}{2}}} \int_{-\infty+ia}^{\infty+ia} e^{\gamma b}(S_1 - D_1)e^{\gamma y}\, e^{-i\alpha x}\, d\alpha \; ; \; -k_2\cos\theta_o < a < k_2\cos\theta_o \tag{2.89}$$

$$= \phi_{sep} + \phi_{int} \tag{2.90}$$

where ϕ_{sep} is the sum of diffracted waves produced by each parallel plate waveguide separately, i.e. acting as though the other parallel plate waveguide were absent. ϕ_{int} is the field due to interaction between the two parallel plate waveguides. Evaluating the integral in (2.89) by the method of steepest descent [59], we recognize ϕ_{sep} to be

$$\begin{aligned}\phi_{sep} = \frac{e^{i(kr-\pi/4)}}{(2\pi kr)^{\frac{1}{2}}} \Bigg\{ & e^{ikd(\cos\theta+\cos\theta_o)} \\ & \left[-\frac{2i\,\cos\theta_o/2\,\cos\theta/2}{\cos\theta_o + \cos\theta} \cdot \left(\frac{\cos(kb\,\sin\theta_o)\cos(kb\,\sin\theta)}{K_+(k\,\cos\theta_o)K_+(k\,\cos\theta)} \right.\right. \\ & \left.\left. + \frac{i\,\sin(kb\,\sin\theta_o)\sin(kb\,\sin\theta)}{L_+(k\,\cos\theta_o)L_+(k\,\cos\theta)2kb\,\cos\theta_o/2\,\cos\theta/2} \right) \right] \\ & + e^{-ikd(\cos\theta_o+\cos\theta)} \left[\frac{2i\,\sin\theta_o/2\,\sin\theta/2}{\cos\theta_o + \cos\theta} \right. \\ & \cdot \left(\frac{\cos(kb\,\sin\theta_o)\cos(kb\,\sin\theta)}{K_-(k\,\cos\theta_o)K_-(k\,\cos\theta)} \right. \\ & \left.\left. \left. + \frac{i\,\sin(kb\,\sin\theta_o)\sin(kb\,\sin\theta)}{L_-(k\,\cos\theta_o)L_-(k\,\cos\theta)2kb\,\sin\theta_o/2\,\sin\theta/2} \right) \right] \Bigg\} \end{aligned} \tag{2.91a}$$

$$= \frac{e^{i(kr-\pi/4)}}{(2\pi kr)^{\frac{1}{2}}} \left\{ a(\theta_o,-\theta) e^{ikd(\cos\theta_o+\cos\theta)} \right.$$

$$\left. + a(\pi - \theta_o, \theta - \pi) e^{-ikd(\cos\theta_o+\cos\theta)} \right\} \qquad (2.91b)$$

where $d = \frac{\ell}{2}$ and $a(\theta_o,\theta)$ represents the diffraction coefficient of a parallel plate waveguide for an E-polarized incident plane wave (Fig. 2.4). As expected, the above equation is symmetrical in θ_o and θ. It resembles the two singly diffracted rays of Keller [2] for a thin slit provided that each term in (2.91) is recognized as the diffraction by an equivalent edge or source located in the middle of each parallel plate waveguide. This concept of an equivalent edge is superior to the simple ray method of considering two edges since for small separations between the two plates, one rather than two diffraction centres needs to be considered. Furthermore, the ray method has been shown to yield results for this problem which are not in complete agreement with the asymptotic form of the exact solution [52].

The interaction field ϕ_{int} may be recognized and arranged as terms involving functions $K'_+(k\cos\theta_o)$, $K'_-(k\cos\theta_o)$, $L_+(k\cos\theta_o)$ and $L_-(k\cos\theta_o)$. After considerable algebraic manipulation, the result for large $k\ell$ simplifies to

$$\phi_{int} = \phi'_{int} + \phi''_{int} \qquad (2.92)$$

where

$$\phi'_{int} = \frac{e^{i(kr-\pi/4)}}{(2\pi kr)^{\frac{1}{2}}} \frac{F_1(\ell)\left[1 + F_2(b,\ell)\right]}{1 + F_1^2(\ell)\left[1 + F_2(b,\ell)\right]^2} \left\{ \phi^a_{int} \right.$$

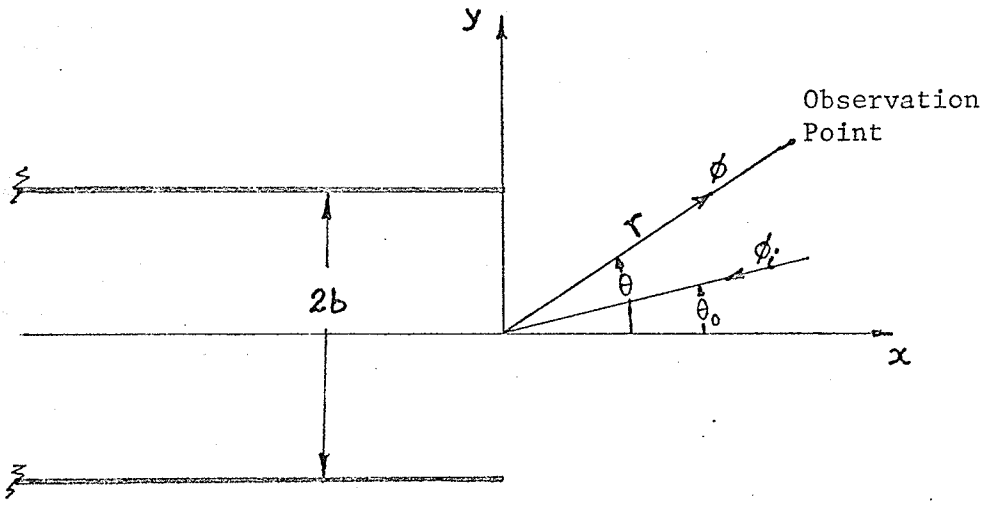

$$\phi = \frac{e^{i(kr-\pi/4)}}{(2\pi kr)^{\frac{1}{2}}} \; a(\theta_o,\theta) \quad , \quad kr >> 1$$

Fig. 2.4 Parallel plate waveguide geometry

$$+ \phi^b_{int} + F_1(\ell)\left[1 + F_2(b,\ell)\right]\left(\phi^c_{int} + \phi^d_{int}\right)\Bigg\} \tag{2.93}$$

$$\phi''_{int} = \frac{e^{i(kr-\pi/4)}}{(2\pi kr)^{\frac{1}{2}}} \frac{F_2(b,\ell)F_3(b,\ell)}{1 - F_2^2(b,\ell)F_3^2(b,\ell)} \Bigg\{\phi^e_{int} + \phi^f_{int}$$

$$+ F_2(b,\ell)F_3(b,\ell)\left[\phi^g_{int} + \phi^h_{int}\right]\Bigg\} \tag{2.94}$$

and

$$F_1(\ell) = \left\{\frac{e^{i(k\ell-\pi/4)}}{(2\pi k\ell)^{\frac{1}{2}}}\right\} \frac{1}{K_+^2(k)} \tag{2.95a}$$

$$F_2(b,\ell) = \frac{i(kb)^2}{k\ell} - \frac{(kb)^4}{(k\ell)^2} + \ldots \tag{2.95b}$$

$$F_3(b,\ell) = \left\{-\frac{e^{i(k\ell-\pi/4)}}{(2\pi k\ell)^{\frac{1}{2}}}\right\} \frac{1}{L_+^2(k)(2kb)} \tag{2.95c}$$

$$\phi^a_{int} = -\frac{e^{ikd(\cos\theta_o - \cos\theta)} \cos(kb\sin\theta_o)\cos(kb\sin\theta)}{K_+(k\cos\theta_o)K_-(k\cos\theta)\cos(\theta_o/2)\sin(\theta/2)} \tag{2.96a}$$

$$\phi^b_{int} = -\frac{e^{-ikd(\cos\theta_o - \cos\theta)} \cos(kb\sin\theta_o)\cos(kb\sin\theta)}{K_-(k\cos\theta_o)K_+(k\cos\theta)\sin(\theta_o/2)\cos(\theta/2)} \tag{2.96b}$$

$$\phi^c_{int} = \frac{i\, e^{ikd(\cos\theta_o + \cos\theta)} \cos(kb\sin\theta_o)\cos(kb\sin\theta)}{K_+(k\cos\theta_o)K_+(k\cos\theta)\cos(\theta_o/2)\cos(\theta/2)} \tag{2.96c}$$

$$\phi^d_{int} = \frac{i\, e^{-ikd(\cos\theta_o + \cos\theta)} \cos(kb\sin\theta_o)\cos(kb\sin\theta)}{K_-(k\cos\theta_o)K_-(k\cos\theta)\sin(\theta_o/2)\sin(\theta/2)} \tag{2.96d}$$

$$\phi^{e}_{int} = \frac{e^{ikd(\cos\theta_o - \cos\theta)} \sin(kb\ \sin\theta_o)\sin(kb\ \sin\theta)}{(2kb)L_+(k\ \cos\theta_o)L_-(k\ \cos\theta)\cos^2(\theta_o/2)\sin^2(\theta/2)} \tag{2.97a}$$

$$\phi^{f}_{int} = \frac{e^{-ikd(\cos\theta_o - \cos\theta)} \sin(kb\ \sin\theta_o)\sin(kb\ \sin\theta)}{(2kb)L_-(k\ \cos\theta_o)L_+(k\ \cos\theta)\sin^2(\theta_o/2)\cos^2(\theta/2)} \tag{2.97b}$$

$$\phi^{g}_{int} = \frac{e^{ikd(\cos\theta_o + \cos\theta)} \sin(kb\ \sin\theta_o)\sin(kb\ \sin\theta)}{(2kb)L_+(k\ \cos\theta_o)L_+(k\ \cos\theta)\cos^2(\theta_o/2)\cos^2(\theta/2)} \tag{2.97c}$$

$$\phi^{h}_{int} = \frac{e^{-ikd(\cos\theta_o + \cos\theta)} \sin(kb\ \sin\theta_o)\sin(kb\ \sin\theta)}{(2kb)L_-(k\ \cos\theta_o)L_-(k\ \cos\theta)\sin^2(\theta_o/2)\sin^2(\theta/2)} \tag{2.97d}$$

The above expressions are valid for θ_o, $\theta \neq 0$ or π.

It may be shown that ϕ'_{int} corresponds to the soft diffraction case due to an equivalent line source (inhomogeneous) representation at the equivalent edge. This interaction field represents the field of four types of higher order rays employed by Keller [2] in the thin slit solution, except for two modifications. The first relates to the factor

$$\frac{\cos(\theta_o/2)\cos(\theta/2)}{\cos\theta_o + \cos\theta}$$

which appears in the ray diffraction coefficient for an E-polarized plane wave incident on a thin half plane. For a parallel plate waveguide with the same type of incident wave, this factor is multiplied by

$$\frac{\cos(kb\ \sin\theta_o)\cos(kb\ \sin\theta)}{K_+(k\ \cos\theta_o)K_+(k\ \cos\theta)} - \frac{i\ \sin(kb\ \sin\theta_o)\sin(kb\ \sin\theta)}{2kb\ \cos(\theta_o/2)\cos(\theta/2)L_+(k\ \cos\theta_o)L_+(k\ \cos\theta)}$$

which is identically unity when $b = 0$, i.e. when each parallel plate

waveguide becomes a half plane.

The second modification is that the factor $\frac{e^{i(k\ell-3\pi/4)}}{(2\pi k\ell)^{\frac{1}{2}}}$, related to the amplitude of the edge-edge ray field for a thin slit, is multiplied in the present case by

$$\left\{1 + F_2(b,\ell)\right\} \frac{1}{K_+^2(k)}$$

which again reduces to unity for $b = 0$.

The second interaction term ϕ''_{int} is a correction to ϕ'_{int} but of lower magnitude by $0(1/k\ell)$, where $k\ell$ is assumed to be larger than unity. Its contribution emerges from the mathematical derivation as proportional to the angular derivative of the ϕ'_{int} field (prior to setting θ equal to 0 or π) as discussed by Morse [60]. This field may be recognized as due to two hypothetical line dipoles located at the two equivalent edges and represents the fields of four types of higher order rays discussed by Karp and Keller [61]. It should be noted that ϕ''_{int} is numerically negligible when compared to ϕ'_{int} for the case $2b/\ell \lesssim 0.5$. For larger values of this ratio, however, its inclusion may result in a better agreement with available results [46]. Also, it is consistent to keep ϕ''_{int} even when the higher terms in the Taylor series expansion of $F_{D_+}(\xi)$ have been neglected. This is because the higher terms in Taylor series for $F_{D_+}(\xi)$ can be neglected if $k\ell >> 1$. However, ϕ''_{int} cannot be neglected if kb also happens to be large along with $k\ell$.

For the special case of $b = 0$, the ϕ''_{int} term vanishes and the interaction field reduces to

$$\phi_{int} = \frac{i\, e^{i(kr+k\ell)}}{(2\pi kr)^{\frac{1}{2}}(2\pi k\ell)^{\frac{1}{2}}} \left(1 + \frac{e^{2ik\ell}}{2\pi ik\ell}\right)^{-1} \left[\left\{\frac{e^{ikd(\cos\theta_o - \cos\theta)}}{\cos(\theta_o/2)\sin(\theta/2)}\right.\right.$$

$$\left. + \frac{e^{-ikd(\cos\theta_o - \cos\theta)}}{\sin(\theta_o/2)\cos(\theta/2)}\right\} + \frac{e^{i(k\ell - 3\pi/4)}}{(2\pi k\ell)^{\frac{1}{2}}} \left\{\frac{e^{-ikd(\cos\theta_o + \cos\theta)}}{\sin(\theta_o/2)\sin(\theta/2)}\right.$$

$$\left.\left. + \frac{e^{ikd(\cos\theta_o + \cos\theta)}}{\cos(\theta_o/2)\cos(\theta/2)}\right\}\right], \quad \theta_o,\ \theta \neq 0 \text{ or } \pi \tag{2.98}$$

which is identical with the result found by Karp and Russek [3]. Furthermore, if the Whittaker function in (2.59) is expressed in terms of a Fresnel integral [58] and the higher order terms of the series in (2.56) neglected, the expression for the interaction field simplifies to

$$\phi_{int} = W_1 \left\{ e^{ikd(\cos\theta_o - \cos\theta)} \frac{F(\ell,0,\theta - \pi)\cos(kb\,\sin\theta)}{K_+(k)K_-(k\,\cos\theta)}\, a(\theta_o,0) \right.$$

$$+ e^{-ikd(\cos\theta_o - \cos\theta)} \frac{F(\ell,0,-\theta)\cos(kb\,\sin\theta)}{K_+(k)K_+(k\,\cos\theta)}\, a(\pi - \theta_o,0)$$

$$+ \frac{F(\ell,0,0)}{K_+^2(k)}$$

$$\cdot \left[e^{-ikd(\cos\theta_o + \cos\theta)} \frac{F(\ell,0,\theta - \pi)\cos(kb\,\sin\theta)}{K_+(k)K_-(k\,\cos\theta)}\, a(\pi - \theta_o,0) \right.$$

$$\left.\left. + e^{ikd(\cos\theta_o + \cos\theta)} \frac{F(\ell,0,-\theta)\cos(kb\,\sin\theta)}{K_+(k)K_+(k\,\cos\theta)}\, a(\theta_o,0)\right]\right\} \tag{2.99a}$$

where

$$W_1 = \frac{1}{1 - \dfrac{F^2(\ell,0,0)}{K_+^4(k)}} \frac{e^{i(kr-\pi/4)}}{(2\pi kr)^{\frac{1}{2}}} \tag{2.99b}$$

$$F(\ell,0,\theta) = e^{-ik\ell\cos\theta}\left\{-1 + (2/i)^{\frac{1}{2}}\int_0^{2(k\ell/\pi)^{\frac{1}{2}}\cos\theta/2} e^{i\pi v^2/2}\,dv\right\} \tag{2.99c}$$

and $a(\theta_o,\theta)$ is the diffraction coefficient for a parallel plate waveguide for an E-polarized incident plane wave (2.91).

For the case of a thin slit ($kb \to 0$), (2.99a) reduces to

$$\phi_{int} = W\left\{-i\,e^{ikd(\cos\theta_o-\cos\theta)}\,\frac{F(\ell,0,\theta-\pi)}{\cos\theta_o/2}\right.$$

$$-i\,e^{-ikd(\cos\theta_o-\cos\theta)}\,\frac{F(\ell,0,-\theta)}{\sin(\theta_o/2)} - i\,F(\ell,0,0)$$

$$\cdot\left[e^{-ikd(\cos\theta_o+\cos\theta)}\,\frac{F(\ell,0,\theta-\pi)}{\sin(\theta_o/2)} + e^{ikd(\cos\theta_o+\cos\theta)}\right.$$

$$\left.\left.\cdot\,\frac{F(\ell,0,-\theta)}{\cos(\theta_o/2)}\right]\right\} \tag{2.100}$$

where

$$W = \frac{1}{1 - F^2(\ell,0,0)}\cdot\frac{e^{i(kr-\pi/4)}}{(2\pi kr)^{\frac{1}{2}}} \tag{2.101}$$

This expression for the interaction field may be shown, by Babinet's principle, to be identical to that obtained by Yu and Rudduck [4] for the complementary narrow strip problem, although the details are omitted here.

The field in region 2 may be expressed in the form

$$\sum_{n=1}^{\infty}\left(c_n^{sep} + c_n^{int}\right)\left(\sin\frac{n\pi(y-b)}{2b}\right)e^{\gamma_n x} \tag{2.102}$$

where

$$\gamma_n = +\sqrt{\left(\frac{n\pi}{2b}\right)^2 - k^2} \quad \text{or} \quad -i\sqrt{k^2 - \left(\frac{n\pi}{2b}\right)^2} \tag{2.103}$$

and c_n^{sep} represents the mode coefficients scattered in the parallel plate waveguide regions, due to the incident plane wave, without considering any interaction effects. c_n^{int} denotes the scattered mode coefficients due to interaction between the waveguides. For the waveguide directly illuminated by the incident wave, they are given by

$$c_n^{sep} = \begin{cases} -\dfrac{2b\cos(kb\sin\theta_o)(k + k\cos\theta_o)^{\frac{1}{2}}(i\gamma_n - k)^{\frac{1}{2}}}{n\pi K_+(k\cos\theta_o)(i\gamma_n - k\cos\theta_o)K_-^{(1)}(i\gamma_n)} & ; n = 1,3,5\ldots \\ \dfrac{2i\sin(kb\sin\theta_o)}{n\pi(i\gamma_n - k\cos\theta_o)L_+(k\cos\theta_o)L_-^{(1)}(i\gamma_n)} & ; n = 2,4,6\ldots \end{cases} \tag{2.104}$$

$$c_n^{int} = \begin{cases} g_n^{int}\left[-\dfrac{i\cos(kb\sin\theta_o)e^{i(k\ell-\pi/4)}e^{-i2kd\cos\theta_o}}{\sin(\theta_o/2)K_-(k\cos\theta_o)K_+(k)(2\pi k\ell)^{\frac{1}{2}}}\right](1 + F_2(b,\ell)); \\ \qquad\qquad n = 1,3,5\ldots \\ -\dfrac{(kb)\sin(kb\sin\theta_o)e^{i(k\ell-\pi/4)}e^{-i2kd\cos\theta_o}(1 + F_2(b,\ell))}{(k\ell)L_-^{(1)}(i\gamma_n)(k - i\gamma_n)n\pi L_+^2(k)L_-(k\cos\theta_o)\sin^2(\theta_o/2)(2\pi k\ell)^{\frac{1}{2}}}; \\ \qquad\qquad n = 2,4,6\ldots \end{cases} \tag{2.105}$$

where

$$g_n^{int} = \frac{2b(2k)^{\frac{1}{2}}(i\gamma_n - k)^{\frac{1}{2}}}{n\pi(k - i\gamma_n)K_-^{(1)}(i\gamma_n)K_+(k)} \tag{2.106}$$

$$K_-^{(1)}(i\gamma_n) = \frac{\partial}{\partial\alpha} K_-(\alpha)\Big|_{\alpha=i\gamma_n} \quad , \quad L_-^{(1)}(i\gamma_n) = \frac{\partial}{\partial\alpha} L_-(\alpha)\Big|_{\alpha=i\gamma_n} \tag{2.107}$$

as shown in Appendix D. It should be noted that c_n^{int} is smaller than c_n^{sep} by $0(1/(2\pi k\ell)^{\frac{1}{2}})$ and can be neglected for $(2\pi k\ell)^{\frac{1}{2}} >> 1$.

2.4 Numerical Results and Discussion

In order to check the accuracy of our approximate solution, computations of the transmission cross-section are performed for various values of plate separation (2b) and slit width (2d). The transmission cross-section is obtained from the imaginary part of F where the far field scattered by the tandem slit is given by $F.(2\pi kr)^{-\frac{1}{2}}\exp\{i(kr + \pi/4)\}$ [62]. Alldredge [46] uses the same definition and proves it to be valid as long as one remembers that it only includes the energy scattered by the slit structure outside the region between the two conducting plates. The computations are based upon (2.91) to (2.101), except that the Fresnel integral approximation, instead of the asymptotic approximation, for the integral I in (2.54) is used for the case of small slit widths. The formulae used for the computation of $K_\pm$ and $L_\pm$ are given in Appendix A. Figures 2.5 to 2.8 show (for $\theta_o = \pi/2$) the results of these computations and comparison with the variational and experimental results of Alldredge [46]. The agreement with available data is satisfactory except for very small slit widths.

Examination of our results shows that, as the tandem slit separation increases, the primary peak in the transmission cross-section decreases and moves towards values corresponding to larger slit widths.

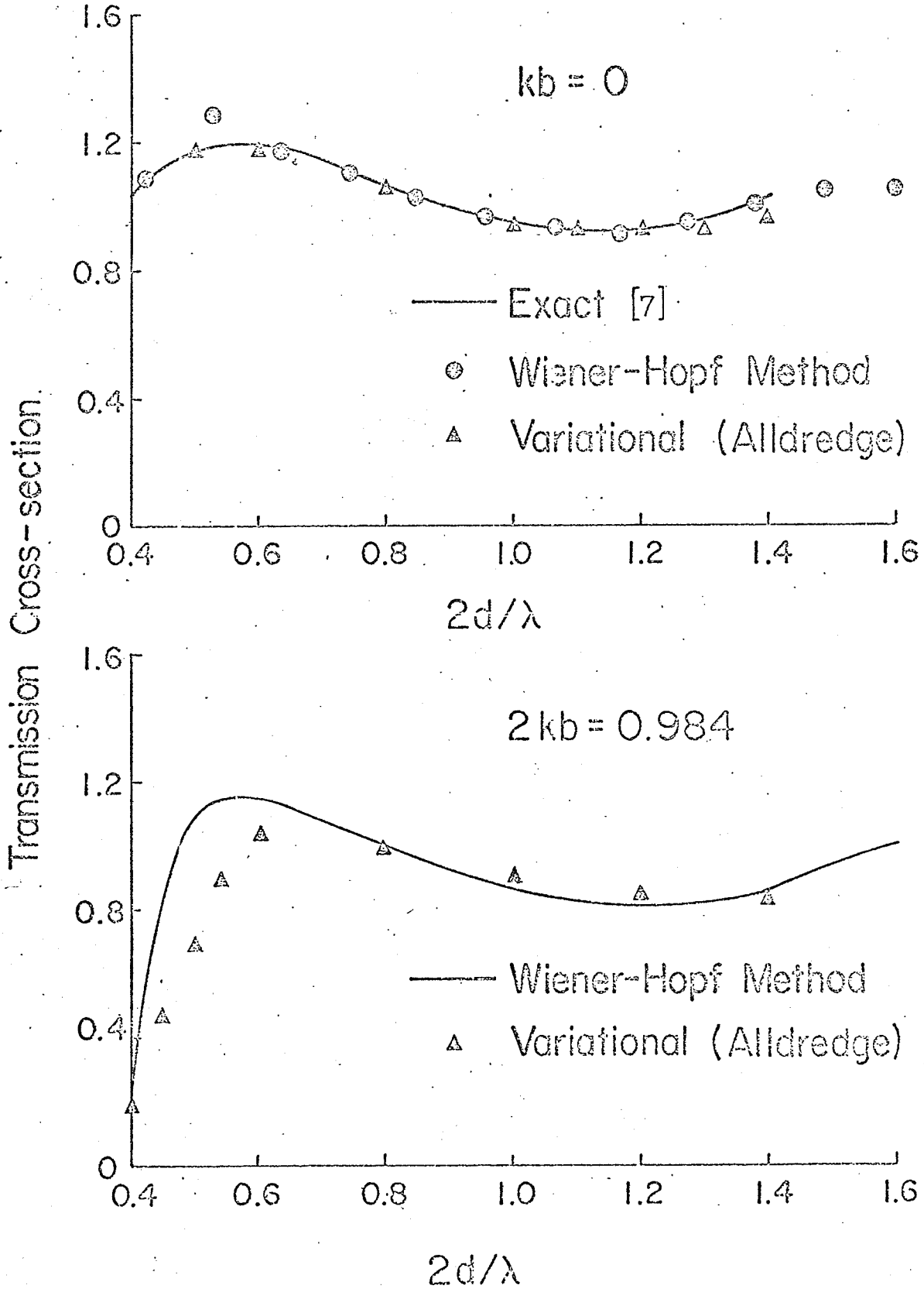

Figure 2.5 Transmission cross-section vs $2d/\lambda$ for a tandem slit.

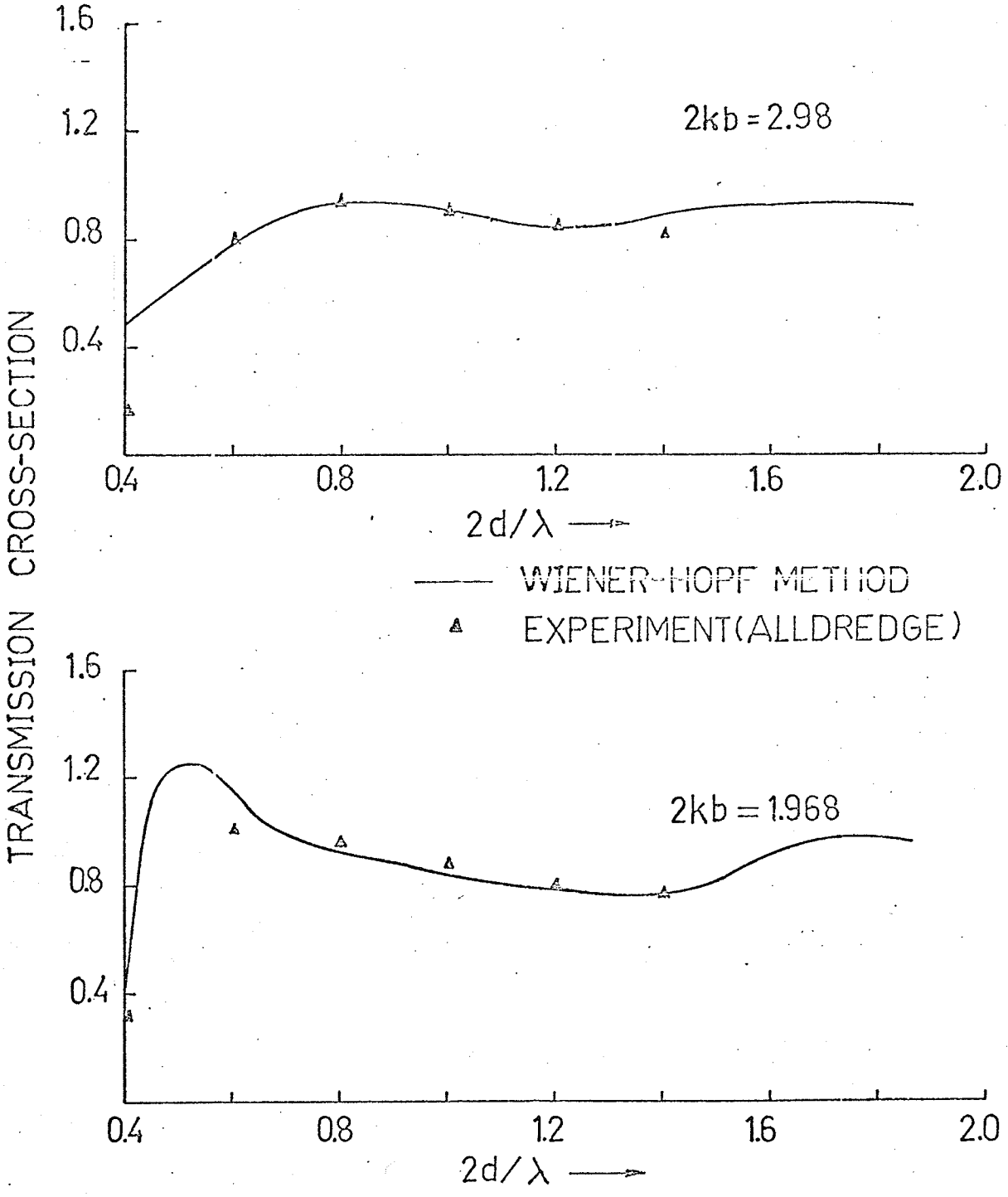

Figure 2.6 Transmission cross-section vs $2d/\lambda$ for a tandem slit.

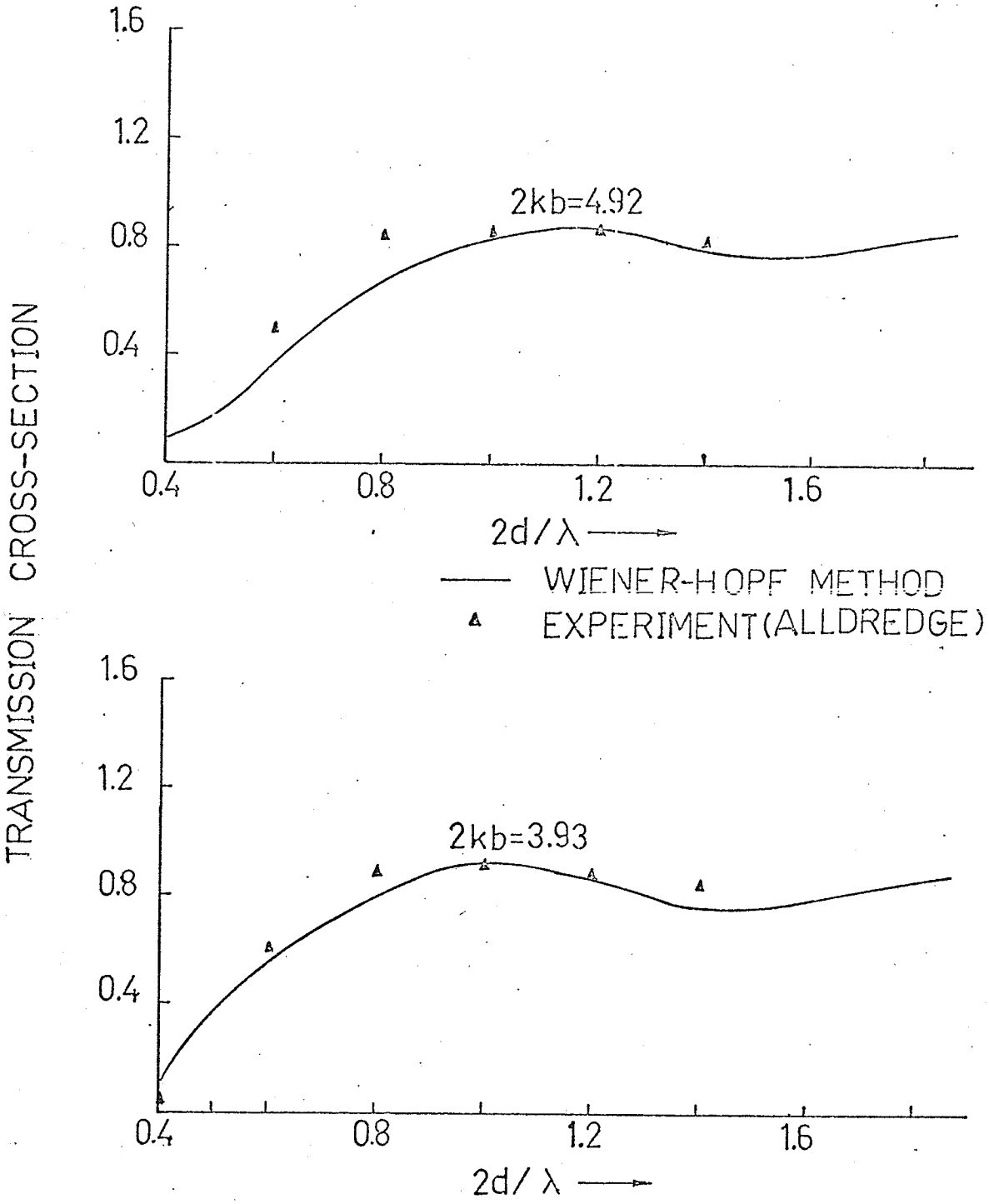

Figure 2.7 Transmission cross section vs 2d/λ for a tandem slit.

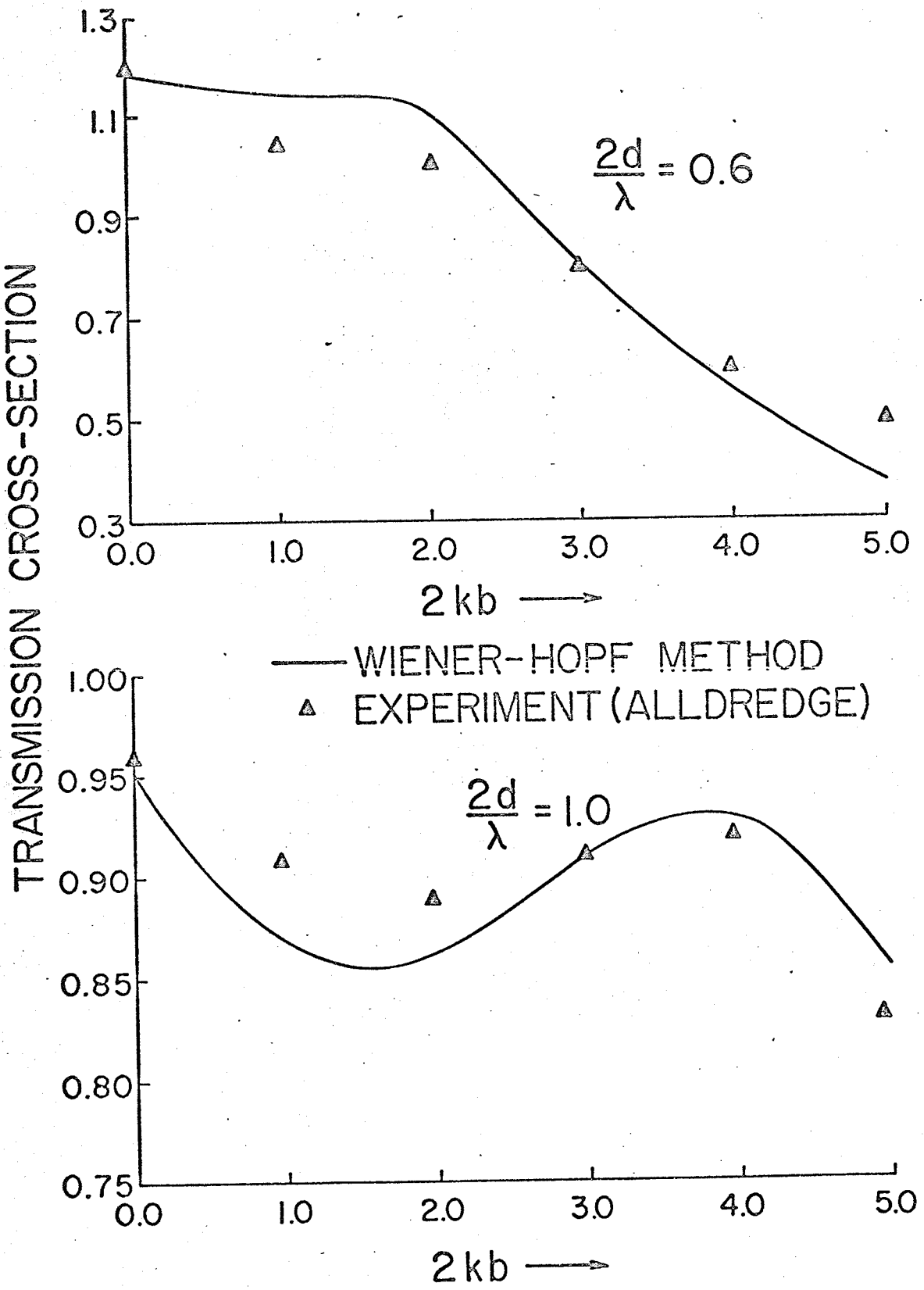

Fig. 2.8 Transmission cross-section vs 2kb for a tandem slit ($2d/\lambda = 0.6, 1.0$)

For example, as the slit separation (2kb) increases from 0 to 4.92, the transmission cross-section peak reduces from 1.26 to 0.88. For the same variation, the location of the primary peak moves from $2d/\lambda = 0.55$ to $2d/\lambda = 1.2$. Furthermore, the curve changes quite significantly when the tandem slit separation changes from 2.98 to 3.93 radians. This may be due to the fact that when $2kb = 3.93$, the space between the plates forming the slits can now operate as a waveguide in the TE_{10} mode. Similar changes will occur when the plate separation is equal to 2π, 3π, etc. This change in behaviour, which seems to be associated with the modes that can be propagated within the plates, appears more significantly in the amplitude data. For example, the maximum normalized amplitude for the case $2kb = 2.98$ is 1.03. This peak amplitude reduces to 0.9 as 2kb is increased to 3.93.

Finally, Fig. 2.8 shows the variation of transmission cross-section with plate-plate separation for two particular values of slit width. For $2d/\lambda = 1.0$, the transmission cross-section shows an oscillatory behaviour, whereas for $2d/\lambda = 0.6$ it decreases almost monotonically with increase of plate-plate separation. This effect might be associated with constructive or destructive interference of the edges for particular values of slit width and plate-plate separation.

It would be interesting to compare some of our results with those of Jones and Williams for the complementary tandem strip problem. In their case the integral I in (2.54) has $K_-(\xi)$ in the denominator and is evaluated as a sum of contributions due to the zeros of $K_-(\xi)$, i.e. $i\gamma_n$, and the branch point $\xi = k$. This leads to an infinite

number of linear equations involving $F(i\gamma_n)$ and $F(k)$. In our case, $K_-(\xi)$ occurs in the numerator of the integrand and therefore the contribution to the integral I comes only from the branch point $\xi = k$. Also, only the alternate terms of the series in (2.58a) contribute to the value of the integral. The first term corresponds to the interaction term which is obtained by replacing the diffraction coefficient for a thin half plane by that for a parallel plate waveguide. The higher order terms, which can be readily included in our analysis, provide the effect of the finite separation between the plates. In particular, for the case $kd > 1$ all higher order terms have the same branch point at $\xi = k$ and are therefore summed as a simple geometric series. The computational advantage of our method, for the practical case of a small separation compared to wavelength or the width (i.e. $kb < 1$ or $2b/\ell \lesssim 0.5$), is that the solution reduces to the ray optical form except for the two modifications discussed previously. Moreover, our solution is not restricted to the case of sufficiently large plate-plate separation which seems to be a limitation in the solution of Jones and Williams. This is because of the difference between the two problems and the interaction mechanism involved. In their case, waveguide modes provide added end-end interaction, whereas in our case there is only an open space coupling between the waveguides.

Although we have concerned ourselves mainly with the E-polarization, it may be shown that the H-polarization can be treated in a similar fashion. The technique may also be generalized to the case of a periodic structure composed of infinite slits. This configuration,

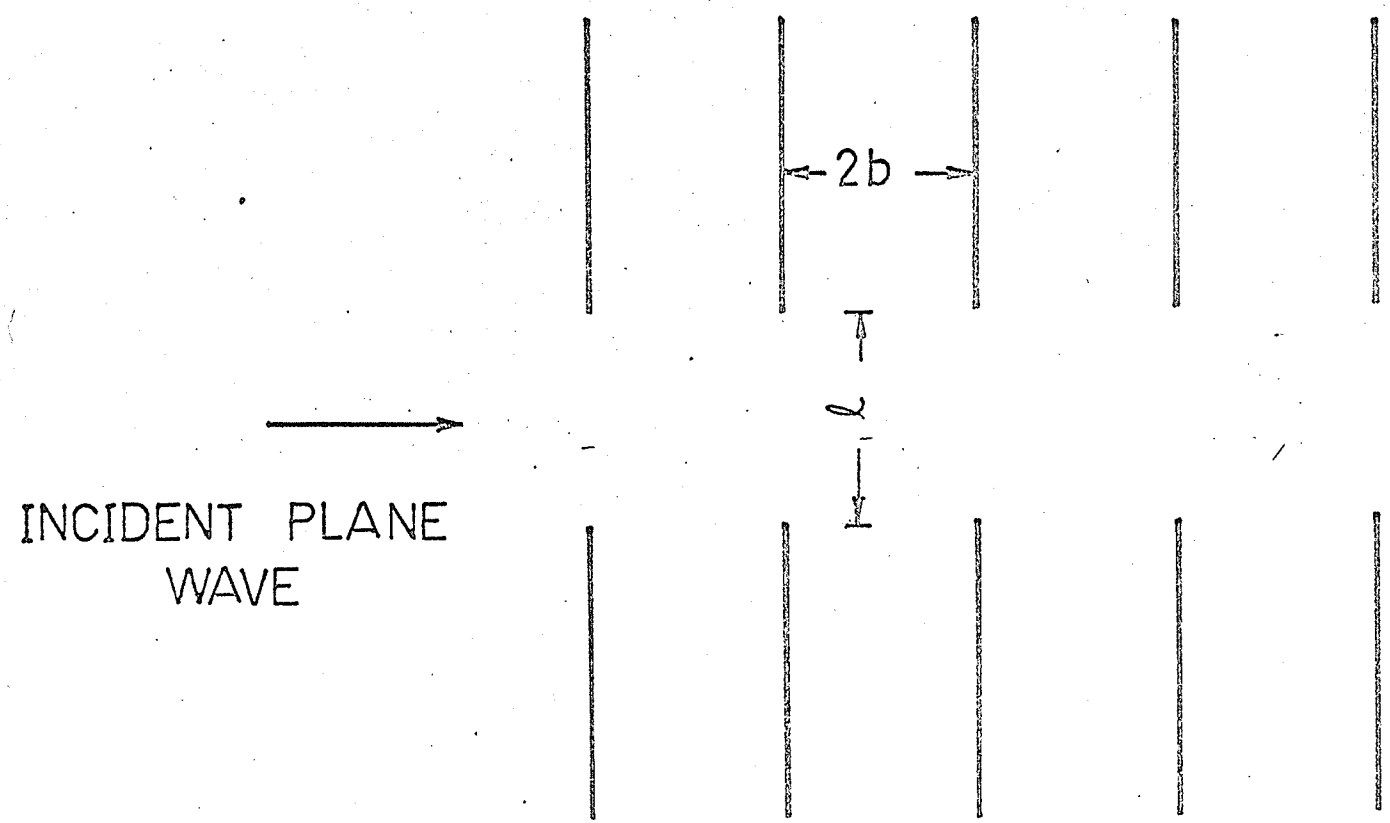

Fig. 2.9 Beam Waveguide Geometry

often referred to as a collimator (see Fig. 2.9), was first investigated by Goubau [63] who considered the question of existence of modal solutions in periodic structures of this type. The field intensity in an iris of this configuration is found to be insensitive to the slit spacing but is very sensitive to the slit width [64]. This may lead to a highly directive beam for particular values of slit width.

CHAPTER III

EXTENSION TO THE SLIT IN A THICK CONDUCTING SCREEN

Studies in aperture diffraction theory have almost entirely been confined to slits or slots in thin screens. A comprehensive review of the literature on the subject shows that only a very few investigations have been concerned with slits or slots in thick screens [30,31,33]. However, finite screen thickness is found to have large effects on performance of numerous practical microwave structures [43,65] and may be used to advantage as a design parameter. Thus a study of the effect of thickness would be useful in spite of the difficulties involved in the mathematical analysis. These difficulties arise because conventional methods of approach cannot be readily extended. Thus, the geometrical theory of diffraction is inconvenient to apply because of the four scattering centres and large number of edge-edge interactions involved, unless a reduction of the number of scattering centres is achieved. Moreover, ray theory is restricted to the case of large screen thickness because of the inherent asymptotic approximations involved. These difficulties may be largely overcome by using the equivalent edge concept as discussed in Chapter II, thus leading to two rather than four scattering centres.

Similar problems have been attempted in the past by a number of investigators in connection with waveguide coupling structures containing thick slits or slots. The analytical approach has been mainly based on the variational method [42,66,67], the integral equation method [45] or

extensions of Bethe's theory [40], and has been mainly confined to slit or slot dimensions very small compared to the wavelength. More recently, Budach [32] presented an approximate solution for an acoustic plane wave incident on a thick slit which is also valid only for slit dimensions very small compared to wavelength. Lehman [33] used the analytic properties of finite Fourier transforms to show that the electromagnetic field distributions for a thick slit can be obtained by solving a single variable Fredholm equation of the second kind. His numerical approach, though restricted to the case of a symmetrical excitation (i.e. two plane waves illuminating the slit symmetrically at angles θ and $-\theta$), spans the Rayleigh to geometrical optics range. However, since the approach is numerical, there is a lack of physical insight into the mechanism of diffraction leading to a very limited application of the results obtained.

The purpose of this chapter is to utilize the results of the tandem slit configuration given in Chapter II to obtain a solution of the thick slit problem in a ray optical form. The solution, which employs simple diffraction coefficients assigned to each thick half plane, is shown to be applicable to a large number of related problems.

Since it is our aim to obtain the solution in a ray-optical form, the results for the diffraction of an E-polarized plane wave by a thick half plane are obtained first.

3.1 Diffraction by a Thick Half Plane (E-Polarization)

The diffraction of a plane wave by a half plane was first investigated by Sommerfeld [68] by a method which involved the use of

Riemann surfaces, and was subsequently analysed by Copson [69] using the Wiener-Hopf technique. Since then, several modifications of the original half plane problem have been investigated by the same technique [70-72]. An assumption common to all these investigations is that the half plane is infinitely thin. The difficulty in considering the finite thickness arises from the fact that the conventional Wiener-Hopf technique cannot be directly applied.

Hanson [34] apparently was the first to investigate the thick half plane problem. Under the assumption that $kb << 1$, where k is the free space wave number and $2b$ is the thickness of the half plane, he was able to obtain a solution correct to the zeroth order in kb. This solution resembles that of a parallel plate waveguide which is also solvable by the Wiener-Hopf technique. Harden in 1952 [36] gave extensive experimental data on the diffraction by a half plane of finite thickness as well as finite conductivity. In 1953 Jones [35] formulated the thick half plane problem in terms of two equations of the Wiener-Hopf type, which, however, could not be solved by standard techniques. He obtained an approximate solution by reducing the equations to two sets of infinite linear simultaneous equations. Under the assumption that $kb << 1$, the two sets of equations could be truncated and an approximate solution obtained. Jones has also shown that when the thickness of a half plane is less than a tenth of a wavelength (λ) and when the incident plane wave is H-polarized, the half plane behaves as a combination of a semi-infinite waveguide with a magnetic line source at the open end. Furthermore, he showed that for the E-polarization

case the thick half plane behaves as a parallel plate waveguide when $2b < \lambda/10$.

In 1968 Lee and Mittra [37] solved the problem of a thick half plane for the H-polarization in terms of a highly convergent Neumann series using scattering matrices. The matrices were formulated on the basis of the well-known Wiener-Hopf solution for the problem of diffraction and radiation by a semi-infinite parallel plate waveguide.

To introduce their approach, consider a perfectly conducting parallel-plate waveguide placed at $x < 0$ $|y| \leq b$ as shown in Fig. 3.1. It is assumed that the medium inside the waveguide is filled with a dielectric which has a dielectric constant ε_r and is recessed from the aperture by a distance δ. Let an E-polarized plane wave

$$\phi_i = e^{-ikx\cos\theta_o - iky\sin\theta_o} \tag{3.1}$$

be incident on the plates. The time dependence $\exp(-i\omega t)$ has again been suppressed. When this wave arrives at junction 1, part of its amplitude is reflected into region A (denoted by $S_1^{AA}\phi_i$) and the remaining part is transmitted into region B (denoted by $S_1^{BA}\phi_i$). The wave $S_1^{BA}\phi_i$ progresses towards junction 2 where it is scattered. The result is a transmitted wave $S_2^{CB}S_1^{BA}\phi_i$ and a reflected wave $S_2^{BB}S_1^{BA}\phi_i$. The reflected wave travels in the positive x direction and is scattered again at junction 1. This process of multiple scattering continues indefinitely. The contributions in region A are summed and we have, for the scattered field ϕ

$$\phi = \left\{S_1^{AA} + S_1^{AB}\, S_2^{BB}\, S_1^{BA} + S_1^{AB}\, S_2^{BB}\, S_1^{BB}\, S_2^{BB}\, S_1^{BA} + \ldots\right\}\phi_i \tag{3.2}$$

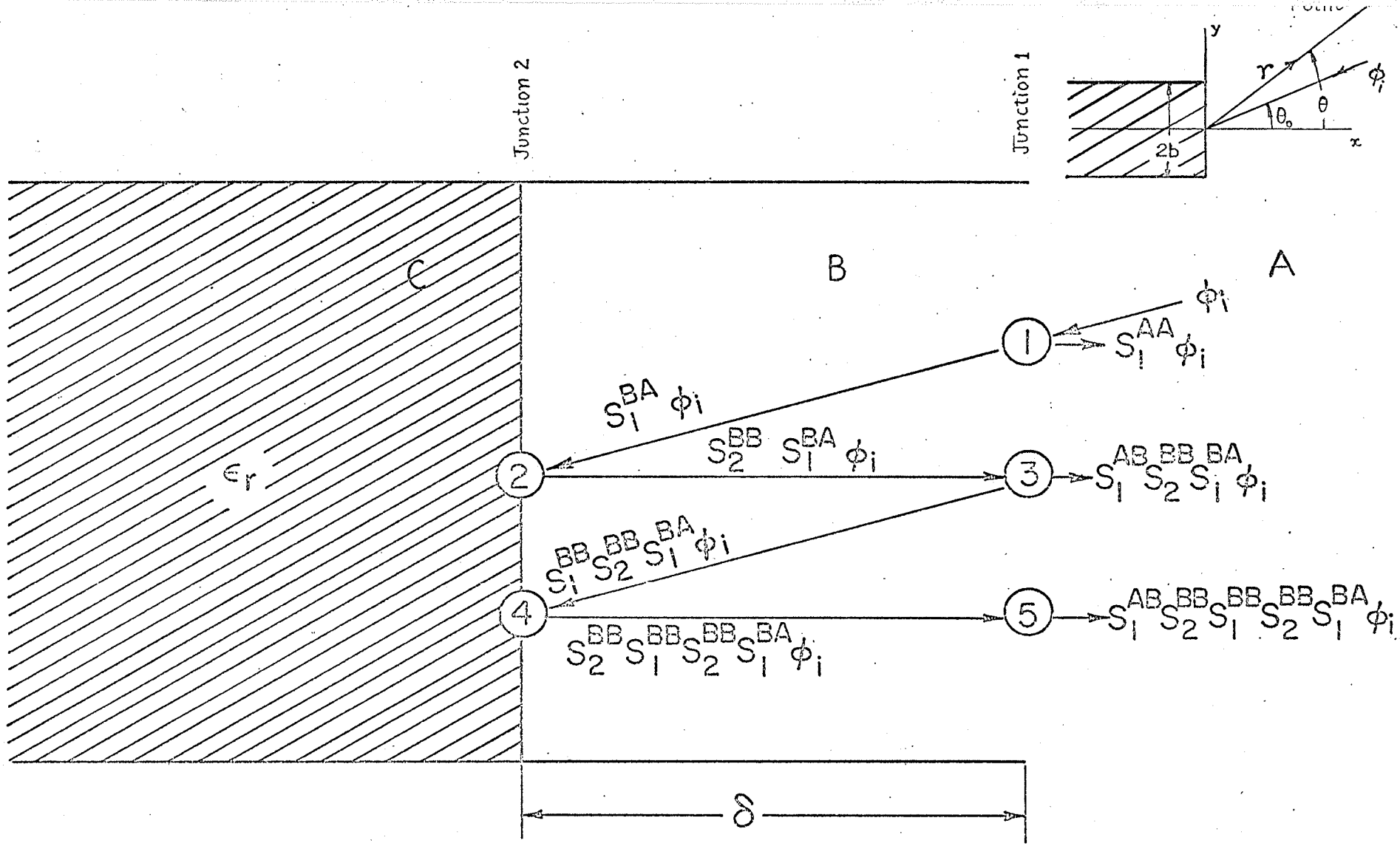

Figure 3.1 Diagram of scattered waves due to multiple scattering at various junctions in a recessed dielectric loaded parallel plate waveguide.

$$= \left\{ S_1^{AA} + S_1^{AB} S_2^{BB} \left(1 - S_1^{BB} S_2^{BB}\right)^{-1} S_1^{BA} \right\} \phi_i \qquad (3.3)$$

Upon letting $\delta \to 0$ and $\varepsilon_r \to \infty$, (3.3) becomes the formally exact solution of the thick half plane problem. We will now determine the explicit expressions for each of these matrices for the case of an E-polarized incident plane wave. The corresponding expressions for the H-polarization case are given by Lee and Mittra.

It is seen by reference to Fig. 3.1 that S_1^{AA} is related to the scattered field in the open region due to an E-polarized plane wave incident on a parallel plate waveguide. This field has already been determined in connection with the tandem slit problem in terms of ϕ_{sep} which represents the field of two such parallel plate waveguides (p. 37). Thus we have

$$S_1^{AA}\phi_i = a(\theta_o,\theta) \frac{e^{i(kr-\pi/4)}}{(2\pi kr)^{\frac{1}{2}}} \qquad \theta \neq \pm (\pi - \theta_o) \qquad (3.4)$$

where

$$a(\theta_o,\theta) = \frac{2i \cos(\theta_o/2)\cos(\theta/2)}{\cos\theta_o + \cos\theta} \left\{ - \frac{\cos(kb \sin\theta_o)\cos(kb \sin\theta)}{K_+(k \cos\theta_o)K_+(k \cos\theta)} \right.$$

$$\left. + \frac{i \sin(kb \sin\theta_o)\sin(kb \sin\theta)}{L_+(k \cos\theta_o)L_+(k \cos\theta)2kb \cos(\theta_o/2)\cos(\theta/2)} \right\} \qquad (3.5)$$

The elements of the scattering matrix S_1^{BA} are related to the scattered mode coefficients inside the parallel plate waveguide due to an E-polarized incident plane wave. These coefficients have been evaluated in connection with the tandem slit problem (see Appendix D). Thus the expression for the field transmitted inside the waveguide is

given by

$$E_z = \sum_{n=1}^{\infty} c_n \sin\left[\frac{n\pi}{2b}(y - b)\right] e^{\gamma_n x} \tag{3.6}$$

where the mode coefficients c_n are given by

$$c_n(\theta_o) = \begin{cases} \dfrac{-2b \cos(kb \sin\theta_o)(k + k\cos\theta_o)^{\frac{1}{2}}(i\gamma_n - k)^{\frac{1}{2}}}{n\pi\, K_+(k\cos\theta_o)(i\gamma_n - k\cos\theta_o)K_-^{(1)}(i\gamma_n)} & ; n = 1,3,5 \\ \dfrac{2i \sin(kb \sin\theta_o)}{n\pi(i\gamma_n - k\cos\theta_o)L_+(k\cos\theta_o)L_-^{(1)}(i\gamma_n)} & ; n = 2,4,6 \end{cases} \tag{3.7}$$

and

$$K_-^{(1)}(i\gamma_n) = \frac{\partial}{\partial\alpha} K_-(\alpha)\Big|_{\alpha=i\gamma_n} \tag{3.8}$$

$$L_-^{(1)}(i\gamma_n) = \frac{\partial}{\partial\alpha} L_-(\alpha)\Big|_{\alpha=i\gamma_n}$$

$$\gamma_n = + \left[\left(\frac{n\pi}{2b}\right)^2 - k^2\right]^{\frac{1}{2}} \quad \text{or} \quad - i\left[k^2 - \left(\frac{n\pi}{2b}\right)^2\right]^{\frac{1}{2}} \tag{3.9}$$

It is easy to recognize that

$$S_1^{BA}\phi_i = \left[c_o, c_1, c_2 \ldots\right]^T \quad , T = \text{transpose operator} \tag{3.10}$$

Thus S_1^{BA} is an (Nx1) matrix, where N denotes the infinite number of modes inside the waveguide.

To find the explicit expression for S_2^{BB} we consider junction 2 which simply corresponds to the junction of two dissimilar homogeneous, dielectric media inside a parallel plate waveguide. If the incident

field is

$$E_z^i = \sin\left[\frac{m\pi}{2b}(y - b)\right] e^{\gamma_m x} \quad , \tag{3.11a}$$

then the reflected field is given by

$$E_z^{BB} = \sum_{n=1}^{\infty} f_{nm} \sin\left[\frac{n\pi}{2b}(y - b)\right] e^{-\gamma_n x} \tag{3.11b}$$

where

$$f_{nm} = \begin{cases} \dfrac{\gamma_n - \gamma_n'}{\gamma_n + \gamma_n'} & , \text{ if } m = n \\ \\ 0 & , \text{ if } m \neq n \end{cases} \tag{3.12}$$

$$\gamma_n' = +\sqrt{\left(\frac{n\pi}{2b}\right)^2 - \varepsilon_r k^2} \quad \text{or} \quad -i\sqrt{\varepsilon_r k^2 - \left(\frac{n\pi}{2b}\right)^2} \tag{3.13}$$

In terms of scattering matrix notation, one can identify S_2^{BB} by

$$S_2^{BB} = \left[f_{mn}\right]_{NxN} \tag{3.14}$$

Also f_{mn} is a diagonal matrix of order NxN and is therefore of infinite order.

S_1^{AB} is related to the problem of radiation from a parallel plate waveguide. The solution to this problem is given by Noble [38], p. 108. Thus for a TE_{m0} mode

$$E_z^i = \sin\left[\frac{m\pi(y - b)}{2b}\right] e^{-\gamma_m x} \tag{3.15}$$

incident from the parallel plate region and of normalized amplitude, the diffracted field outside the waveguide is found to be

$$\phi = \frac{m}{4b} \frac{K_+(i\gamma_m)}{(i\gamma_m + k)^{\frac{1}{2}}} \int_{-\infty+i\tau}^{\infty+i\tau} \frac{K_+(\alpha)}{(\alpha + i\gamma_m)(\alpha + k)^{\frac{1}{2}}} e^{\gamma(b-|y|)-i\alpha x} \, d\alpha \quad ; \quad m = 1,3,5... \tag{3.16}$$

$$\phi = \pm \frac{m}{4i} L_+(i\gamma_m) \int_{-\infty+i\tau}^{\infty+i\tau} \frac{L_+(\alpha)}{(\alpha + i\gamma_m)} e^{\gamma(b-|y|)-i\alpha x} \, d\alpha \quad ; \quad m = 2,4,6... \tag{3.17}$$

$$-k_2 < \tau < k_2 \ , \ |y| > b$$

where the upper and lower signs correspond to $y \geq b$ and $y \leq -b$, respectively. Evaluation of these integrals by the method of steepest descent yields

$$\phi = \frac{e^{i(kr-\pi/4)}}{(2\pi kr)^{\frac{1}{2}}} e_m(\theta) \quad , \quad kr \to \infty \tag{3.18a}$$

where

$$e_m(\theta) = \begin{cases} \dfrac{m\pi \cos(\theta/2) K_+(i\gamma_m) \cos(kb \sin\theta) k^{\frac{1}{2}}}{\sqrt{2}\, b (k + i\gamma_m)^{\frac{1}{2}} (i\gamma_m - k\cos\theta) K_+(k\cos\theta)} \quad ; \quad m = 1,3,5... \\ \dfrac{m\pi \, L_+(i\gamma_m) \sin(kb \sin\theta)}{2b \, i(i\gamma_m - k\cos\theta) L_+(k\cos\theta)} \quad ; \quad m = 2,4,6... \end{cases} \tag{3.18b}$$

Thus, we may identify

$$S_1^{AB} = \frac{e^{i(kr-\pi/4)}}{(2\pi kr)^{\frac{1}{2}}} \left[e_o, \ e_1, \ e_2 \ \ldots \right]^T \tag{3.19}$$

Similar to S_1^{BA}, S_1^{AB} is also an infinitely large column matrix.

The matrix S_1^{BB} is associated with the reflected field inside the waveguide due to an incident field given by (3.15). The problem

has been solved by Noble [38], p. 108 and we have

$$\phi = \frac{m}{4b} \frac{K_+(i\gamma_m)}{(k + i\gamma_m)^{\frac{1}{2}}} \int_{-\infty+i\tau}^{\infty+i\tau} \frac{K_+(\alpha)}{(\alpha + i\gamma_m)(\alpha + k)^{\frac{1}{2}}} \frac{\cosh \gamma y}{\cosh \gamma b} e^{-i\alpha x} \, d\alpha$$

$$- b \leq y \leq b \ , \ m = 1,3,5... \tag{3.20}$$

$$\phi = \frac{m}{4i} L_+(i\gamma_m) \int_{-\infty+i\tau}^{\infty+i\tau} \frac{L_+(\alpha)\sinh \gamma y}{(\alpha + i\gamma_m)\sinh \gamma b} e^{-i\alpha x} \, d\alpha$$

$$(- b \leq y \leq b) \ , \ m = 2,4,6... \tag{3.21}$$

In the region $-b \leq y \leq b$, $x < 0$, we can close the contour in the upper half plane. It is found that there are no branch points in this region and an infinite number of poles at the roots of $L_-(\alpha) = 0$ or $K_-(\alpha) = 0$. Evaluating the integrals in (3.20) and (3.21), we have for the reflected field

$$E_z = \sum_{n=1}^{\infty} d_{nm} \sin\left[\frac{n\pi(y - b)}{2b}\right] e^{\gamma_n x} \tag{3.22a}$$

where

$$d_{nm}\Big|_{m \text{ odd}} = \begin{cases} \dfrac{- i \, m\pi \, K_+(i\gamma_m)}{2b(k + i\gamma_m)^{\frac{1}{2}}(k + i\gamma_n)^{\frac{1}{2}}(\gamma_m + \gamma_n)K_-^{(1)}(i\gamma_n)} \ ; & n = 1,3,5... \\ \\ 0 \quad ; \quad & n = 2,4,6... \end{cases} \tag{3.22b}$$

$$d_{nm}\Big|_{m \text{ even}} = \begin{cases} 0 \quad ; & n = 1,3,5\ldots \\ \dfrac{-\,im\, L_{+}(i\gamma_m)}{n(\gamma_m + \gamma_n)L_{-}^{(1)}(i\gamma_n)} \quad ; & n = 2,4,6\ldots \end{cases} \tag{3.22c}$$

Thus one may identify

$$S_1^{BB} = \left[d_{nm}\right]_{NxN}$$

Before calculating the diffraction pattern, it is desirable to summarize and rearrange the results obtained in (3.1) to (3.22). Since we are interested in the far field ϕ, we may write

$$\phi = \frac{e^{i(kr-\pi/4)}}{(2\pi kr)^{\frac{1}{2}}} P(\theta_o,\theta) \qquad kr >> 1 \tag{3.23}$$

where the far field diffraction pattern (or coefficient) is given by

$$P(\theta_o,\theta) = a(\theta_o,\theta) + \{e_n\}^T[f_{nm}](I - [d_{nm}][f_{nm}])^{-1}\{c_n\} \tag{3.24}$$

where { } signifies (Nx1) column vector, [ ] signifies (NxN) square matrix, and I is an (NxN) identity matrix. To be exact one has to let $N \to \infty$ and, consequently, $(I - [d_{nm}][f_{nm}])$ is a matrix of infinite order. As yet no method is available for inverting the matrix in a closed form. However, it has been demonstrated in a large number of examples [37] that accurate computations of a form similar to (3.24) are possible for a finite N. Even for $N = 1$ the results have been found to be quite close to the limiting values [37]. Thus if we retain only one term and let $\varepsilon_r \to \infty$, the E-polarization diffraction pattern $P(\theta_o,\theta)$ for a thick half plane is given by

$$P(\theta_o,\theta) = a(\theta_o,\theta) - \frac{e_1(\theta)c_1(\theta_o)}{1 + d_{11}} \tag{3.25}$$

Fig. 3.2 shows the typical calculated diffraction patterns, based on (3.25), of a thick half plane due to an E-polarized plane wave for various angles of incidence (θ_o) and screen thickness $(2kb)$. It was found that the difference between $P(\theta_o,\theta)$ and $a(\theta_o,\theta)$ was negligible for $2kb < 1$ (which also corresponds to $2b < \lambda/10$) as predicted by Jones [35]. The results indicate that the pattern is relatively insensitive to the effect of thickness in the neighbourhood of the geometrical shadow boundaries $\theta = \pm(\theta_o - 180°)$, as expected. The insensitivity is caused by the first term in (3.25) which gives the dominant contribution whereas the second term, representing the thickness effect, becomes relatively small in magnitude. However, the effect of increasing the thickness is clearly seen along the direction $\theta = 0°$. The scattered field along this direction shows a distinct increase with increase of kb. Of particular interest is the peak in the patterns which tends to coincide with $\theta = -\theta_o$ as the thickness increases. For example, for a half plane of electrical thickness 2 radians, the peak occurs at $\theta = -22°$ for $\theta_o = 30°$, while the same peak shifts to $\theta = -42°$ when $\theta_o = 50°$. This is to be expected, since for the limiting case of an infinitely thick half plane, the reflected field by geometrical optics should occur at $\theta = -\theta_o$.

3.2 Diffraction by a Thick Slit

The scattering matrix technique as well as the solution of the tandem slit given in the previous chapter are utilized to find the

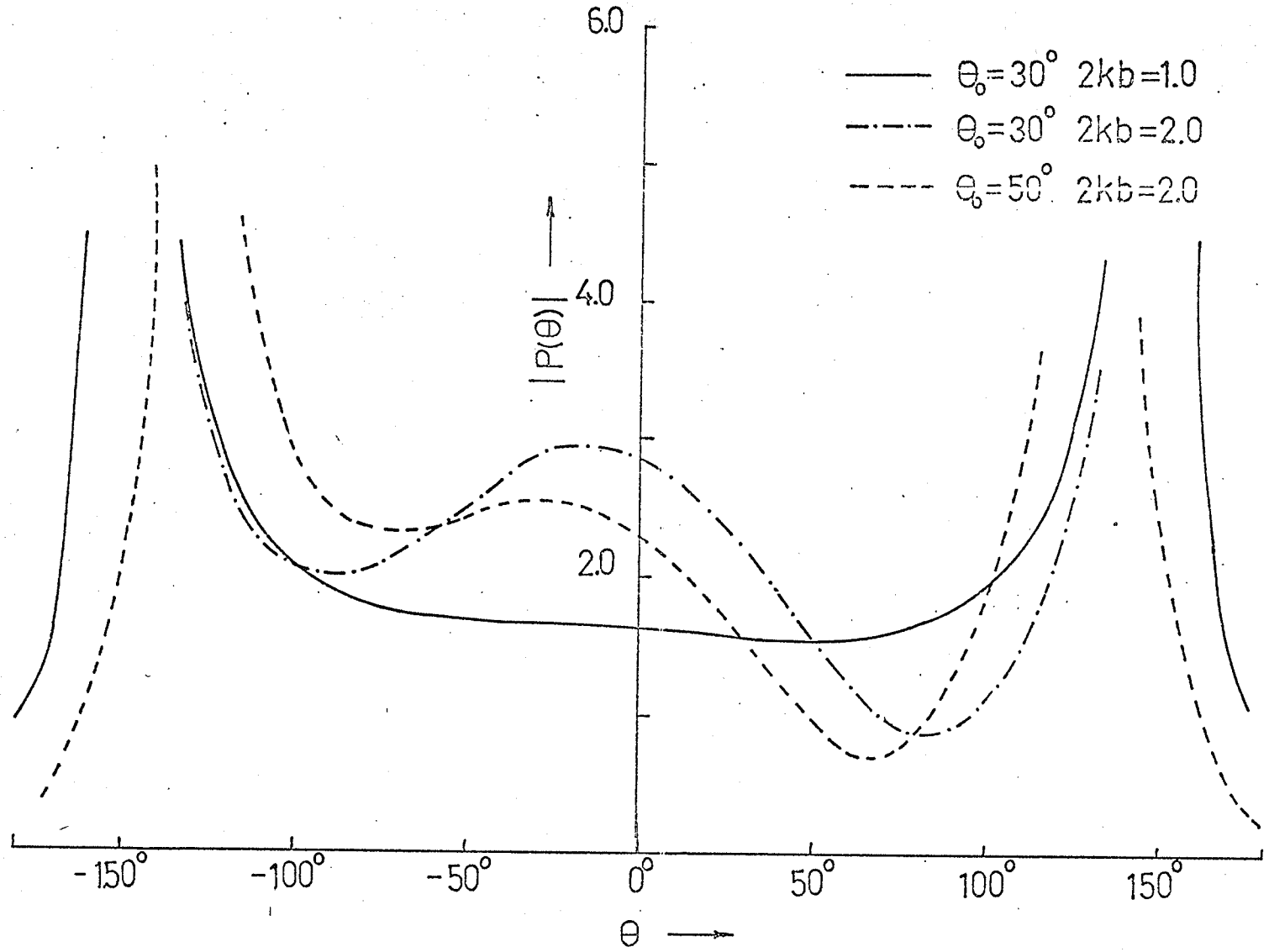

Figure 3.2 Scattering patterns of half planes of various thicknesses

diffraction by a slit in a thick conducting screen. The expression for the total field can again be written as the sum of non-interaction (ϕ^t_{sep}) and interaction (ϕ^t_{int}) terms. ϕ^t_{sep} is obtained by adding the contribution from the two thick half plane edges when assumed to be isolated from each other. The computation of this term is carried out in a ray-optical sense employing the diffraction coefficient for a thick half plane derived in the previous section.

For the derivation of ϕ^t_{int}, the diffraction from a tandem slit is utilized as the first term in the series solution (3.2) for the diffraction by a dielectric-loaded tandem slit, where each parallel plate waveguide is filled by a dielectric slab (of relative permittivity ε_r and recessed from the aperture by a distance δ) as shown in Fig. 3.3. The second and higher order terms are due to reflections at the air dielectric interfaces and are essentially similar to the terms derived in the last section except for one basic modification. The coefficients of the modes excited in either waveguide due to the incident plane wave, which are related to the matrix elements S_1^{BA}, are modified by the addition of the interaction mode coefficients (2.105) due to the presence of the other waveguide. To obtain the solution for the diffraction by a slit in a thick conducting screen, we let $\delta \to 0$ and $\varepsilon_r \to \infty$. This procedure leads to the relation

$$\phi^t = \phi^t_{sep} + \phi^t_{int} \tag{3.26}$$

where

$$\phi^t_{sep} = \frac{e^{i(kr-\pi/4)}}{(2\pi kr)^{\frac{1}{2}}} \left\{ e^{ikd(\cos\theta_o+\cos\theta)} P(\theta_o,-\theta) \right.$$

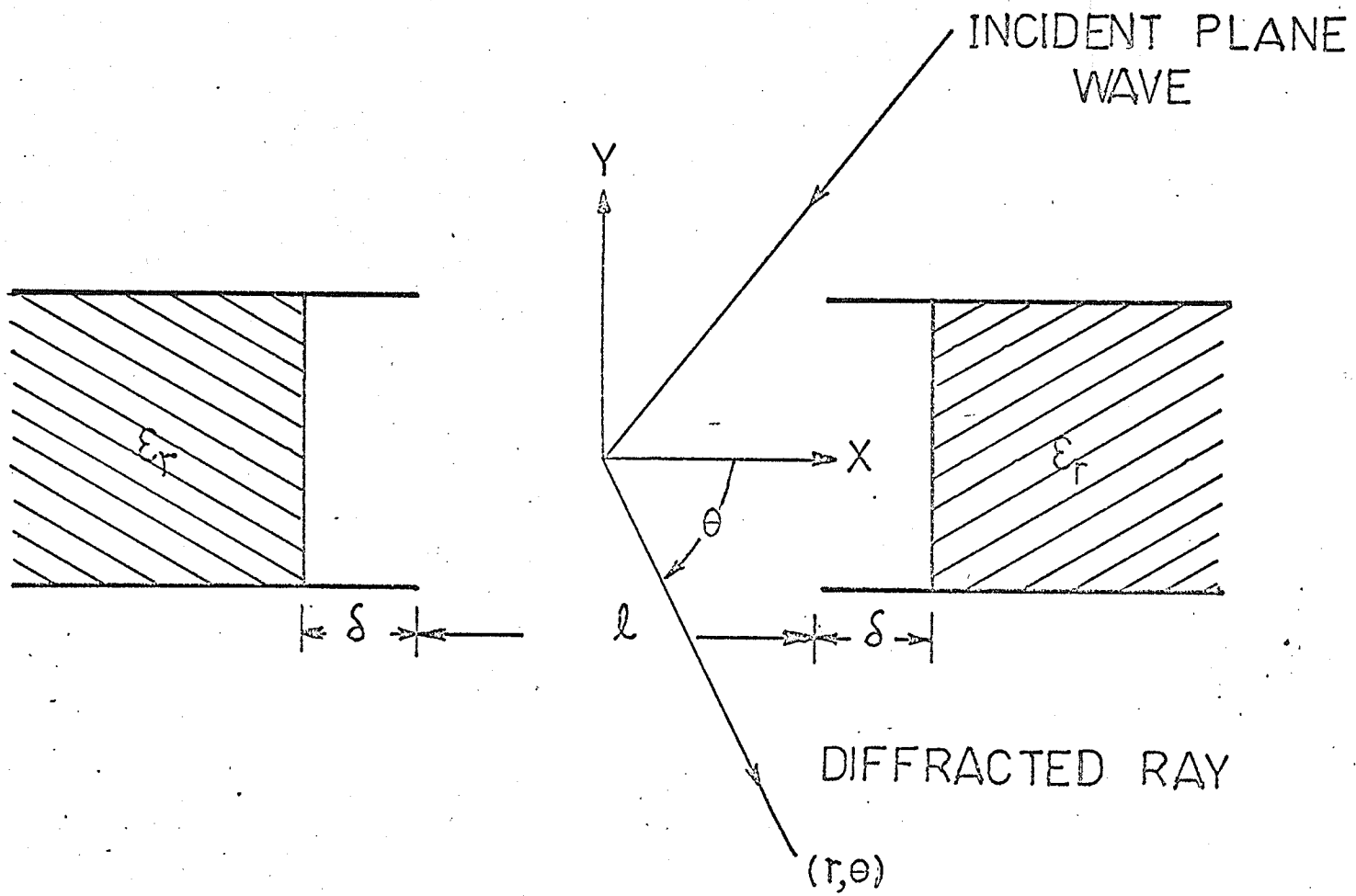

Figure 3.3 Tandem slit loaded with a recessed dielectric.

$$+ e^{-ikd(\cos\theta_o + \cos\theta)} P(\pi - \theta_o, \theta - \pi)\Big\} \tag{3.27}$$

and $P(\theta_o,\theta)$ is the diffraction coefficient due to an E-polarized plane wave incident on the thick half plane derived in the previous section. The expression for ϕ^t_{int} is similar to (2.93) and for large ℓ (or 2d) is given by

$$\phi^t_{int} = \frac{e^{i(kr-\pi/4)}}{(2\pi kr)^{\frac{1}{2}}} \frac{K_+^2(k)F_1(\ell)\left[1 + F_2(b,\ell)\right]}{1 + \{F_1(\ell)\left[1 + F_2(b,\ell)\right]\}^2}$$

$$\cdot \left[\phi^t_a + \phi^t_b + F_1(\ell)\left[1 + F_2(b,\ell)\right](\phi^t_c + \phi^t_d)\right] \tag{3.28}$$

where F_1, F_2 are given by (2.95) and

$$\phi^t_a = e^{ikd(\cos\theta_o - \cos\theta)} a(\theta_o,0)a(0,\theta - \pi)$$

$$\cdot \left[1 - \frac{e_1(0)c_1^1(\theta_o)}{(1 + d_{11})a(\theta_o,0)}\right]\left[1 - \frac{e_1(\theta - \pi)c_1^2(0)}{(1 + d_{11})a(0,\theta - \pi)}\right] \tag{3.29}$$

$$\phi^t_b = e^{-ikd(\cos\theta_o - \cos\theta)} a(\pi - \theta_o,0)a(0,-\theta)$$

$$\cdot \left[1 - \frac{e_1(0)c_1^1(\pi - \theta_o)}{(1 + d_{11})a(\pi - \theta_o,0)}\right]\left[1 - \frac{e_1(-\theta)c_1^3(0)}{(1 + d_{11})a(0,-\theta)}\right] \tag{3.30}$$

$$\phi^t_c = -ie^{ikd(\cos\theta_o + \cos\theta)} a(\theta_o,0)a(0,-\theta)$$

$$\cdot \left[1 - \frac{e_1(0)c_1^1(\theta_o)}{(1 + d_{11})a(\theta_o,0)}\right]\left[1 - \frac{e_1(-\theta)c_1^3(0)}{(1 + d_{11})a(0,-\theta)}\right] \tag{3.31}$$

$$\phi_d^t = -ie^{-ikd(\cos\theta_o+\cos\theta)} a(\pi-\theta_o,0)a(0,\theta-\pi) \cdot \left[1 - \frac{e_1(0)c_1^1(\pi-\theta_o)}{(1+d_{11})a(\pi-\theta_o,0)}\right]\left[1 - \frac{e_1(\theta-\pi)c_1^2(0)}{(1+d_{11})a(0,\theta-\pi)}\right] \quad (3.32)$$

Here $a(\theta_o,\theta)$ is the parallel plate waveguide diffraction coefficient due to an E-polarized plane wave and is given by (3.5). $e_n(\theta)$ and d_{nm} are given by (3.18) and (3.22). c_n^1, c_n^2, c_n^3 represent the total (non-interaction and interaction) mode coefficients inside the parallel plate waveguide and are given by

$$c_n^1(\theta_o) = c_n^{sep}(\theta_o) + c_n^{int}(\theta_o) \quad (3.33a)$$

$$c_n^2(0) = c_n^{sep}(0) + c_n^{int}(\pi-\theta_o) \quad (3.33b)$$

$$c_n^3(0) = c_n^{sep}(0) + c_n^{int}(\theta_o) \quad (3.33c)$$

where c_n^{sep} and c_n^{int} are given by (2.104) and (2.105). The above expressions do not take ϕ''_{int} into account since it is negligible for $2b/\ell \lesssim 0.5$ which is the practical case of interest.

Examination of these results shows that for $b \to 0$ the asymptotic solution (3.26) reduces to that obtained by Karp and Russek [3] and Keller [2] for the case of a wide slit in a thin conducting screen. However, without the asymptotic approximation, our solution may be shown, with the aid of Babinet's principle, to lead to the same expression as given by Yu and Rudduck [4] for the complementary strip problem.

It may also be shown that if the interaction mode coefficients c_n^{int} are neglected, the solution reduces to that of a thin screen except for two modifications. The first is that the diffraction

coefficient for a thin half plane is replaced by that of a thick half plane. The second is the same as the second modification mentioned in the previous chapter in connection with the tandem slit problem (p. 42).

Finally, it should be noted that when $kb << \pi/2$, the solution for the thick slit reduces to that for the tandem slit, as expected, since the parallel plate waveguides in the tandem slit configuration would be operating below cutoff.

3.3 Experimental and Numerical Results

In order to verify the validity of our approximate solution for the slit in a thick conducting screen, an experiment was conducted (for normal plane wave incidence) at 10 GHz for slit widths of 2,4,6 and 8 cm and thicknesses of 0.125, 1, 2 and 4 cm. In each case, each half of the slit was constructed from aluminum plates of dimensions 40λ (length) x 30λ (width) x $2b$ (thickness). These dimensions were dictated by the size of the quiet zone of a large microwave anechoic chamber where the experiment was conducted. Fig. 3.4 shows part of the experimental setup where the slit assembly along with the transmitter was rotated around the vertical axis while the receiver was fixed at appropriate far field distance from the slit. Using an antenna positioner and a pattern recorder, initial measurements were taken at $2d = 0$ to determine the error due to the outer edges of the plates within the complete range of the polar angle θ (Fig. 3.5). It was found that the error was negligible for $-40° \leq \theta \leq +40°$ since the received signal was in the noise level of the measuring equipment in

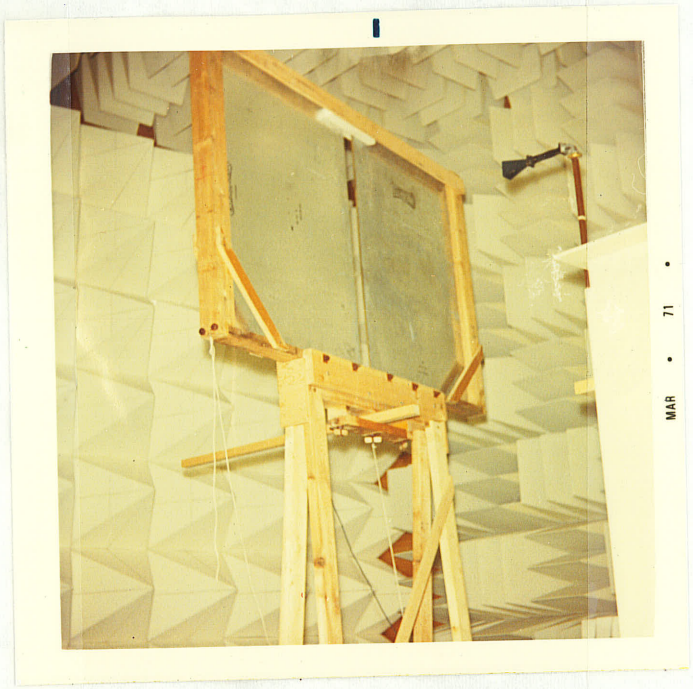

Fig. 3.4 Experimental setup for thick slit pattern measurement

this range. Outside this range, undesirable signals were obtained because the outer edges of the screens were too close to the receiver. Fig. 3.5 shows typical patterns (for normal plane wave incidence) compared with theory while the essential experimental data from the rest of the patterns are summarized and compared with theory in Tables 3.1 and 3.2.

3.4 Discussion of the Results

In this chapter we have investigated the diffraction of an E-polarized plane wave by a slit in a thick conducting screen. For this, the Wiener-Hopf solution of the tandem slit problem presented in Chapter II is employed. This solution, which is the first term of a scattering matrix series and compares favourably with Alldredge's variational and experimental results [46], is used to solve the thick slit problem, thus extending the method of Lee and Mittra [37]. Using the equivalent edge concept, the analytical results for large slit widths reduce to a simple ray-optical form similar to that of Keller for the thin slit [2]. For smaller values of slit width, the formulation leads to results which are identical to those of Yu and Rudduck [4] for the complementary thin strip problem. Furthermore, our approximate solutions agree favourably with experiment for $2b/\ell \lesssim 0.5$ and reduce asymptotically to Keller's solution for $b \to 0$.

Examination of Fig. 3.5 and Tables 3.1 and 3.2 indicates that the 6 dB beam width increases as the screen thickness is increased to $2b/\ell \lesssim 0.5$ and then decreases for larger values of this ratio. Also, the first minima shift away from the main beam with increasing

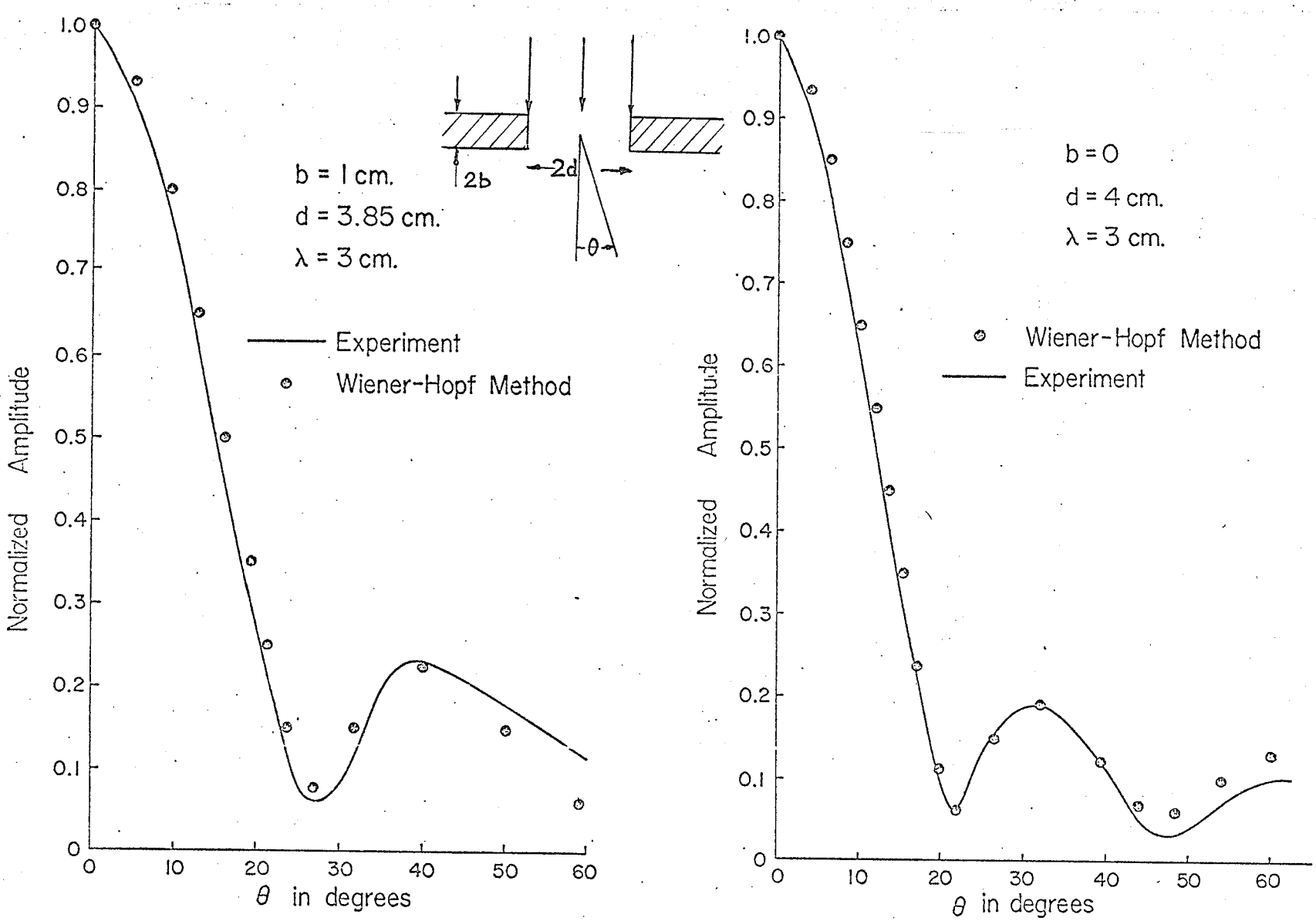

Figure 3.5 Diffraction patterns for various slit widths and screen thicknesses

Table 3.1 6dB Beamwidth vs slit width and thickness

Slit thickness (2kb) \ Slit width (kℓ)	4.18 Experiment	8.36 Theory	8.36 Expt.	12.56 Theory	12.56 Expt.	16.75 Theory	16.75 Expt.
0.125	100°	58°	58°	36°	36°	27°	26°
2.090	101°	62°	57°	40°	38°	30°	28°
4.180	97°	68°	66°	45°	39°	36°	33°
8.360	96°	--	65°	--	46°	--	--

Table 3.2 Main to side lobe ratio and locations of first null and first side lobe for $k\ell = 16.75$

Slit thickness (2kb)	Main to side lobe ratio in dB		Location of first null		Location of first side lobe	
	Theory	Expt.	Theory	Expt.	Theory	Expt.
0.125	11.7	11.7	22°	21°	32°	31°
2.090	11.06	12.0	23°	24°	33°	37°
4.180	10.30	10.0	27°	27°	40°	44°

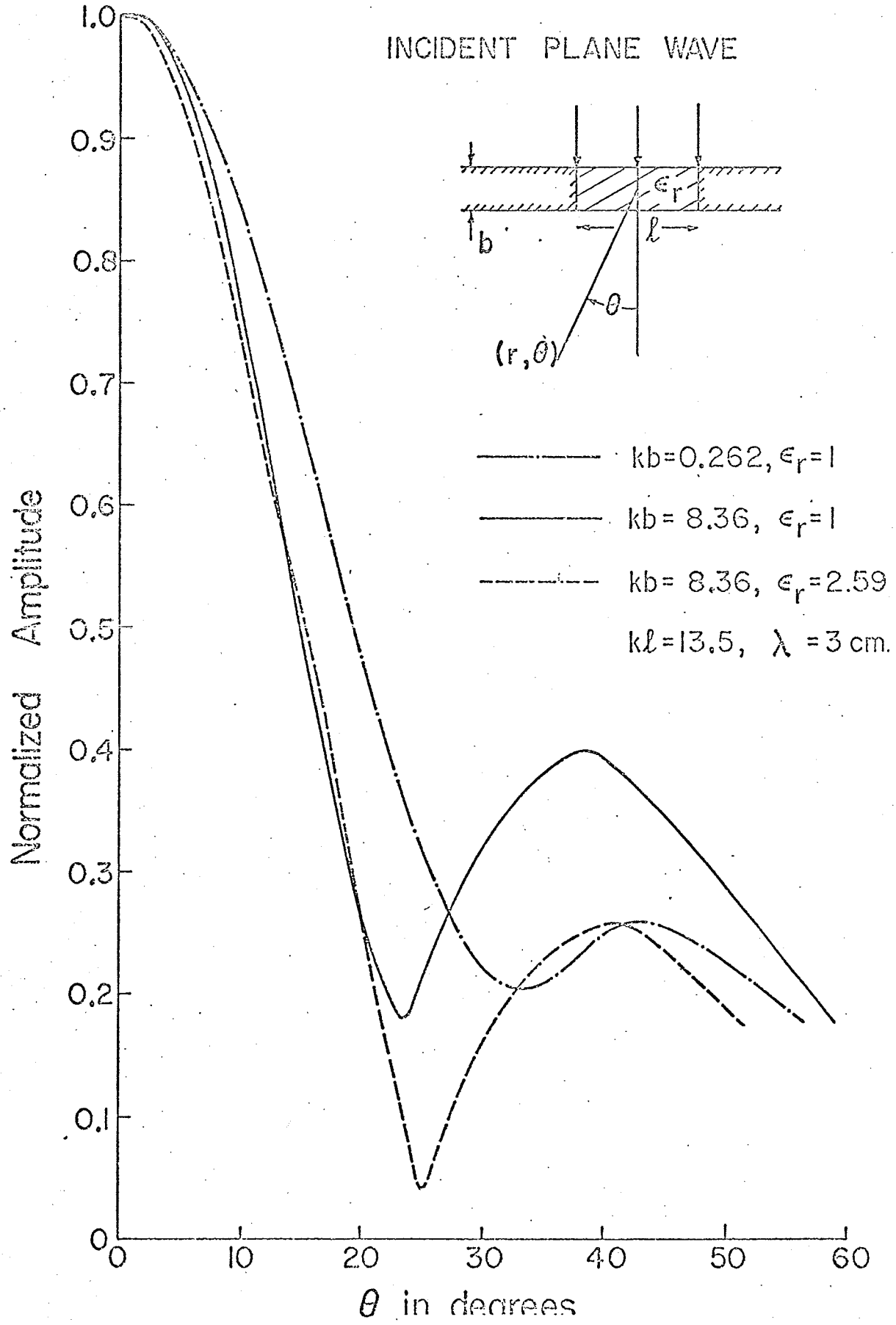

Figure 3.6 Experimental diffraction patterns of a thick slit for an H-polarized plane wave incidence.

Table 3.3 3dB Beamwidth vs slit width and thickness ($\varepsilon_r = 1.0$)

Slit thickness (kb) \ Slit width (kℓ)	4.18	8.36	12.56	16.75
0.262	76°	40°	27.5°	22.5°
2.090	80°	37°	27.0°	21.5°
8.360	76°	37°	21.5°	— —

Table 3.4 Main to side lobe ratio and locations of first null and first side lobe for $k\ell = 16.75$ ($\varepsilon_r = 1.0$)

Slit Thickness (kb)	Main to side lobe ratio in dB	Location of first null	Location of first side lobe
0.262	10.0	25°	29°
2.090	10.2	24°	30°
8.360	8.0	23°	38°

thickness (e.g. for a slit of 6 cm width, the first minimum shifts from 31° to 34° as the thickness varies from 0.125 to 2 cm and from 20° to 27° for a width of 8 cm). On the other hand, the first side lobe level increases with thickness and shifts away from the main beam (e.g. from 11.7 to 10 dB below the main beam for a slit width of 8 cm as the thickness varies from 0.125 to 2 cm. For the same variation, the first side lobe location shifts from 31° to 34°).

One may conclude from these results that in general the effective width of a slit in a thick conducting screen reduces as the screen thickness increases. This fact has been observed by some authors in the past [45] and may be effectively used in the design of waveguide discontinuities and filters [1].

Although we have concerned ourselves mainly with the E-polarization, it may be shown that the H-polarization can be treated in a similar fashion. Some interesting experimental results obtained for the latter case are summarized in Tables 3.3 and 3.4. Fig. 3.6 also shows the effect of loading the aperture by a dielectric slab.

CHAPTER IV

APPLICATION TO THICK WAVEGUIDE DIAPHRAGMS

In this chapter the solution for the far field diffracted by a thick slit is utilized to investigate the scattering properties of various thick waveguide discontinuities. Fig. 4.1 shows a typical transverse thick strip discontinuity located in a parallel plate waveguide of width a. Imaged with respect to the waveguide walls, it leads to an infinite array of strips or slits. The imaged configuration has been solved using the generalized Wiener-Hopf technique [73]. It has also been solved by a ray-optical approach employing the far field scattering properties of a thin strip and a thin slit which are elements of the infinite set [25]. The finite screen thickness of such waveguide discontinuities (e.g. asymmetric and symmetric diaphragms) has a large effect on the performance of various microwave structures and is the main concern of this chapter.

The problem of finite screen thickness of various waveguide coupling structures has been the subject of a number of investigations in the past and has resulted in some interesting observations. Thus the effective width of a thick iris was found to decrease with increasing screen thickness [45,65]. Some approximate solutions have been obtained to account for the effect of thickness. Mumford [39] proposed an empirical formula deduced from experimental results for thick irises. Akhiezer [40] extended Bethe's theory for small holes [41] to include the effect of thickness on the transmission through a

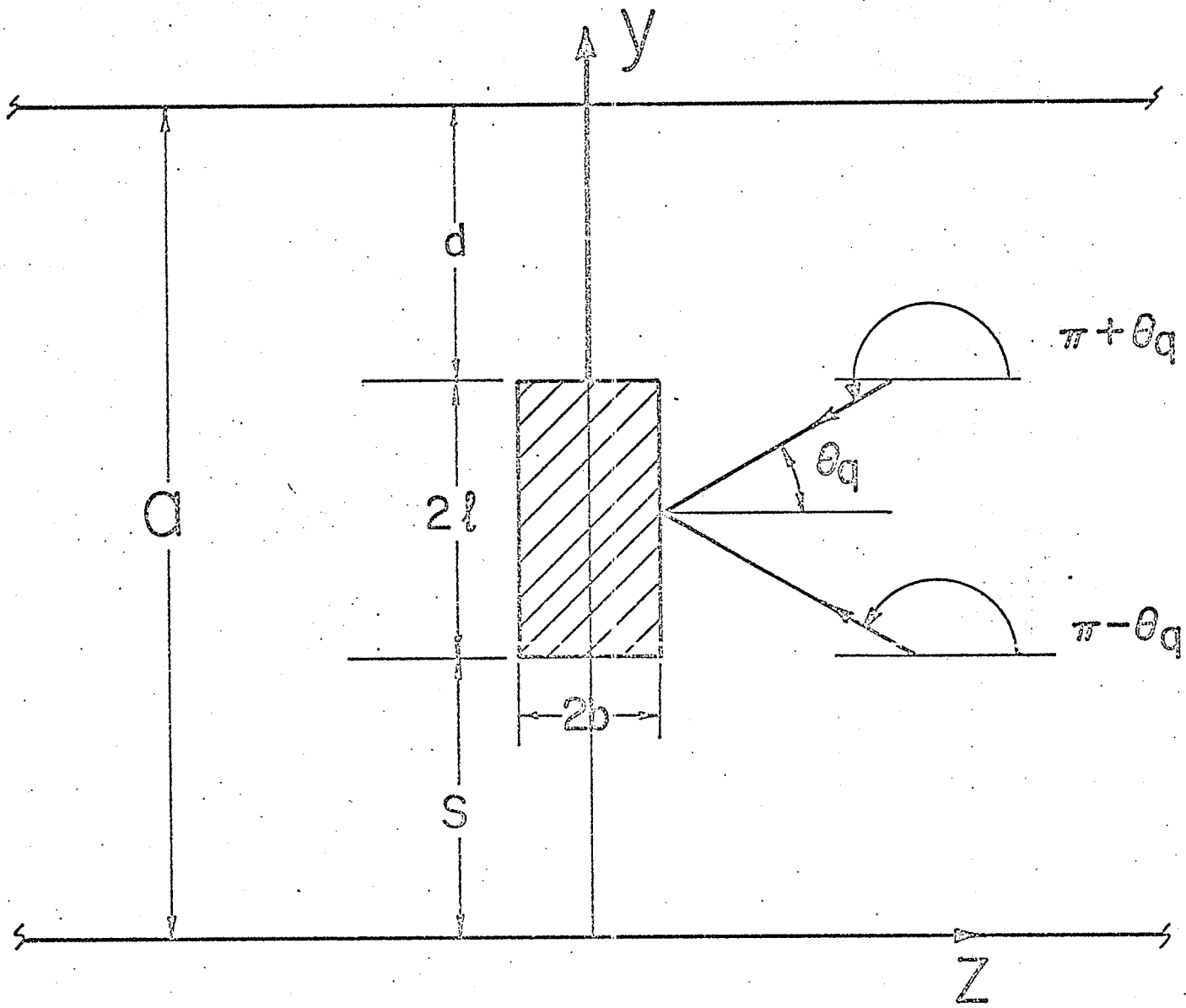

Figure 4.1 Transverse thick strip discontinuity in a waveguide.

waveguide slot. Oliner [42] investigated the properties of a narrow slot and viewed it as a composite structure consisting of a length of waveguide section equal to the slot wall thickness and of cross-sectional dimensions equal to those of the slot. His results are also only valid for apertures with dimensions small compared to the wavelength. Cohn [43] used a conformal mapping technique proposed by Davy [44] and obtained an approximate formula for the capacitance between two infinite plates of finite thickness. The thickness of a capacitive iris was accounted for by considering a line section of certain length and the formulae obtained are applicable only for $2b << \lambda$ and $2b/\ell << 1$ (where $2b$ is the thickness and ℓ the width of the aperture). Garb et al. [45] proposed an integral equation formulation for the fields on both sides of a thick slot connecting two cavities. Though their solution is applicable for any $2b$ to ℓ ratio, it is valid only for both $2b, \ell << \lambda$. Thus most of these investigations are confined to slit or slot dimensions small compared to the wavelength and are mainly confined to the dominant mode range.

Recently, the growing importance of multimode waveguide technology [74] and the accompanying need for the study of waveguide discontinuities has motivated the use of quasi-optical techniques adapted to the high frequency range [75-77] rather than conventional methods [78] which are more suited to the dominant mode range. These techniques utilize quasi-optical ray constructions to determine approximately the field in the discontinuity region and to calculate therefrom the field scattered into various modes. The nature of the

field approximation near the discontinuity determines the accuracy of the calculation of scattered mode amplitudes far from the discontinuity. In contrast, the recent ray-optical approach of Yee and Felsen [25], for dealing with waveguide discontinuities of infinitesimal thickness, employs far field scattering properties of the scattering centres constituting the discontinuity. Although the technique is best suited to the high frequency range (except near the modal cutoffs), it is capable of providing satisfactory results in the range of propagation of only the dominant mode.

It is the purpose of this chapter to apply the solution of the thick slit problem previously obtained to the scattering by an asymmetric waveguide diaphragm of finite thickness and a symmetric diaphragm of infinitesimal as well as finite thickness. Furthermore, the results obtained here have been employed in the analysis and design of waveguide multicavity filters with thick diaphragms as reported elsewhere [1].

4.1 Asymmetric Waveguide Diaphragm

Consider a discontinuity in a waveguide composed of a transverse thick strip as shown in Fig. 4.1. The width and thickness of the strip are denoted by 2ℓ and $2b$, respectively, while the distances from the walls to the upper and lower edges are denoted by d and s, respectively. In order to obtain reasonably accurate results by asymptotic theory, certain restrictions on these dimensions in terms of the waveguide dimension, are necessary as will be discussed later. The results obtained for this structure can be adapted to the case of an asymmetric

diaphragm, as will also be shown later.

In order to formulate this problem, we require the field of a line source in a waveguide. This can be found by the ray-optical approach as shown by Yee, Felsen and Keller [24]. Basically, the field at a point in the waveguide is obtained as the sum of contributions from the rays passing through that point either directly or after multiple scattering at the walls. Alternatively, the ray diagram may be constructed to show the rays from the source as well as its images taken successively with respect to the walls. The result is an infinite set of images whose intensities and locations are determined from the boundary conditions at the walls. Thus consider a line source whose far field is given by

$$U(r,\theta) \sim f(\theta) \frac{e^{i(kr-\pi/4)}}{(2\pi kr)^{\frac{1}{2}}} \quad , \quad kr \to \infty \tag{4.1}$$

where $f(\theta)$ is the pattern function of the line source, θ is measured from the positive z-axis and the time dependence $\exp(-i\omega t)$ has been assumed throughout. If this line source is placed at $y = y'$, $z = 0$ in the waveguide, the infinite set of images are located at

$$y_j^{\pm} = 2ja \pm y' \quad , \quad j = 0, \pm 1, \pm 2 \ldots \tag{4.2}$$

Due to the boundary conditions at a perfectly conducting surface, each of the images at y_j^+ or y_j^- has the radiation pattern $f(\theta_j^+)$ or $-f(-\theta_j^-)$, respectively, where $r_j^{\pm}$ are measured from the jth image to the observation point and $\theta_j^{\pm}$ are the angles between $r_j^{\pm}$ and the positive z-axis. Thus the field $E_x(y,z)$ is given by

$$E_x(y,z) \sim \sum_j \frac{f(\theta_j^+)e^{i(kr_j^+ - \pi/4)}}{(2\pi kr_j^+)^{1/2}} - \sum_j \frac{f(-\theta_j^-)e^{i(kr_j^- - \pi/4)}}{(2\pi kr_j^-)^{1/2}} \tag{4.3}$$

$$= h(y - y', z) - h(-y - y', z) \tag{4.4}$$

Here $h(y,z)$ denotes the field of an array of line sources centred at $y = 0$ with each source having the radiation pattern $f(\theta)$. The explicit expression for $h(y,z)$ has been obtained by Yee, Felsen and Keller [24] as well as Morse and Feshbach [79]. Thus $h(y,z)$ can be written as an infinite sum of modes

$$h(y,z) = \sum_{n=-\infty}^{\infty} C_n(z) e^{i2\pi ny/2a} \tag{4.5}$$

where $C_n(z)$ is obtained by Fourier inversion and simplifies to

$$C_n(z) \sim \frac{e^{-i\pi/4}}{2a(2\pi k)^{1/2}} \sum_{j=-\infty}^{\infty} \int_{-2ja}^{-2(j-1)a} (z^2 + \eta^2)^{-1/4} f(\tan^{-1}\eta/z) e^{ik(z^2+\eta^2)^{1/2} - 2\pi in\eta/2a} \, d\eta \tag{4.6}$$

after the change of variable $\eta = y - 2ja$.

Saddle point evaluation of this integral for large k, leads to

$$h(y,z) \sim \frac{1}{2} \sum_{n=-\infty}^{\infty} (\beta_n a)^{-1} f(\theta_n) e^{ik(y \sin\theta_n + z \cos\theta_n)} \tag{4.7}$$

where $\beta_n = [k^2 - (n\pi/a)^2]^{1/2}$ with $\mathrm{Im}\beta_n \geq 0$ and $\cos\theta_n = (\mathrm{sgn}\ z)\beta_n/k$. Using (4.7) in (4.4), we obtain

$$E_x(y,z) = i \sum_{n=1}^{\infty} \left[f(\theta_n) e^{-in\pi y'/a} - f(-\theta_n) e^{in\pi y'/a} \right] \frac{\sin(n\pi y/a)}{\beta_n a} e^{i\beta_n |z|} \tag{4.8}$$

This is the exact field expression when the line source is located at $y = y'$, $z = 0$ inside the parallel plate waveguide of Fig. 4.1.

Alternatively, it could be obtained by expressing the field of a line source in terms of a Hankel function and applying the Poisson sum formula and the Fourier transform of the Hankel function to find $C_n(z)$ [79]. The resulting integral may be evaluated exactly leading to the same expression as (4.8). The reason why (4.8) is exact in the first case even after two asymptotic approximations is discussed in terms of Floquet's theorem by Hamid and Johnson [80].

The amplitude of a particular mode can be determined from (4.8) and the amplitudes of the pattern function $f(\theta)$ along the characteristic angles $\theta = \pm \theta_n$, which represent the propagation directions of the two modal plane waves constituting the nth waveguide mode.

Let the normalized electric field due to the qth mode, incident on the strip from the right, be given by

$$E_x^i(y,z) = \sin(q\pi y/a)e^{-i\beta_q z} \tag{4.9}$$

which may be decomposed into two plane waves, i.e.

$$E_x^i(y,z) = -(i/2)e^{i(-\beta_q z+q\pi y/a)} + (i/2)e^{i(-\beta_q z-q\pi y/a)} \tag{4.10}$$

where the first and second terms correspond to the two waves which propagate along the $\pi - \theta_q$, $\pi + \theta_q$ directions, respectively. These waves are incident upon the two thick edges of the strip where each thick edge behaves like a line source and is considered as mathematically equivalent to a thin edge with a modified diffraction coefficient as discussed in Chapter III. The fields scattered at this discontinuity may be expressed as

$$E_x^r(y,z) = \sum_{n=1}^{\infty} R_{qn} \sin(n\pi y/a) e^{i\beta_n |z|} \quad , \quad z > 0 \tag{4.11}$$

$$E_x^t(y,z) = \sum_{n=1}^{\infty} \tau_{qn} \sin(n\pi y/a) e^{i\beta_n |z|} \quad , \quad z < 0 \tag{4.12}$$

where the superscripts r and t refer to reflected and transmitted fields, respectively. Furthermore, the subscripts q and n denote the incident and reflected (or transmitted) modes, respectively, with the implication that all modes are TE_{qo} or TE_{no}. In order to calculate the reflection (or transmission) coefficient R_{qn} (or τ_{qn}) we equate (4.11) (or (4.12)) with (4.8). For this, it is required to determine the pattern function $f(\theta_n)$ for the strip along the direction of the nth excited mode. Thus we consider the diffraction of the two incident plane waves (4.10) at the two edges of the strip. Here the total diffracted field consists of the sum of contributions due to primary and secondary diffracted fields. The primary field is due to the initial diffraction of the plane waves at the two edges of the strip. The secondary diffracted field is due to the interaction between the two edges of the strip and also between the edges and the neighbouring waveguide walls. However, the latter contribution dominates since the former is smaller by $0(1/k\ell)$ where $k\ell$ is assumed to be larger than unity. This statement is true only when the strip to waveguide width ratio $(2\ell/a)$ is not appreciably less than 0.5 as was established numerically. By summing these fields and expressing them with respect to the midpoint $(y = s + \ell, z = 0)$, we obtain the pattern function $f(\theta_n)$ needed in (4.8).

Thus the primary field due to initial diffraction of the two plane waves corresponding to the qth mode at the two thick edges is given by

$$U^P(r,\theta) = \left[i\, f^P(\theta_q,\theta) - i\, f^P(-\theta_q,\theta) \right] \frac{e^{i(kr-\pi/4)}}{(2\pi kr)^{\frac{1}{2}}} \tag{4.13a}$$

where

$$f^P(\alpha,\beta) = \frac{e^{-ik(\ell+s)\sin\alpha}}{2} \left[P(\pi/2 - \alpha,\ \pi/2 - \beta) e^{-ik\ell(\sin\alpha+\sin\beta)} + P(\pi/2 + \alpha,\ \pi/2 + \beta) e^{ik\ell(\sin\alpha+\sin\beta)} \right] \tag{4.13b}$$

$P(\theta_o,\theta)$ is the diffraction coefficient for a thick half plane due to an E-polarized incident plane wave as derived in Chapter III, (3.25). The first term in the above expression (4.13b) has been obtained by recognizing that the ray impinging on the upper edge at an angle α has a phase factor

$$e^{-ik(2\ell+s)\sin\alpha}$$

and the field due to the ray diffracted by this edge in the direction $\theta = \beta$ is obtained by multiplying the incident ray field by

$$P(\pi/2 - \alpha,\ \pi/2 - \beta) e^{-ik\ell\sin\beta} \frac{e^{i(kr-\pi/4)}}{(2\pi kr)^{\frac{1}{2}}}$$

where r is measured from the midpoint of the strip. The second term in (4.13b) is due to diffraction at the lower edge and is obtained in a similar manner.

Equating (4.8) and (4.11) and using (4.13), we obtain the following expression for the primary reflection coefficient

$$R^{p}_{qn} = -\frac{\cos(n+q)\psi}{a\beta_n}\left[P(\pi/2-\theta_q,\ \pi/2-\theta_n)e^{-i\gamma(q+n)}\right.$$

$$\left.+\ P(\pi/2+\theta_q,\ \pi/2+\theta_n)e^{i\gamma(q+n)}\right]$$

$$+\frac{\cos(q-n)\psi}{a\beta_n}\left[P(\pi/2+\theta_q,\ \pi/2-\theta_n)e^{-i\gamma(n-q)}\right.$$

$$\left.+\ P(\pi/2-\theta_q,\ \pi/2+\theta_n)e^{i\gamma(n-q)}\right] \tag{4.14}$$

where

$$\gamma = \pi\ell/a \quad , \quad \psi = \pi(s+\ell)/a \tag{4.15}$$

For the case of an infinitesimally thin strip, (4.14) reduces to

$$R^{p}_{qq} = \frac{1}{a\beta_n}\left\{\left[\frac{\sin(n+q)\gamma}{\sin[(\theta_n+\theta_q)/2]} + \frac{i\cos(n+q)\gamma}{\cos[(\theta_n-\theta_q)/2]}\right]\cos(q+n)\psi\right.$$

$$\left.-\left[\frac{\sin(n-q)\gamma}{\sin[(\theta_n-\theta_q)/2]} + \frac{i\cos(n-q)\gamma}{\cos[(\theta_n+\theta_q)/2]}\right]\right\}\cos(q-n)\psi \tag{4.16}$$

and hence

$$R^{p}_{qq} = -\frac{2\ell}{a} - \frac{ik}{a\beta_q^2} + \left[\frac{ka}{q\pi}\sin(2q\gamma) + i\cos(2q\gamma)\right]\frac{\cos(2q\psi)}{a\beta_q} \tag{4.17}$$

which agrees with the expression obtained by Yee and Felsen [25].

As discussed earlier, the secondary diffracted field is due to the interaction between the strip edges and the waveguide walls (or between the edges and their images). Following the interaction procedure for the thick slit described in Chapter III, one may show that the composite field U^{i}_{A} impinging on the upper edge of the strip due to multiple interaction with the upper wall and the composite field U^{i}_{B} impinging on the lower wall due to multiple interaction with the lower

wall, are given by

$$U_A^i = U_A(2d,0)/\{1 - i\, F_1(2d)[1 + F_2(b,2d)]\} \tag{4.18a}$$

$$U_B^i = U_B(2s,0)/\{1 - i\, F_1(2s)[1 + F_2(b,2d)]\} \tag{4.18b}$$

where F_1, F_2 are given by (2.95) and the parameters $2ks$ and $2kd$ should be larger than $1/2\pi$ for (4.18) to be convergent. $U_A(2d,0)$ and $U_B(2s,0)$ are the corresponding fields due to single interaction of the primary diffracted field with the upper and lower wall, respectively

$$U_A(2d,0) = -\frac{F_1(2d)[1 + F_2(b,2d)]}{2}\left\{i\, e^{-iq(\gamma+\psi)}\, P(\pi/2 - \theta_q,0) - i\, e^{iq(\gamma+\psi)}\, P(\pi/2 + \theta_q,0)\right\} K_+^2(k) \tag{4.19a}$$

$$U_B(2s,0) = -\frac{F_1(2s)[1 + F_2(b,2s)]}{2}\left\{i\, e^{-iq(\psi-\gamma)}\, P(\pi/2 + \theta_q,0) - i\, e^{iq(\psi-\gamma)}\, P(\pi/2 - \theta_q,0)\right\} K_+^2(k) \tag{4.19b}$$

When (3.25) is applied to the upper edge, with $E_\pm^i$ in (4.10) taken as the incident fields and θ (in the argument of $P(\theta_o,\theta)$) set equal to zero, the primary diffracted field impinging on the wall in the plane of the strip is obtained. The result (4.19a) is obtained by taking the reflection coefficient at the wall as -1 and the total distance from the edge to the neighbouring wall and back to the edge as $2d$. (4.19b) is obtained in a similar manner and applies to the scattering between the lower edge and the neighbouring wall.

Thus the far field contribution in the direction θ_n due to

the interaction between the upper edge and the neighbouring wall is given by

$$U_A^i \, P(0,\pi/2 - \theta_n) e^{-i\gamma n} \, \frac{e^{i(kr-\pi/4)}}{(2\pi kr)^{\frac{1}{2}}} \tag{4.20a}$$

whereas that for the lower edge and the neighbouring wall is given by

$$U_B^i \, P(0,\pi/2 + \theta_n) e^{i\gamma n} \, \frac{e^{i(kr-\pi/4)}}{(2\pi kr)^{\frac{1}{2}}} \tag{4.20b}$$

Thus $f(\theta_n)$, to be used in (4.8), is given by

$$f(\theta_n) = U_A^i \, P(0,\pi/2 - \theta_n) e^{-i\gamma n} + U_B^i \, P(0,\pi/2 + \theta_n) e^{i\gamma n} \tag{4.21}$$

Using (4.8), (4.11), (4.19) and (4.21) and simplifying, we obtain the following expression for the reflection coefficient due to the secondary diffracted field

$$R_{qn}^s = \frac{1}{2\beta_n a} \left[W_2(d) Q_1(n) Q_1(q) + W_2(s) Q_2(n) Q_2(q) \right] \tag{4.22}$$

where

$$W_2(\xi) = \frac{F_1(2\xi)\left[1 + F_2(b,2\xi)\right] K_+^2(k)}{1 - i \, F_1(2\xi)\left[1 + F_2(b,2\xi)\right]} \tag{4.23}$$

$$\begin{aligned} Q_1(m) &= P(0,\pi/2 - \theta_m) e^{-i(\gamma+\psi)m} - P(0,\pi/2 + \theta_m) e^{i(\gamma+\psi)m} \\ Q_2(m) &= P(0,\pi/2 + \theta_m) e^{-i(\psi-\gamma)m} - P(0,\pi/2 - \theta_m) e^{i(\psi-\gamma)m} \end{aligned} \tag{4.24}$$

and γ and ψ are given in (4.15).

Since the total diffracted field consists of primary and secondary diffracted fields, the composite reflection coefficient is given by

$$R_{qn} = R_{qn}^p + R_{qn}^s \tag{4.25}$$

Because ray optics is essentially a high frequency technique, it is to be expected that the above formulae, when applied to a particular mode, have their greatest accuracy in the frequency range well above the cutoff frequency of the mode. Even within the high frequency range, the results deteriorate as the cutoff frequency of a particular mode is approached. The difficulty arises from the fact that the constituent modal plane waves now propagate almost perpendicular to the axis of the waveguide and strike the strip at almost grazing angles of incidence. Since the accuracy of our results for the thick slit is questionable at these angles of incidence and reflection ($\theta_q \approx \pm \pi/2$, $\theta_n \approx \pm \pi/2$), the value of R^p_{qq} obtained from (4.14) is inaccurate near the cutoff frequency of the qth mode.

Another difficulty arises in the calculation of interaction near the point of emergence of the nth mode from cutoff since the mode angle θ_n is then nearly equal to $\pi/2$. While calculating R_{qq}, one does not, in general, consider R_{qn} for $n \neq q$. However, at the frequencies where new modes emerge, the constituent modal plane waves travel almost perpendicular to the axis of the waveguide and are in the same region as the transition region ($y = 0$ to $y = s$; $y = 2\ell + s$ to $y = a$ in Fig. 4.1) for the multiply diffracted rays. It is difficult to include these modes by the ordinary ray theory and therefore our results are inaccurate near the modal cutoffs.

An improved expression for the secondary reflection coefficient can be obtained by considering the Fresnel integral expression for the thick slit problem. Thus following the above steps and simplifying,

the far field contribution in the direction θ_n due to the interaction between the upper edge and the neighbouring wall (corresponding to (4.20a)) is now given by [25]

$$
\begin{aligned}
&- \frac{F(2d,0,\pi/2 - \theta_n)}{1 + \dfrac{F(2d,0,0)}{K_+^2(k)}} \; \frac{\cos(kb\,\cos\theta_n)}{2K_+(k\,\sin\theta_n)K_+(k)} \\
&\cdot \left\{ i\, e^{-iq(\gamma+\psi)} \; \frac{F(2d,0,\pi/2 - \theta_q)\cos(kb\,\cos\theta_q)}{K_+(k\,\sin\theta_q)K_+(k)} \right. \\
&\left. - i\, e^{iq(\gamma+\psi)} \; \frac{F(2d,0,\pi/2 + \theta_q)\cos(kb\,\cos\theta_q)}{K_-(k\,\sin\theta_q)K_+(k)} \right\} \\
&\cdot \frac{e^{-i\gamma n}\, e^{i(kr-\pi/4)}}{F_1(2d)K_+^2(k)(2\pi kr)^{\frac{1}{2}}}
\end{aligned}
\tag{4.26}
$$

where $F(\xi,0,\theta)$ and $F_1(\xi)$ are given by (2.99c) and (2.95a), respectively. Similar expression can be obtained for the lower edge. Using (4.5), (4.8) and (4.26) and simplifying, the expression for the improved secondary reflection coefficient, corresponding to (4.19), is given by

$$
R^s_{qn} = \frac{1}{2\beta_n a} \left[W'(d)Q_3(q)Q_3(n) + W'(s)Q_4(q)Q_4(n) \right] \tag{4.27}
$$

where Q_3, Q_4 are given by

$$
\begin{aligned}
Q_3(n) = &\frac{-e^{i(\psi+\gamma)n}F(2d,0,\pi/2 - \theta_n)\cos(kb\,\cos\theta_n)}{K_+(k\,\sin\theta_n)K_+(k)} \\
&- \frac{e^{i(\psi+\gamma)n}F(2d,0,\pi/2 + \theta_n)\cos(kb\,\cos\theta_n)}{K_-(k\,\sin\theta_n)K_+(k)}
\end{aligned}
\tag{4.28a}
$$

$$Q_4(n) = e^{-i(\psi-\gamma)n}\frac{F(2s,0,\pi/2+\theta_n)\cos(kb\cos\theta_n)}{K_-(k\sin\theta_n)K_+(k)}$$

$$-\frac{e^{i(\psi-\gamma)n}F(2s,0,\pi/2-\theta_n)\cos(kb\cos\theta_n)}{K_+(k\sin\theta_n)K_+(k)} \qquad (4.28b)$$

$$W'(\xi) = \frac{1}{1+\dfrac{F(2\xi,0,0)}{K_+^2(k)}}\cdot\frac{1}{F_1(2\xi)K_+^2(k)} \qquad (4.29)$$

Since our results for the thick slit are more suitable for large slit widths, the above simplified expressions have been derived by assuming a tandem slit type of interaction (2.99). $P(\theta_o,\theta)$ in (4.14), however, still represents the thick half plane diffraction coefficient (3.25).

The results in this section can be easily adapted to the case of an asymmetrical diaphragm as shown in Fig. 4.2. Thus, if $s = d$ and a is replaced by $2a$ in Fig. 4.1, an even numbered mode incident on the strip in Fig. 4.1 excites by symmetry about the plane $y = a$, only even numbered modes. Thus the entire configuration can be bisected at the plane $y = a$ thereby generating Fig. 4.2 which has been simplified to the case $d = \ell = a/2$. It follows that the asymmetric diaphragm nth mode reflection coefficient for an incident qth mode can be obtained by making the following replacements in the above results

$$n \to 2n \ , \ q \to 2q \ , \ a \to 2a \ , \ s = d \qquad (4.30)$$

Moreover, since the diaphragm in Fig. 4.2 is adjacent to the lower waveguide wall, it is necessary by comparison with the bisected structure of Fig. 4.1, to replace y by $a - y$, thereby introducing

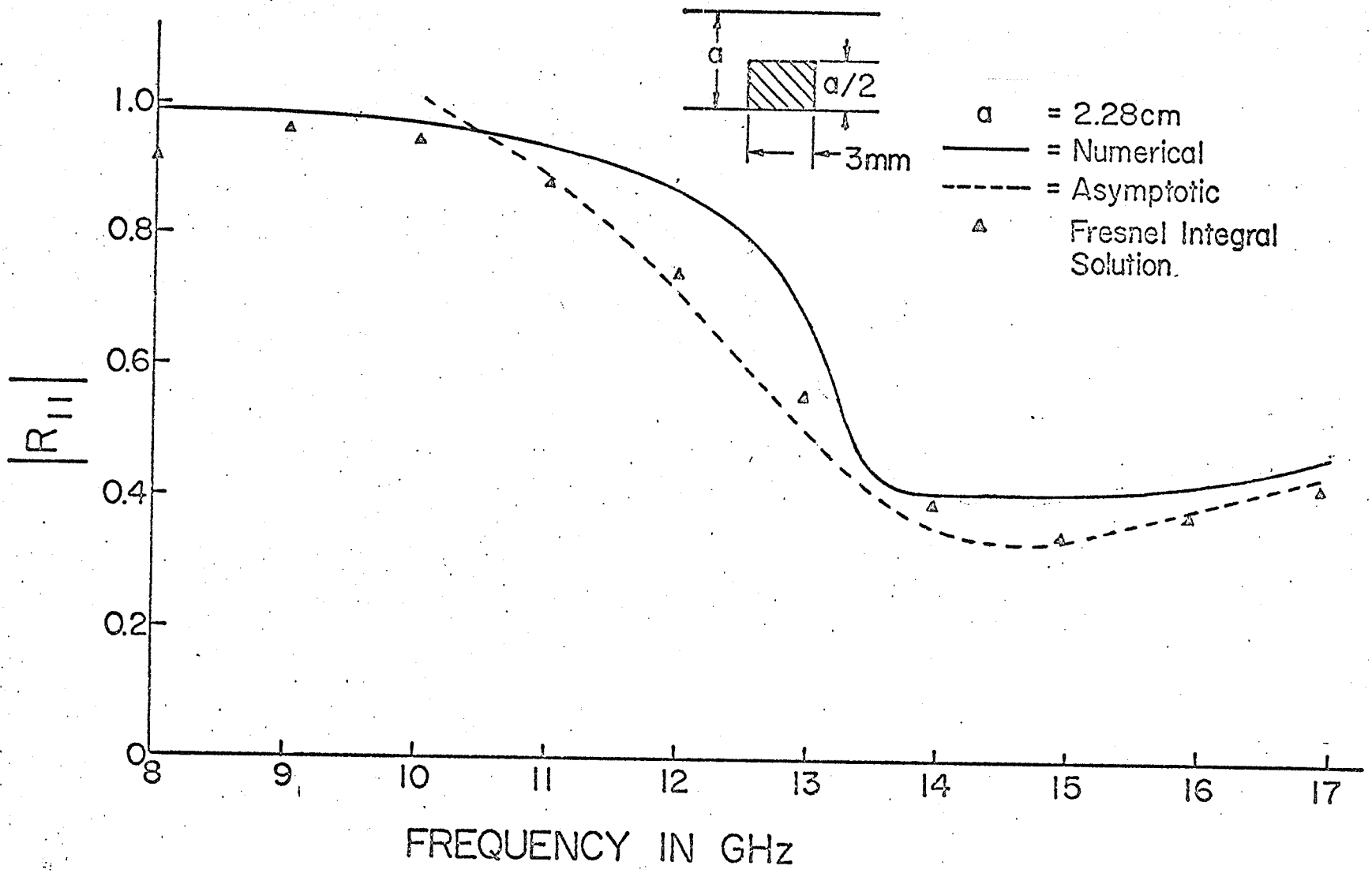

Fig. 4.2 Reflection coefficient vs frequency for an asymmetric diaphragm of 3mm thickness

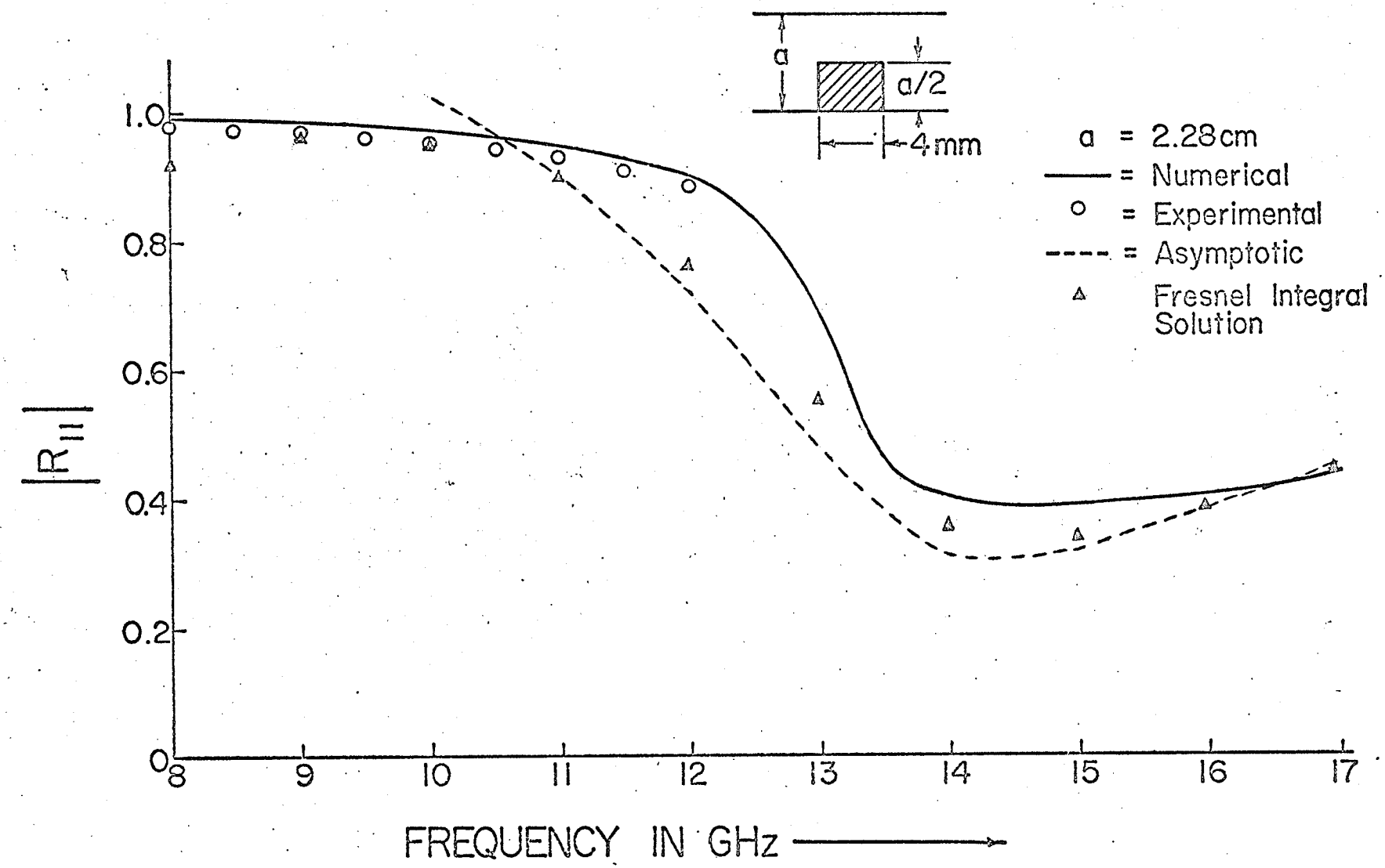

Fig. 4.3 Reflection coefficient vs frequency for an asymmetric diaphragm of 4mm thickness

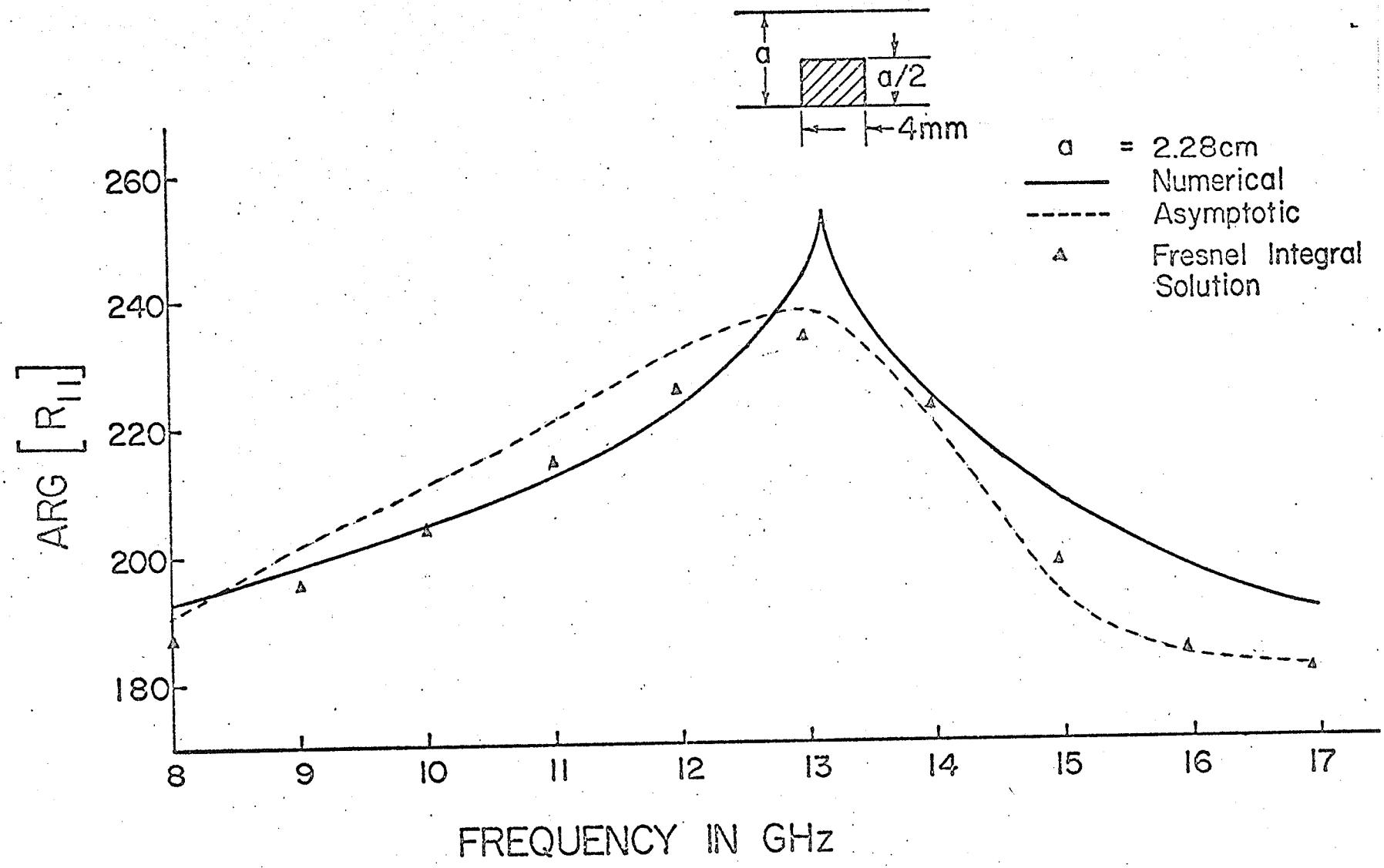

Fig. 4.4 Argument of reflection coefficient vs frequency for an asymmetric diaphragm of 4mm thickness

Table 4.1

R_{11} vs thickness for an asymmetric diaphragm

(a/λ = 0.835 , Frequency = 11.0 GHz)

Thickness 2b in mm	Magnitude of R_{11}		Argument of R_{11}	
	Ray Theory (Asymptotic)	Numerical	Ray Theory (Asymptotic)	Numerical
0.5	0.808	0.848	219.0°	212.0°
1.0	0.829	0.872	218.8°	212.1°
2.0	0.864	0.906	219.4°	212.1°
3.0	0.888	0.938	220.3°	211.9°
4.0	0.905	0.955	221.5°	211.8°
5.0	0.916	0.966	221.8°	211.6°
6.0	0.923	0.975	224.3°	211.5°
7.0	0.928	0.981	225.9°	211.4°

a factor $(-1)^q$ in (4.9) and $(-1)^n$ in (4.11), (4.12).

In order to check the accuracy of our approximate solution, computations of the reflection coefficient were performed for a diaphragm of $\ell = a/2$ and the results compared with data based on numerical [47] or experimental solution. The experiment was conducted at X-band using standard measurement techniques whereas the numerical solution was obtained by using a modal analysis method of transverse field matching and was found to be accurate for thick irises when compared with experimental results or data available in the Waveguide Handbook [78]. The maximum deviation was approximately 8% for the infinitesimally thin (approximated by a thickness of 0.3 mm) case.

Our approximate calculations are based on (4.14) along with (4.22) for the asymptotic solution and (4.27) for the Fresnel integral solution. The agreement with experimental or numerical data for $|R_{11}|$ versus frequency is satisfactory except near the modal cutoffs as shown in Figs. 4.2 and 4.3. The magnitude and argument of R_{11} are given in Table 4.1 for various values of thickness $(2b)$ while the argument of R_{11} versus frequency is shown for a particular case in Fig. 4.4.

4.2 Symmetric Waveguide Diaphragm

When two asymmetric diaphragms are placed facing each other in a waveguide, the resulting configuration is known as a symmetric diaphragm. In this section the ray-optical method is applied to deal with a symmetric diaphragm of infinitesimal as well as of finite thickness.

Consider a symmetric diaphragm placed at $z = 0$ in a waveguide as shown in Fig. 4.5. The width and thickness of the window in the diaphragm are denoted by 2ℓ and $2b$, respectively, while the distances from the edges adjacent to the upper and lower walls are denoted by d and s, respectively. Similar to the case of a thick strip discontinuity, certain restrictions, as will be given later, have to be placed on these dimensions for obtaining reasonably accurate results from asymptotic theory.

Let the normalized electric field due to a TE_{qo} waveguide mode incident on the diaphragm from the right be given by

$$E_x^i(y,z) = \sin(q\pi y/a)e^{-i\beta_q|z|} \tag{4.31}$$

which may be decomposed into two plane waves, i.e.

$$E_x^i(y,z) = -(i/2)e^{i(-\beta_q z+q\pi y/a)} + (i/2)e^{i(-\beta_q z-q\pi y/a)} \tag{4.32}$$

These waves are scattered at the discontinuity where each of the two thick edges behaves like an induced line source and, as before, is considered mathematically equivalent to a thin edge with a modified diffraction coefficient as discussed in Chapter III.

In order to calculate the reflection coefficient R_{qn} in (4.11) due to this discontinuity, it is required to determine, as in the case of a strip discontinuity, the pattern function $f(\theta_n)$ along the direction of the nth excited mode. Thus we consider the diffraction of the two plane waves (4.32) at the two thick edges of the waveguide diaphragm. The total diffracted field consists of contributions due to the primary and the secondary diffracted fields. The primary

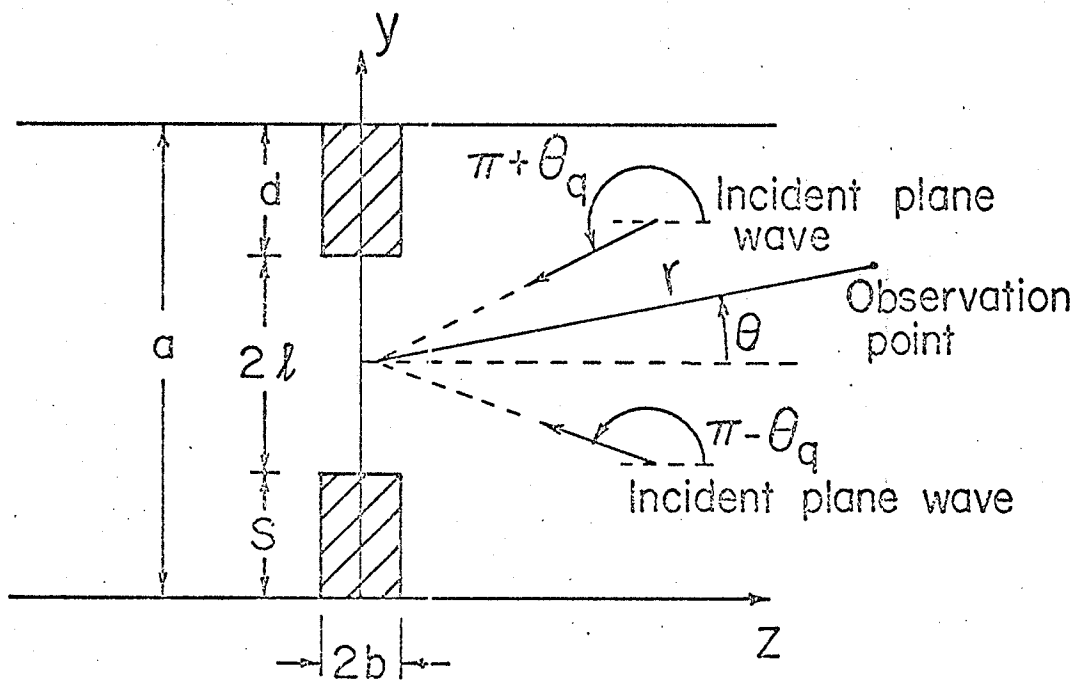

Figure 4.5 Thick symmetric diaphragm in a rectangular waveguide.

diffracted field is due to the initial diffraction of the two plane waves at the two edges of the diaphragm. The secondary diffracted field is due to interaction between the two edges of the diaphragm and between the diaphragm edges and the neighbouring waveguide walls. However, the former contribution dominates since the latter is smaller by $0(1/kd$ or $1/ks)$ where kd or ks is assumed to be larger than unity. This is true only when the diaphragm width (2ℓ) is not appreciably larger than half the waveguide width. Summation of these fields and their combination with respect to the midpoint $(y = s + \ell,\ z = 0)$ leads to the pattern function $f(\theta_n)$ needed in (4.8).

Thus the primary field due to initial diffraction of the two waves by the two equivalent edges is given as

$$U^P(r,\theta) = \left[i\ f^P(\theta_q,\theta) - i\ f^P(-\theta_q,\theta) \right] \frac{e^{i(kr-\pi/4)}}{(2\pi kr)^{\frac{1}{2}}} \tag{4.33a}$$

where the (r,θ) polar coordinates are shown in Fig. 4.5, and

$$f^P(\alpha,\beta) = \frac{1}{2}\, e^{-ik(\ell+s)\sin\alpha} \left[P(\pi/2 + \alpha,\ \pi/2 + \beta) e^{-ik\ell(\sin\alpha+\sin\beta)} + P(\pi/2 - \alpha,\ \pi/2 - \beta) e^{ik\ell(\sin\alpha+\sin\beta)} \right] \tag{4.33b}$$

Here $P(\theta_o,\theta)$ is the diffraction coefficient for a thick half plane due to an E-polarized incident plane wave and has been given in Chapter III, (3.25). As discussed in connection with the thick strip discontinuity, the first term in (4.33b) has been obtained by recognizing that the ray incident at the upper edge at an angle α has a phase factor

$$e^{-ik(2\ell+s)\sin\alpha}$$

The field due to the ray diffracted by this edge in the direction $\theta = \beta$

is obtained by multiplying the incident ray field by

$$P(\pi/2 + \alpha, \pi/2 + \beta)e^{-ik\ell\sin\beta} \frac{e^{i(kr-\pi/4)}}{(2\pi kr)^{\frac{1}{2}}}$$

where r is measured from the middle of the window. The second term in (4.33b) is due to diffraction at the lower edge and is obtained in a similar way.

Now following (2.2), the total field in the illumination region in our case is given by

$$\phi_t = \phi + e^{-iky\sin\theta_q - ikz\cos\theta_q} - e^{-iky\sin\theta_q + ik(z-2b)\cos\theta_q}$$

Subtracting the incident field from this expression and remembering that there are two plane waves incident on the diaphragm, the total field reflected in the illumination region is given by

$$\phi^r = \phi - \sin(\frac{q\pi y}{a})\, e^{-i\beta_q|z|}\, e^{-i2b\beta_q}$$

Thus for finding the field at an observation point in the illumination region, it is required to add the term

$$-\sin(\frac{q\pi y}{a})\, e^{-i\beta_q|z|}\, e^{-i2b\beta_q}$$

to (4.33). This term reduces to

$$-\sin(\frac{q\pi y}{a})\, e^{-i\beta_q|z|}$$

or -1 when normalized with respect to the incident field for an infinitesimally thin diaphragm. This term does not appear for the transmission region of a thin diaphragm as expected since $\tau = 1 + R$ for a thin lossless discontinuity.

Using (4.8), (4.11) and (4.33) and simplifying, it follows from the above discussion that the primary reflection coefficient of the nth excited mode is given by

$$R^{p}_{qn} = -\frac{\cos(n+q)\psi}{a\beta_n}\left[P(\pi/2+\theta_q,\ \pi/2+\theta_n)e^{-i\gamma(q+n)} + P(\pi/2-\theta_q,\ \pi/2-\theta_n)e^{i\gamma(q+n)}\right] + \frac{\cos(q-n)\psi}{a\beta_n} \cdot \left[P(\pi/2-\theta_q,\ \pi/2+\theta_n)e^{i\gamma(q-n)} + P(\pi/2+\theta_q,\ \pi/2-\theta_n)e^{-i\gamma(q-n)}\right] - e^{-i2b\beta_q} \tag{4.34}$$

where γ and ψ are given in (4.15).

For the case of an infinitesimally thin symmetric diaphragm, (4.34) reduces to

$$R^{p}_{qn} = \frac{1}{a\beta_n}\left\{\left[-\frac{\sin(q+n)\gamma}{\sin\frac{\theta_n+\theta_q}{2}} + i\frac{\cos(q+n)\gamma}{\cos\frac{\theta_n-\theta_q}{2}}\right]\cos(q+n)\psi + \left[\frac{\sin(n-q)\gamma}{\sin\frac{\theta_n-\theta_q}{2}} - i\frac{\cos(n-q)\gamma}{\cos\frac{\theta_n+\theta_q}{2}}\right]\cos(n-q)\psi\right\} - 1 \tag{4.35}$$

and hence

$$R^{p}_{qq} = \frac{2\ell}{a} - 1 - \frac{ik}{a\beta_q^2} - \frac{k\sin(2q\gamma)\cos(2q\psi)}{q\pi\beta_q} + \frac{i\cos(2q\gamma)\cos(2q\psi)}{a\beta_q} \tag{4.36}$$

It is interesting to note that the infinite frequency limit (i.e. $a/\lambda \to \infty$) of the dominant mode reflection coefficient R_{11} of a thin symmetric diaphragm with $2\ell = a/2$ is -0.182 as compared to -0.5 for an asymmetric diaphragm of the same aperture dimensions.

As discussed earlier, the secondary diffracted field is due to the interaction between the two edges of the diaphragm. Following the interaction procedure for the thick slit described in Chapter III and using (4.8) and (4.11), we obtain the following expression for the secondary reflection coefficient

$$R^s_{qn} = \frac{i}{a\beta_n}\left(e^{-in\psi}\left[i\, f^s(\theta_q,\theta_n) - i\, f^s(-\theta_q,\theta_n)\right]\right.$$
$$\left. - e^{in\psi}\left[i\, f^s(\theta_q,-\theta_n) - i\, f^s(-\theta_q,-\theta_n)\right]\right) \tag{4.37}$$

where

$$f^s(\alpha,\beta) = \frac{W_3}{2}\, e^{-ik(\ell+s)\sin\alpha}\left\{e^{-ik\ell(\sin\alpha-\sin\beta)}P(0,\pi/2+\alpha)P(0,\pi/2-\beta)\right.$$
$$+ e^{ik\ell(\sin\alpha-\sin\beta)}P(0,\pi/2-\alpha)P(0,\pi/2+\beta)$$
$$- i\, F_1(2\ell)[1 + F_2(b,2\ell)]$$
$$\cdot\left[e^{ik\ell(\sin\alpha+\sin\beta)}\, P(0,\pi/2-\alpha)P(0,\pi/2-\beta)\right.$$
$$\left.\left. + e^{-ik\ell\,(\sin\alpha+\sin\beta)}\, P(0,\pi/2+\beta)P(0,\pi/2+\alpha)\right]\right\} \tag{4.38}$$

$$W_3 = \frac{F_1(2\ell)[1 + F_2(b,2\ell)]K_+^2(k)}{1 + F_1^2(2\ell)[1 + F_2(b,2\ell)]^2} \tag{4.39}$$

and F_1, F_2 are given by (2.95). Also, the parameter $2k\ell$ should be greater than $1/2\pi$ for (4.39) to converge.

As discussed before the first term in (4.38) has been obtained by recognizing that the ray incident on the upper edge at an angle α has the phase factor

$$e^{-ik(2\ell+s)\sin\alpha}$$

and the field due to diffracted ray in the direction $\theta = \beta$, after a

single diffraction at the lower edge is obtained by multiplying the incident ray by

$$F_1(2\ell)\left[1 + F_2(b,2\ell)\right]K_+^2(k)P(0,\pi/2 + \alpha)P(0,\pi/2 - \beta)e^{ik\ell \sin\beta} \cdot \frac{e^{i(kr-\pi/4)}}{(2\pi kr)^{\frac{1}{2}}}$$

where r is measured from the middle of the diaphragm. The term $F_1^2(2\ell)\left[1 + F_2(b,2\ell)\right]^2$ in the denominator of (4.39) denotes the continuation of this process indefinitely. The second term corresponds to the ray initially incident on the lower edge and emerging at an angle $\theta = \beta$ after a single diffraction at the upper edge. The third and the fourth terms in (4.38) correspond to the rays initially incident at either edge and emerging at an angle $\theta = \beta$ from the same edge. It is to be noted the interaction mode coefficients c_n^{int} have been neglected in the derivation of (4.38) since their effect is negligible for the practical case of interest $(2b/\ell \lesssim 0.5)$.

As in the previous case of a thick strip discontinuity (or a thick asymmetric diaphragm), the accuracy of our results can be improved by considering the interaction in terms of Fresnel integrals as given in (2.99). The resulting expression for $f^s(\alpha,\beta)$ is given by

$$f^s(\alpha,\beta) = \frac{W_4}{2} e^{-ik(\ell+s)\sin\alpha} \cdot \left\{ e^{-ik\ell(\sin\alpha-\sin\beta)} \frac{F(2\ell,0,\pi/2 - \beta)P(0,\pi/2 + \alpha)\cos(kb\cos\beta)}{K_+(k)K_+(k\sin\beta)} + e^{ik\ell(\sin\alpha-\sin\beta)} \frac{F(2\ell,0,\pi/2 + \beta)P(0,\pi/2 - \alpha)\cos(kb\cos\beta)}{K_+(k)K_-(k\sin\beta)} \right.$$

$$+ \frac{F(2\ell,0,0)}{K_+^2(k)} \left[e^{-ik\ell(\sin\alpha+\sin\beta)} \cdot \frac{F(2\ell,0,\pi/2+\beta)P(0,\pi/2+\alpha)\cos(kb\cos\beta)}{K_+(k)K_-(k\sin\beta)} + e^{ik\ell(\sin\alpha+\sin\beta)} \frac{F(2\ell,0,\pi/2-\beta)P(0,\pi/2-\alpha)\cos(kb\sin\beta)}{K_+(k)K_+(k\sin\beta)} \right] \tag{4.40}$$

where

$$W_4 = \frac{1}{1 - \frac{F^2(2\ell,0,0)}{K_+^4(k)}} \tag{4.41}$$

and $F(\xi,0,\theta)$ is given by (2.99c).

Since our results for the thick slit are more suitable for large slit widths, the above simplified expression has again been obtained by assuming a tandem slit type of interaction. $P(\theta_o,\theta)$, in (4.41), however still represents the thick half plane diffraction coefficient.

In order to check the accuracy of our approximate theory, computations of the reflection coefficient were performed for a symmetric diaphragm of aperture width $a/2$ and thickness $2b$ and the results compared with experimental and/or numerical data [47]. The calculations are based on (4.36) to (4.38) for the asymptotic solution and (4.36), (4.37) and (4.40) for the Fresnel integral solution. The agreement with numerical data is satisfactory except near $a/\lambda = 0.5$, 1.5, 2.5 ... as shown in Figs. 4.6 and 4.7. These discrepancies occur mainly because of two reasons. As discussed for the case of an

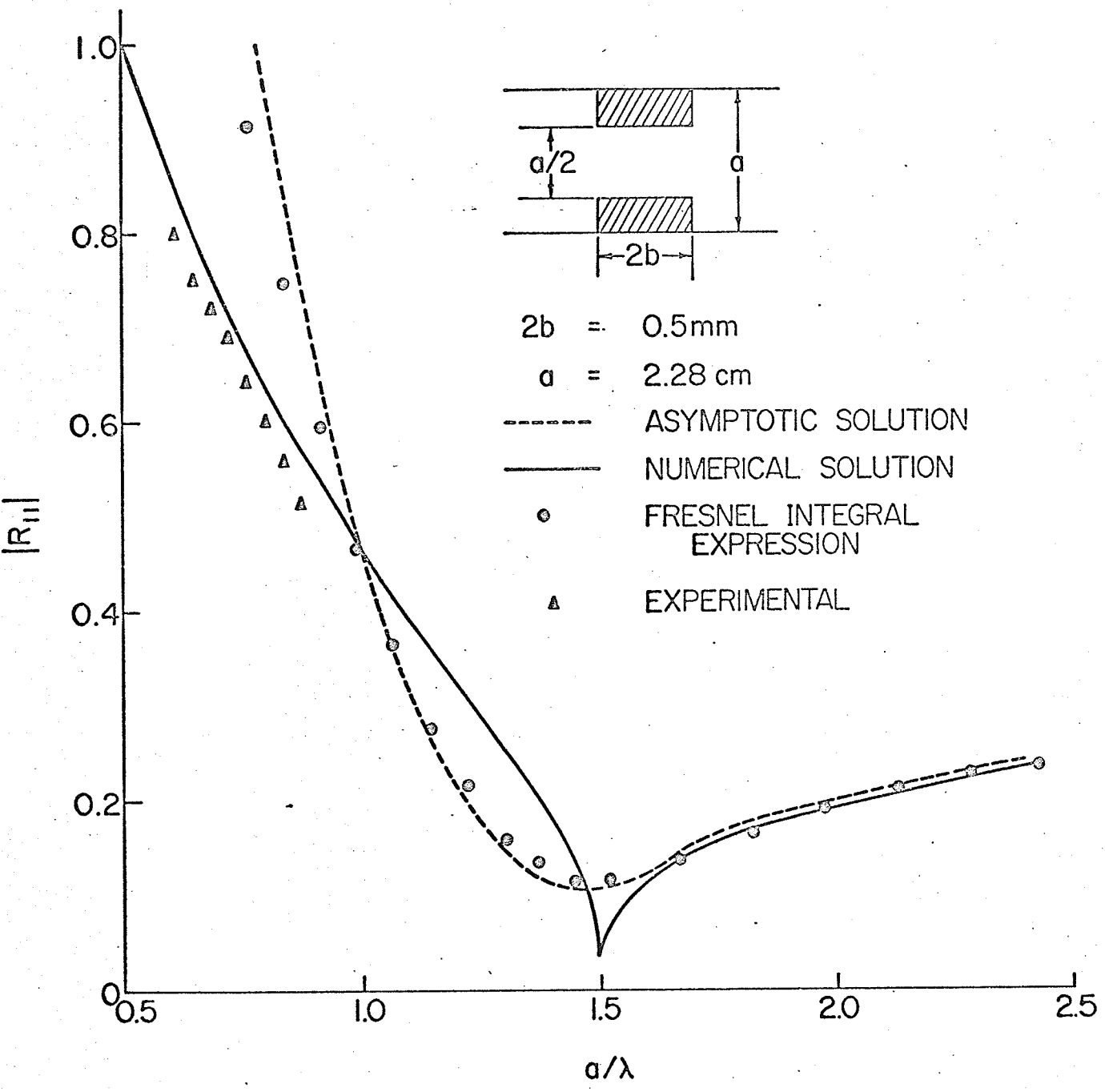

Fig. 4.6 Reflection coefficient vs frequency for a symmetric diaphragm of 0.5 mm thickness

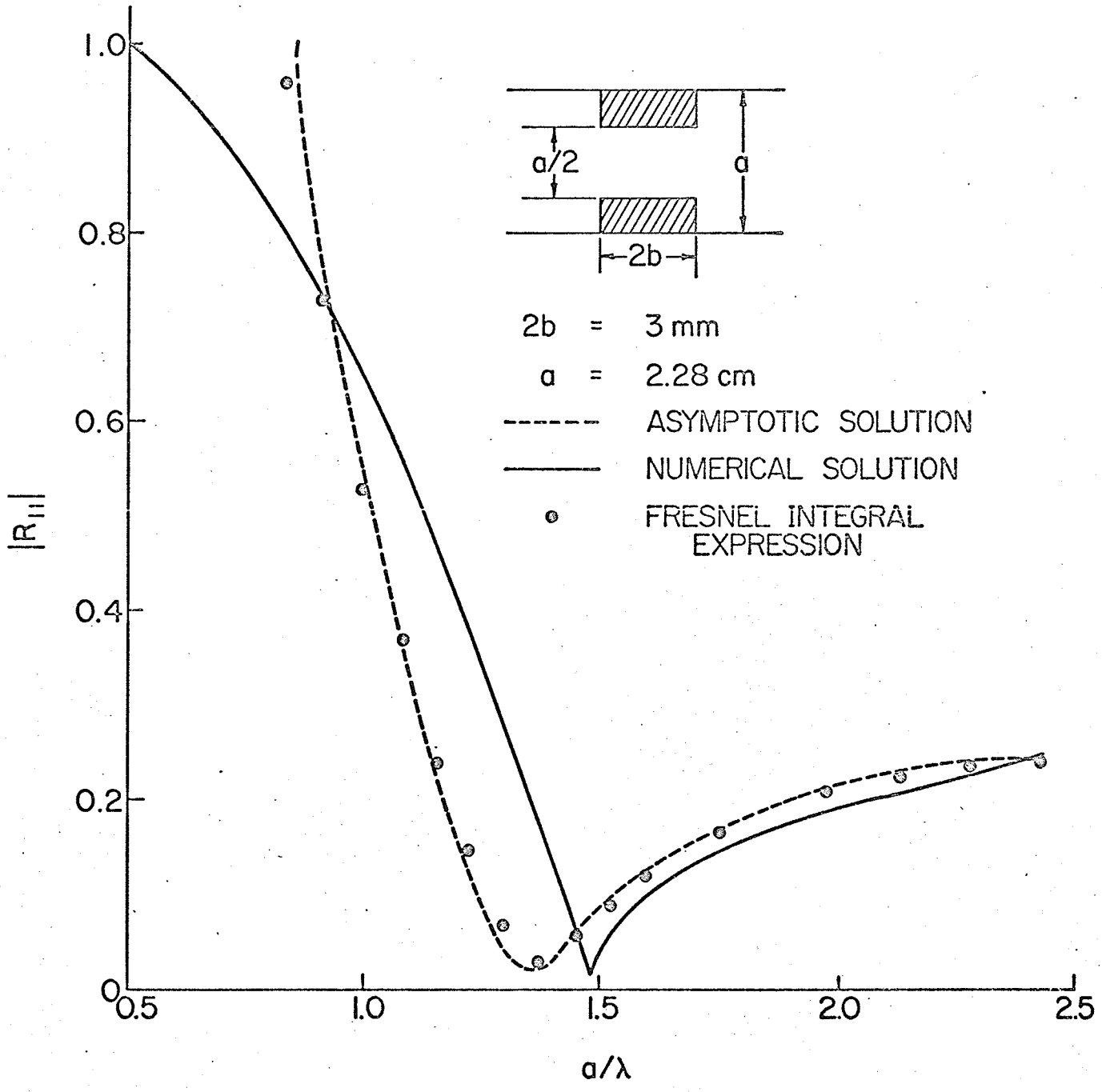

Fig. 4.7 Reflection coefficient vs frequency for a symmetric diaphragm of 3 mm thickness

asymmetric diaphragm, primary reflection coefficient R^p_{qq} is inaccurate near the cutoff frequency of the qth mode ($a/\lambda = 0.5$ for R^p_{11}) because of the nearly grazing angles of incidence and reflection. An additional difficulty arises in the calculation of interaction near the point of emergence of the nth mode from cutoff since the mode angle θ_n is then nearly equal to $\pi/2$ and is in the transition region ($y = 0$ to $y = s$ and $y = 2\ell + s$ to $y = a$ in Fig. 4.1, $y = s$ to $y = 2\ell + s$ in Fig. 4.5) for multiply diffracted rays. It follows from the discussion on page 92 that our results for the symmetric diaphragm will be inaccurate near the modal cutoffs. Now for a symmetric discontinuity the reflection coefficient R_{qn} vanishes for $q + n =$ odd, i.e. an incident mode does not excite any reflected modes of opposite parity [24]. Thus for a TE_{10} mode incident on a symmetric diaphragm, new modes emerge at $a/\lambda = 1.5, 2.5, 3.5 \ldots$ (corresponding to $n = 3,5,7\ldots$). Similarly for an asymmetric diaphragm new modes emerge at $a/\lambda = 1,1.5,2\ldots$ (corresponding to $n = 4,6,8\ldots$ according to the discussion on page 94). The emergence of these modes may thus explain the discrepancies in our results at these particular values of a/λ (in addition to $a/\lambda = 0.5$) for both asymmetric and symmetric diaphragms.

Finally, Tables 4.2 and 4.3 give the magnitude of the reflection coefficient at two particular values of a/λ for various values of screen thickness.

4.3 Discussion of the Results

We have shown that the ray-optical analysis of Yee and Felsen [25]

TABLE 4.2

Magnitude of R_{11} vs. thickness for a symmetric diaphragm

($a/\lambda = 0.91$, $a = 2.28$ cm)

Thickness 2b in mm	Asymptotic Solution	Fresnel Integral Solution	Numerical Solution
0.5	0.642	0.598	0.537
1.0	0.682	0.635	0.591
1.5	0.714	0.665	0.635
2.0	0.742	0.691	0.673
2.5	0.765	0.712	0.707
3.0	0.784	0.728	0.737
3.5	0.797	0.741	0.763
4.0	0.805	0.748	0.788

TABLE 4.3

Magnitude of R_{11} vs. thickness for a symmetric diaphragm

($a/\lambda = 2.43$, $a = 2.28$ cm)

Thickness 2b in mm	Asymptotic Solution	Fresnel Integral Solution	Numerical Solution
0.5	0.241	0.239	0.237
1.0	0.242	0.240	0.240
1.5	0.241	0.239	0.240
2.0	0.240	0.239	0.241
2.5	0.240	0.239	0.243
3.0	0.240	0.240	0.244
3.5	0.241	0.242	0.245
4.0	0.244	0.244	0.244

may be extended to deal with an asymmetric diaphragm of finite thickness and a symmetric diaphragm of infinitesimal as well as finite thickness. Our approximate results reduce to those of Yee and Felsen [25] when the thickness (2b) of an asymmetric diaphragm reduces to zero. Our results for both asymmetric and symmetric diaphragms compare favourably with experimental and/or numerical data except near the modal cutoffs. Furthermore, the approximate results for an infinitesimally thin diaphragm are in better agreement with numerical data as $ka \to \infty$ than for a thick diaphragm, since truncation in the series for the evaluation of $K_{\pm}(\alpha)$, $L_{\pm}(\alpha)$ (A.1,A.2) and $P(\theta_o,\theta)$ (3.24) introduces additional errors.

Examination of our results for the asymmetric diaphragm shows that as the screen thickness increases, the reflection coefficient also increases thereby decreasing the effective distance between the diaphragm edge (or strip edges) and the waveguide wall. For example, it is shown in Table 4.1 that the magnitude of the reflection coefficient at 11.0 GHz increases by 3% and 15% as the screen thickness increases from 0.5 mm to 1 mm and 7 mm, respectively. However, the argument of the reflection coefficient increases very slightly as the diaphragm thickness is increased.

Examination of Tables 4.2 and 4.3 for the symmetric diaphragm shows that the reflection coefficient increases with thickness at lower frequencies ($a/\lambda \lesssim 1.5$) but remains approximately constant at very high frequencies. For example, Table 4.2 shows that the reflection coefficient at 12.0 GHz increases by about 47% as the screen thickness

increases from 0.5 mm to 4 mm, whereas Table 4.3 shows that the reflection coefficient at 32 GHz remains approximately constant for the same variation in thickness.

CHAPTER V

DISCUSSION AND CONCLUSIONS

5.1 Discussion

Examination of our results suggests that the ray-optical technique leads to a good agreement with available theoretical and experimental results for a number of free space and waveguide problems. The accuracy and limitations of the results in each case are discussed in this chapter.

The first part of the analytical results was concerned with the solution of the tandem slit configuration by the Wiener-Hopf technique. The integral equations arising in the formulation (2.26 and 2.31) are similar to those of Jones [53] and Williams [54] for the complementary problem of two parallel strips. Our approach to the solution of these equations is similar to these authors but not restricted to the case of large plate-plate separation which seems to be a limitation in their solution. This is because of the difference in the mechanism of interaction between these two complementary problems. Our approximate results agree favourably with Alldredge's experimental and variational solution [46]. The results indicate that as the tandem slit separation increases the main peak in the scattered cross-section decreases and moves towards values corresponding to larger slit widths (Figs. 2.5 to 2.7). Furthermore, the curve for the cross-section changes quite significantly when the tandem slit separation is of certain magnitude (e.g. π, 2π, 3π). The change (see Fig. 2.7) may be associated with the fact that at these values of the separation the parallel plate can now act as a waveguide

for the propagation of a particular mode. This change in behaviour appears more significantly in the amplitude data. Also, we have been able to observe these changes in spite of the fact that $K_+(\xi)$ is not a slowly varying function near $\xi = k$ for these values of plate separation (p. 30) and that more than one term is required in its Taylor series expansion.

It should be noted that the asymptotic tandem slit solution is, in general, valid for $2b/\ell \lesssim 0.5$. The validity for small $k\ell$, for the cases considered in Figs. 2.5 to 2.8 was increased to $2b/\ell \approx 1$ by including the first two terms of the series in (2.58b) in terms of Fresnel integrals. For larger values of this ratio, the deviation from experimental results becomes significant. This is because of the difficulties involved in including higher order terms representing the effect of finite plate separation when the slit width is small compared to the wavelength (additional errors occur because of neglecting of ϕ''_{int} and higher terms in the Taylor series expansion of $F_{D_+}(\xi)$ and $K_+(\xi)$). However, when the slit width is large, asymptotic approximations can be applied and the terms can be included in the form of a simple geometric series (2.65). When the slit separation is also large ($2kb > 10$) the numerical computation of $K_\pm(\alpha)$, $L_\pm(\alpha)$ is laborious [37] and it might be more effective to use the conventional ray-optical technique for this specific case.

The analytical results for the thick slit are presented in a ray-optical form where the diffraction by each edge of the slit has been viewed as that due to a thin edge centred at the middle of the thick

edge modified by an appropriate diffraction coefficient. The edge-edge interaction term, on the other hand, has also been modified such that each thick edge is viewed by the other as a combination of a line source as well as a line dipole which vanishes when the thickness approaches zero. Our analytical results for large slit widths reduce to a simple ray-optical form similar to that of Keller for the thin slit [2]. For smaller values of the slit width, the formulation leads to results which are identical to those of Yu and Rudduck [4] for the complementary strip problem. Our computations for the diffraction patterns agree favourably with experiment and indicate (see Tables 3.1 and 3.2) that the 6dB beamwidth increases as the screen thickness increases as long as $2b/\ell \lesssim 0.5$ and decreases for larger values of this ratio. Also the first minima shift away from the main beam with increasing thickness. On the other hand, the first side lobe level increases with thickness and shifts away from the main beam.

It should be noted that these results are only valid for $2b/\ell \lesssim 0.5$. However, this limitation does not seem to be serious since the dimensions of most practical slits fall within this range. It may be possible to improve the overall accuracy by including ϕ''_{int} and the higher order terms in the Taylor series expansion of $F_{D_+}(\xi)$ and $K_+(\xi)$ (2.56). However, the analysis in this case becomes extremely complicated. It may also be effective to use the conventional ray-optical method when the dimensions of the slit are large compared to the wavelength.

The solution for the far field scattered by a thick slit was

utilized to find the scattering properties of asymmetric and symmetric waveguide diaphragms of finite thickness. Our approximate results (4.14 and 4.22) reduce to those of Yee and Felsen [25] when the thickness of the asymmetric diaphragm reduces to zero. The results for both asymmetric and symmetric diaphragms compare favourably with experimental and/or available numerical [47] data except near the modal cutoffs. Examination of the results for these diaphragms shows that as the screen thickness increases the reflection coefficient increases at lower frequencies $(a/\lambda \lesssim 1.5)$ thereby decreasing the effective distance between the two edges of the diaphragm (symmetric case) or between the edges of the diaphragm and the waveguide wall (asymmetric case). At higher frequencies, however, the effect of increasing thickness is less pronounced.

Comparison of the results in the dominant mode range for asymmetric and symmetric diaphragms shows that the results for the former case are in better agreement with experimental and/or numerical data than for the latter case (see Figs. 4.2 and 4.6). This is because of the fact that the distance between the edges of the equivalent slit is larger in the former case and the ray-optical results are more accurate for smaller values of a/λ. It should also be noted that in both cases our approximate results for an infinitesimally thin diaphragm are in better agreement with available numerical data [47] as $ka \to \infty$ than for a thick diaphragm. This may be explained by the fact that as $ka \to \infty$, kb also approaches ∞ and the truncation in the series (A.1 and A.2) to evaluate $K_{\pm}(\alpha)$, $L_{\pm}(\alpha)$ and the series (3.24) to evaluate

$P(\theta_o,\theta)$, introduces additional errors.

Although favourable agreement has been obtained with experimental or available theoretical results in most of the problems discussed, there are, nevertheless, a number of limitations of the study. Thus we have concerned ourselves only with the evaluation of the fields at distances far away from the tandem slit or the thick slit. The variation of the fields in the aperture with the tandem slit separation or the thickness of the slit has not been evaluated. For the case of a tandem slit, an expression for the field in the aperture has been obtained in terms of a Fourier inversion integral (from (2.85)). However, this inversion cannot be performed in a closed form and the asymptotic evaluation of the integral leads to inaccurate results for the fields in the aperture. It may be possible to evaluate the integral numerically and to obtain the aperture fields for the tandem slit but it would seem difficult to extend the results to a thick slit in free space or a waveguide.

Finally, the deviation of the results from experimental and available numerical data [47] in all cases is due to the nature of the edge-edge interaction which is accounted for only approximately by the present procedure. It may be possible to deal with the interaction by more rigorous means [81]. It may also be effective in some cases to combine numerical techniques for the lower frequency range and in the vicinity of modal cutoffs with the ray-optical procedure for the remaining frequency range. These aspects remain to be explored. Nevertheless, it would seem that the simplicity and versatility exhibited

by our technique renders it worthy of consideration for a large number of problems where screen thickness is an important parameter.

5.2 Conclusions

The diffraction of a plane electromagnetic wave by a tandem slit or a slit in a thick conducting screen has been solved. The final results have been expressed in a ray-optical form using simple diffraction coefficients assigned to each thick half plane and have been shown to be a simple modification of the conventional ray-optical thin slit solution. This has been achieved by using the concept of an equivalent edge which has facilitated the reduction of scattering centres as well as large number of edge-edge interactions. The far field scattering properties of a thick slit thus obtained in free space have been utilized to find the scattering properties of thick diaphragms in a waveguide. This application, though best suited to the high frequency range far from modal cutoffs, has been shown to lead to accurate results even in the dominant mode range. Finally, the favourable agreement with experimental or available analytical results in most cases shows that the procedure can be used with confidence for both free space and waveguide problems.

5.3 Suggestions for Future Research

A number of promising problems arise from the study and their investigation may lead to some useful results and applications. Thus it may be possible to extend the Wiener-Hopf technique for the tandem slit to the diffraction by an array of slits. The existence and character of modal fields in such a two-dimensional periodic structure

has been investigated in the past and some interesting results have been obtained [63,64]. It would also be interesting to consider the effect of finite thickness of the screens on the fields associated with such structures.

The filling of the aperture in a thick screen by a dielectric has resulted in some attractive experimental results. It may be possible to deal with the problem analytically by an extension of the present technique. The recent work of Bates and Mittra [82] on the excitation of a dielectric slab by means of a parallel plate waveguide may be employed in this investigation. The results may lead to the use of dielectric as another parameter in the design of filters [65].

Recently, the exact solution for the electromagnetic scattering by a semi-infinite parallel plate waveguide was asymptotically expanded by Bowman [52] for waveguide dimensions large compared to the wavelength. The results yielded term-by-term comparison with the corresponding results derived by means of ray theory. It was shown that the conventional ray method using two scattering centres does not yield complete agreement with the asymptotic form of the exact solution. It would be interesting to follow this procedure for the scattering by a thin waveguide diaphragm. The term-by-term comparison of the asymptotic form of the exact solution with the corresponding one derived by means of ray theory could lead to an explanation of deviation at the modal cutoffs. The improvement in dealing with edge-edge interaction thus obtained could lead to a better application of the ray-optical method to a large number of waveguide and free space scattering problems involving thin and thick screens.

APPENDIX A

EXPRESSIONS FOR $K_{\pm}(\alpha)$ AND $L_{\pm}(\alpha)$

The formulae used for the computation of $K_{\pm}(\alpha)$ and $L_{\pm}(\alpha)$ are given by (Noble [38], p. 104)

$$K_{\pm}(\alpha) = \exp\left[\mp X_1(\alpha) - T_{\pm}(\alpha)\right] \cdot \prod_{n=1,3,5}^{\infty} \left(\frac{2ib}{n\pi}\right)(\mp\alpha - i\gamma_n) \cdot \exp\left[\pm \frac{2i\alpha b}{n\pi}\right] \tag{A.1}$$

$$L_{\pm}(\alpha) = \exp\left[\mp X_2(\alpha) - T_{\pm}(\alpha)\right] \cdot \prod_{n=2,4,6}^{\infty} \left(\frac{2ib}{n\pi}\right)(\mp\alpha - i\gamma_n) \cdot \exp\left[\pm \frac{2i\alpha b}{n\pi}\right] \tag{A.2}$$

where

$$\gamma_n = +\sqrt{\left[\frac{n\pi}{2b}\right]^2 - k^2} \quad \text{or} \quad -i\sqrt{k^2 - \left[\frac{n\pi}{2b}\right]^2} \tag{A.3}$$

$$X_1(\alpha) = -\frac{i\alpha b}{\pi}\left[0.4228 + \ell n(\pi/2kb) + b\alpha/2\right] \tag{A.4}$$

$$X_2(\alpha) = -\frac{i\alpha b}{\pi}\left[0.4228 + \ell n(2\pi/kb) + b\alpha/2\right] \tag{A.5}$$

$$T_+(\alpha) = T_-(-\alpha) = \frac{b\gamma}{\pi} \text{ arc } \cos(\alpha/k) \tag{A.6}$$

$$\gamma = \sqrt{\alpha^2 - k^2} \tag{A.7}$$

APPENDIX B

BEHAVIOUR OF $F_{D_+}(\alpha)$ NEAR $\alpha = k$

From (2.75), (2.29) and (2.18), we have

$$F_{D_+}(\alpha) = \psi_{D_+}(\alpha) \pm \psi_{D_-}(-\alpha)$$

$$= D_+'^{(o)} - D_+'^{(i)} \pm \psi_{D_-}(-\alpha)$$

$$= \Phi_+'(b + 0) - \Phi_+'(-b - 0) - \Phi_+'(b - 0) + \Phi_+'(-b + 0) \pm \psi_{D_-}(-\alpha)$$

$$= \text{function of } \Phi_+'(\pm b \pm 0) \pm \psi_{D_-}(-\alpha) \qquad \text{(B.1)}$$

Also from (2.12a)

$$\Phi_+' = \int_q^\infty \frac{\partial \phi}{\partial y} e^{i\alpha x}\, dx \qquad \text{(B.2)}$$

where $\left.\frac{\partial \phi}{\partial y}\right|_{y=\pm b\pm 0}$ represents the magnetic field at the upper and lower surfaces of the half planes. Also, the field scattered by a half plane for an E-polarized incident plane wave is of the form

$$\phi = -\frac{e^{i(kr+\pi/4)}}{(2\pi kr)^{\frac{1}{2}}} \left\{ \frac{1}{\cos\left(\frac{\theta_o + \theta}{2}\right)} + \frac{1}{\cos\left(\frac{\theta - \theta_o}{2}\right)} \right\} ; \; kr >> 1 \qquad \text{(B.3)}$$

where r and θ are shown in Fig. 3.1. Thus use of (B.3) and Maxwell equations leads to the following form for Φ_+'

$$\Phi_+' \approx \int \left(\frac{A_1 e^{ikr}}{k^{\frac{1}{2}} r^{3/2}} + \frac{A_2 e^{ikr}}{k^{-\frac{1}{2}} r^{\frac{1}{2}}} \right) e^{i\alpha r}\, dr \; ; \; kr >> 1 \qquad \text{(B.4)}$$

where A_1, A_2 are independent of k and r. Since the transform of

r^{-n} is of the form α^{n-1} (or k^{n-1} for $\alpha = k$) in the α-plane, it is evident from (B.4) that to a first approximation, Φ_+' (or $F_{D_+}(\alpha)$) is a slowly varying function of α near $\alpha = k$. (Similar results may be obtained for intermediate and smaller values of r.)

APPENDIX C

EVALUATION OF $U(\alpha)$

The procedure in deriving (2.53) from (2.31) is applied to (2.26) and leads to an integral equation containing $L_{\pm}$ terms. All the integrals in the resulting equation are of the form

$$I = \frac{1}{2\pi i} \int_{ia-\infty}^{ia+\infty} \frac{F_{D_+}(\xi)\, e^{i\xi\ell}\, L_-(\xi)}{(\xi + \alpha)}\, d\xi \qquad (C.1)$$

which has a branch point singularity at $\xi = k$. If the functions $L_+(\xi)$ and $F_{D_+}(\xi)$ are expanded about this branch point in terms of a Taylor's series and only the first term retained, the integral reduces to

$$\frac{F_{D_+}(k)}{2\pi i\, L_+(k)(2k)^{\frac{1}{2}}} \int_{ia-\infty}^{ia+\infty} \frac{e^{-\gamma b}\, \sinh \gamma b\, e^{i\xi\ell}}{(\xi - k)^{\frac{1}{2}}\, b(\xi + \alpha)}\, d\xi = \frac{F_{D_+}(k)\, U(\alpha)}{L_+(k)} \qquad (C.2)$$

where

$$U(\alpha) = \frac{1}{(2k)^{\frac{1}{2}}\, 2\pi i} \int_{ia-\infty}^{ia+\infty} \frac{e^{-\gamma b}\, \sinh \gamma b\, e^{i\xi\ell}}{(\xi - k)^{\frac{1}{2}}\, b(\xi + \alpha)}\, d\xi \qquad (C.3)$$

Now

$$\frac{e^{-\gamma b}\, \sinh \gamma b}{b} = \gamma - \gamma^2 b + \frac{2\gamma^3 b^2}{3} - \ldots \qquad (C.4)$$

Substituting (C.4) into (C.3) we obtain

$$U(\alpha) = \frac{1}{(2k)^{\frac{1}{2}}\, 2\pi i} \int_{ia-\infty}^{ia+\infty} \frac{(\gamma - \gamma^2 b + 2\gamma^3 b^2/3 - \ldots) e^{i\xi\ell}}{(\xi + \alpha)(\xi - k)^{\frac{1}{2}}}\, d\xi \qquad (C.5)$$

Following the procedure in deriving (2.59) to (2.65), the asymptotic expression for $U(\alpha)$ is given by

$$U(\alpha) = \frac{-e^{+i\pi/4}\, e^{ik\ell}\, k^{\frac{1}{2}} b}{(2\pi)^{\frac{1}{2}}\, (\alpha + k)\ell^{3/2}} \left[1 + \frac{i(kb)^2}{k\ell} - \frac{(kb)^4}{(k\ell)^2} + \ldots\right] \qquad (C.6)$$

which is only valid for $(kb)^2/k\ell < 1$. As in the evaluation of $T(\alpha)$, only the alternate terms of (C.5) contribute to the value of the integral. The first term in (C.6) corresponds to the second term in (C.5).

APPENDIX D

EVALUATION OF THE SCATTERED MODE COEFFICIENTS (c_n^{sep} , c_n^{int})

The transform of the field scattered by a tandem slit is given by (2.9), i.e.

$$\Phi = A\, e^{-\gamma y} \quad , \quad y \geq b \tag{D.1a}$$

$$= D\, e^{\gamma y} \quad , \quad y \leq -b \tag{D.1b}$$

$$= B\, e^{\gamma y} + C\, e^{-\gamma y} \quad , \quad -b \leq y \leq b \tag{D.1c}$$

Equating the fields at $y = \pm b$, we obtain

$$D = B + C\, e^{2\gamma b} \tag{D.2a}$$

$$A = C + B\, e^{2\gamma b} \tag{D.2b}$$

Also, using (2.18) and remembering that $S_1^{(o)} = S_1^{(i)} = S_1, D_1^{(o)} = D_1^{(i)} = D_1$, and $\Phi_1(\pm b) = \Phi(\pm b)$, we obtain

$$A = \frac{e^{\gamma b}}{2}\,(S_1 + D_1) \tag{D.3a}$$

$$D = \frac{e^{\gamma b}}{2}\,(S_1 - D_1) \tag{D.3b}$$

Substitution of (D.3) into (D.2) yields

$$B = \frac{S_1}{4\cosh \gamma b} + \frac{D_1}{4\sinh \gamma b} \tag{D.4a}$$

$$C = \frac{S_1}{4\cosh \gamma b} - \frac{D_1}{4\sinh \gamma b} \tag{D.4b}$$

The transform of the field in the waveguide region is thus given by

$$\Phi = \frac{S_1 \cosh \gamma y}{2\cosh \gamma b} + \frac{D_1 \sinh \gamma y}{2\sinh \gamma b} \tag{D.5}$$

The inverse transform of (D.5) yields an integral expression for the field inside the two waveguides, which may also be expressed as a modal series, i.e.

$$\phi = \frac{1}{(2\pi)^{\frac{1}{2}}} \int_{-\infty+i\tau}^{\infty+i\tau} \left[\frac{S_1 \cosh \gamma y}{2 \cosh \gamma b} + \frac{D_1 \sinh \gamma y}{2 \sinh \gamma b} \right] e^{-i\alpha x} \, dx \, , \quad -b \leq y \leq b \tag{D.6a}$$

$$= \sum_{n=1}^{\infty} (c_n^{sep} + c_n^{int}) \sin n\pi \left(\frac{y - b}{2b} \right) e^{\gamma_n |x \pm d|} \tag{D.6b}$$

where c_n^{sep} , c_n^{int} have been previously defined (p. 45) and the upper and lower signs correspond to the left and right hand side waveguide, respectively (Fig. 2.1). Also the first and second terms in (D.6a) denote the contribution from the odd and even mode coefficients, respectively. Using (2.78) the first term in the integrand of (D.6a) reduces to

$$\frac{k \sin\theta_o \, K'(\alpha) e^{-ikb \sin\theta_o} \cosh \gamma y}{2\pi \cosh \gamma b} \left(\frac{e^{i\alpha d}}{K'_+(\alpha)} \left[G_1(\alpha) + \frac{T(\alpha) \left[G_1(k) T(k) + G_2(k) K'_+(k) K_+(k) \right]}{\left[K'_+(k) K_+(k) \right]^2 - T^2(k)} \right] \right.$$

$$+ \frac{e^{-i\alpha d}}{K'_-(\alpha)} \left[G_2(-\alpha) + \frac{T(-\alpha) \left[G_2(k) T(k) + G_1(k) K'_+(k) K_+(k) \right]}{\left[K'_+(k) K_+(k) \right]^2 - T^2(k)} \right]$$

$$\left. - G(\alpha) \right) e^{-i\alpha x} \tag{D.7}$$

A similar expression can be obtained for the second term in (D.6a). Now consider the first term in the second square bracket of (D.7), i.e.

$$\frac{k \sin\theta_o \, K'(\alpha) \, e^{-ikb \sin\theta_o} \cosh \gamma y \, G_2(-\alpha) e^{-i\alpha d}}{2\pi \cosh \gamma b \, K'_-(\alpha)}$$

where $G_2(\alpha)$ is given by (2.74). For this term the contour in (D.6a) can be closed in the upper half plane and contribution to the value of the integral evaluated from the poles, i.e. $\alpha = k \cos\theta_o$ and $\alpha = i\gamma_n$. There are no branch points in this region. Adding the contribution from the second term in (D.6a) and evaluating the residues, the pole at $\alpha = k \cos\theta_o$ gives a contribution $-\exp(-ikx \cos\theta_o - iky \sin\theta_o)$ which exactly cancels the incident wave. The poles at $\alpha = i\gamma_n$ represent the scattered propagating and non-propagating modes inside the waveguide (left hand side for the above term). Evaluating the integral at these poles and treating the other terms in the integrand in a similar fashion, the expressions for c_n^{sep} and c_n^{int} (for large ℓ) for the left hand side waveguide simplify to

$$c_n^{sep} = \begin{cases} \dfrac{-2b \cos(kb \sin\theta_o)(k + k \cos\theta_o)^{\frac{1}{2}}(i\gamma_n - k)^{\frac{1}{2}}}{n\pi \, K_+(k \cos\theta_o)(i\gamma_n - k \cos\theta_o)K_-^{(1)}(i\gamma_n)} & ; \; n = 1,3,5\ldots \\ \dfrac{2i \sin(kb \sin\theta_o)}{n\pi \, (i\gamma_n - k \cos\theta_o)L_+(k \cos\theta_o)L_-^{(1)}(i\gamma_n)} & ; \; n = 2,4,6\ldots \end{cases} \tag{D.8}$$

where

$$L_-^{(1)}(i\gamma_n) = \frac{\partial}{\partial\alpha} L_-(\alpha)\Big|_{\alpha=i\gamma_n}, \quad K_-^{(1)}(i\gamma_n) = \frac{\partial}{\partial\alpha} K_-(\alpha)\Big|_{\alpha=i\gamma_n} \tag{D.9}$$

and

$$c_n^{int} = \begin{cases} -\dfrac{i2b\cos(kb\sin\theta_o)(2k)^{\frac{1}{2}}(i\gamma_n - k)^{\frac{1}{2}}\, e^{i(k\ell-\pi/4)}\, e^{-i2kd\cos\theta_o}}{n\pi\, K_-(k\cos\theta_o)(k - i\gamma_n)K_-^{(1)}(i\gamma_n)K_+^2(k)(2\pi k\ell)^{\frac{1}{2}}\sin(\theta_o/2)} \cdot \\ (1 + F_2(b,\ell)) \\ \qquad\qquad ;\ n = 1,3,5\ldots \\ \\ -\dfrac{\sin(kb\sin\theta_o)(kb)e^{i(k\ell-\pi/4)}\, e^{-i2kd\cos\theta_o}\,(1 + F_2(b,\ell))}{n\pi\, L_-(k\cos\theta_o)(k - i\gamma_n)L_-^{(1)}(i\gamma_n)L_+^2(k)(k\ell)(2\pi k\ell)^{\frac{1}{2}}\sin^2(\theta_o/2)}\ ; \\ \qquad\qquad n = 2,4,6\ldots \end{cases}$$

(D.10)

Also, for the sake of convenience, (D.8) and (D.10) have been normalized with respect to $e^{ikd\cos\theta_o}$, the incident field at the aperture of the left hand side waveguide. For the second waveguide, the expressions for c_n^{sep} and c_n^{int} are obtained from (D.8) and (D.10) with θ_o replaced by $\pi - \theta_o$.

REFERENCES

[1] S.C. Kashyap and M.A.K. Hamid, "Frequency response of filters with thick diaphragms", accepted for publication in Int. J. Electronics.

[2] J.B. Keller, "Diffraction by an aperture", J. Appl. Phys., Vol. 28, No. 4, pp. 426-444, 1957.

[3] S.N. Karp and A. Russek, "Diffraction by a wide slit", J. Appl. Phys., Vol. 27, pp. 886-894, 1956.

[4] J.S. Yu and R.C. Rudduck, "On higher order diffraction concepts applied to a conducting strip", IEEE Trans. on Antennas and Propagation, Vol. AP-15, pp. 662-668, 1967.

[5] H.S. Tan, "Electromagnetic diffraction by a plane slit aperture", Australian J. Phys., Vol. 21, pp. 35-41, 1968.

[6] P. Ya. Ufimtsev, "Asymptotic investigation of the problem of diffraction of a strip", Radio Eng'g. Elect. Phys., Vol. 14, No. 7, pp. 1016-1025, 1969.

[7] P.M. Morse and P.J. Rubenstein, "The diffraction of waves by ribbons and by slits", Physical Review, Vol. 54, pp. 895-898, 1938.

[8] H.P. Hsu, "Study of aperture fields in the diffraction by a slit", Scientific Rept. No. 5, Case Institute of Technology, 1959.

[9] E. Groschwitz and H. Hönl, "Die beugung elektromagntischer wellen am spalt. I.", Z. Phys., Vol. 131, pp. 305-319, 1952.

[10] H. Hönl and E. Zimmer, "Intensität und polarization bei der beugung elektromagnetischer wellen am spalt. II.", Z. Phys., Vol. 135, pp. 196-218, 1953.

[11] R. Müller and K. Westpfahl, "Eine strenge behandlung der beugung elektromagnetischer wellen am spalt", Z. Phys., Vol. 134, pp. 245-263, 1953.

[12] C.J. Bouwkamp, "Diffraction theory", Rep. Prop. Phys., Vol. 17, pp. 35-100, 1954.

[13] P.C. Clemmow, "Edge currents in diffraction theory", IRE Trans. on Antennas and Propagation, Vol. 4, pp. 282-287, 1956.

[14] R.F. Millar, "Diffraction by a wide slit and complementary strip", Proc. Camb. Phil. Soc. Math. Phys. Sci., Vol. 54, pp. 479-496, 1958.

[15] H. Levine, "Diffraction by an infinite slit", J. Appl. Phys., Vol. 30, pp. 1673-1682, 1959.

[16] J.B. Keller, "The geometrical theory of diffraction", Symposium on Microwave Optics, Eaton Electronic Research Laboratory, McGill University, Montreal, Canada, 1953.

[17] J.B. Keller, R.M. Lewis and B.D. Seckler, "Diffraction by an aperture. II.", J. Appl. Phys., Vol. 28, No. 5, pp. 570-579, 1957.

[18] A. Mohsen and M.A.K. Hamid, "Higher order asymptotic terms of the two-dimensional diffraction by a small aperture", Radio Science, Vol. 3, No. 11, pp. 1105-1108, 1968.

[19] B.R. Levy and J.B. Keller, "Diffraction by a smooth object", Comm. on Pure and Appl. Maths., Vol. 12, No. 1, pp. 159-209, 1959.

[20] J.E. Burke and J.B. Keller, "Diffraction of finite bodies of revolution", Sylvania Electronic Systems Engineering Rept. No. EDL-E49, 1960.

[21] Y. Ohba, "On the radiation pattern of a corner reflector finite in width", IEEE Trans. on Antennas and Propagation, Vol. AP-11, No. 2, pp. 127-132, 1963.

[22] M.A.K. Hamid, "Near field transmission between horn antennas", Research Rept. No. 43, University of Toronto, 1966.

[23] S.J. Maurer and L.B. Felsen, "Ray optical techniques for guided waves", Proc. IEEE, Vol. 55, No. 10, pp. 1718-1729, 1967.

[24] H.Y. Yee, L.B. Felsen and J.B. Keller, "Ray theory of reflection from the open end of a waveguide", SIAM J. Appl. Math., Vol. 16, pp. 268-300, 1968.

[25] H.Y. Yee and L.B. Felsen, "Ray optics - a novel approach to scattering by discontinuities in a waveguide", IEEE Trans. on Microwave Theory and Techniques, Vol. MTT-17, No. 2, pp. 73-85, 1969.

[26] L.B. Felsen and H.Y. Yee, "Ray method of sound wave reflection in an open-ended circular pipe", J. Acous. Soc. Am., Vol. 40, pp. 1028-1039, 1968.

[27] H.Y. Yee and L.B. Felsen, "Ray-optical analysis of electromagnetic scattering in waveguides", IEEE Trans. on Microwave Theory and Techniques, Vol. MTT-17, No. 9, pp. 671-683, 1969.

[28] M.D. Khaskind and L.A. Vainshteyn, "Diffraction of plane waves by a slit and a tape", Radio Eng'g. Electronic Phys., Vol. 9, pp. 1492-1502, 1964.

[29] G. Ya. Popov, "Approximate method of solving the integral equation for the diffraction of electromagnetic waves by a band of finite width", Soviet Phys. Tech. Phys., Vol. 10, pp. 305-309, 1965.

[30] Y. Nomura and S. Inawashiro, "On the transmission of acoustic waves through circular channel of a thick wall", Rept. Tohoku Univ. Res. Inst. Elect. Commun., No. 2, pp. 57-71, 1960.

[31] G.P. Wilson and W.W. Soroka, "Approximation to the diffraction of sound by a circular aperture in a rigid wall of finite thickness", J. Acous. Soc. Am., Vol. 37, No. 2, pp. 286-297, 1964.

[32] Von P. Budach, "Der transmissionsgrad einer schlitzförmigen öffnung geringer tiefe in einer ebenen unendlich ausgedehnten wand bei senkrechtem schalleinfall", Hoch frequenztechnik und Elektroakustik, Vol. 77, pp. 134-143, 1968.

[33] G.W. Lehman, "Diffraction of electromagnetic waves by planar dielectric structures. I. Transverse electric excitation", J. Math. Phys., Vol. 11, No. 5, pp. 1522-1535, 1970.

[34] E.T. Hanson, "Diffraction", Phil. Trans. (GB), A, Vol. 229, pp. 87-124, 1930.

[35] D.S. Jones, "Diffraction by a thick semi-infinite plate", Proc. Roy. Soc., Vol. A 217, pp. 153-175, 1953.

[36] B.N. Harden, "Diffraction of electromagnetic waves by a half-plane", Proc. IEE, Vol. 99, Part III, No. 61, pp. 229-235, 1952.

[37] S.W. Lee and R. Mittra, "Diffraction by a thick conducting half plane and a dielectric loaded waveguide", IEEE Trans. on Antennas and Propagation, Vol. AP-16, No. 4, pp. 454-461, 1968.

[38] B. Noble, "Methods based on the Wiener-Hopf technique", Pergamon Press, 1958.

[39] W.W. Mumford, "Maximally-flat filters in waveguides", Bell Systems Tech. J., pp. 684-714, 1948.

[40] A.N. Akhiezer, "On the inclusion of effect of thickness of the screen in certain diffraction problems", Soviet Phys. Tech. Phys., Vol. 2(6), pp. 1190-1196, 1957.

[41] H.A. Bethe, "Theory of diffraction by small holes", Physical Review, Vol. 66, pp. 163-182, 1944.

[42] A.A. Oliner, "The impedance properties of narrow radiating slots in the broad face of a rectangular waveguide", I and II, IRE Trans. on Antennas and Propagation, Vol. 5, pp. 4-20, 1957.

[43] S.B. Cohn, "Thickness corrections for capacitive obstacles and strip conductors", IRE Trans. on Microwave Theory and Techniques, Vol. MTT-8, pp. 638-644, 1960.

[44] N. Davy, "The field between equal semi-infinite rectangular electrodes or magnetic pole pieces", Phil. Mag., Vol. 35, Ser. 7, pp. 819-840, 1944.

[45] Kh. L. Garb, J.B. Levinson and P. Sh. Fridberg, "Effect of wall thickness in slit problems in electrodynamics", Radio Eng'g. and Electronic Phys., Vol. 13, No. 12, pp. 1888-1896, 1968.

[46] L.R. Alldredge, "Diffraction of microwaves by tandem slits", IRE Trans. on Antennas and Propagation, Vol. 4, pp. 640-649, 1956.

[47] C.W. Hasselfield, "Modal analysis of planar waveguide junctions", M.Sc. Thesis, Department of Electrical Engineering, University of Manitoba, May 1971.

[48] M.A.K. Hamid, S.C. Kashyap, A. Mohsen, W.M. Boerner and R.J. Boulanger, "A ray-optical approach to the analysis of microwave filters", Proc. European Microwave Conference, IEE Conference Publication No. 58, pp. 189-193, 1969.

[49] S.C. Kashyap and M.A.K. Hamid, "Diffraction by a slit in a thick conducting screen", IEEE Trans. on Antennas and Propagation, Vol. AP-19, No. 4, 1971.

[50] S.C. Kashyap and M.A.K. Hamid, "Diffraction pattern of a slit in a thick conducting screen", J. Appl. Phys., Vol. 42, No. 2, pp. 894-895, 1971.

[51] S.C. Kashyap and M.A.K. Hamid, "Ray-optical scattering by a thick waveguide diaphragm", accepted for publication in Int. J. Electron.

[52] J.J. Bowman, "Comparison of ray theory with exact theory for scattering by an open waveguide", IEEE Trans. on Antennas and Propagation, Vol. AP-18, No. 1, pp. 131-132, 1970.

[53] D.S. Jones, "Diffraction by a waveguide of finite length", Proc. Camb. Phil. Soc., Vol. 48, pp. 118-134, 1952.

[54] W.E. Williams, "Diffraction by two parallel planes of finite length", Proc. Camb. Phyl. Soc., Vol. 50, pp. 309-318, 1954.

[55] J. Meixner, "Die kantenbedingung in der theorie der beugung elektromagnetischer wellen an volkommen leitenden ebenen schirmen", Ann. Phys., Vol. 6, pp. 2-9, 1949.

[56] R.A. Hurd, "The admittance of a linear antenna in a uniaxial medium", Canadian J. Phys., Vol. 43, pp. 2276-2309, 1965.

[57] R.A. Hurd, "Admittance of a long linear antenna", Can. J. Phys., Vol. 44, pp. 1723-1744, 1966.

[58] I.S. Gradshyteyn and I.M. Ryzhik, "Tables of integrals, series and products", Academic Press, p. 1060, 1965.

[59] M. Born and E. Wolf, "Principles of Optics", The Macmillan Company, New York, pp. 747-752, 1964.

[60] B.J. Morse, "Diffraction by polygonal cylinders", J. Math. Phys., Vol. 5, No. 2, pp. 199-214, 1964.

[61] S.N. Karp and J.B. Keller, "Multiple diffraction by an aperture in a hard screen", Optica Acta, Vol. 8, No. 1, pp. 61-72, 1961.

[62] P.C. Clemmow, "The plane wave representation of electromagnetic fields", Pergamon Press, pp. 79-81, 1966.

[63] G. Goubau, "On the existence of reiterative wavebeams", paper presented at URSI Spring meeting, 1965; also in Advances in Microwaves, Vol. 3, Academic Press, New York, N.Y.

[64] G.S. Brown and R. Mittra, "Wave propagation in an open, periodic two-dimensional iris waveguide", Radio Science, Vol. 4, No. 5, pp. 471-482, 1969.

[65] G. Craven, "Relationship between direct coupled waveguide filters and evanescent-mode filters", Electronics Letters, Vol. 4, No. 3, pp. 45-46, 1968.

[66] B.A. Panchenko, "Diffraction of an electromagnetic wave by a flat screen having a finite thickness and evenly distributed apertures", Radio Eng'g. and Electronic Phys., Vol. 12, No. 4, pp. 719-721, 1967.

[67] M.A. Allen and G.S. Kino, "On the theory of strongly coupled cavity chains", IRE Trans. on Microwave Theory and Techniques, Vol. 8, pp. 362-372, 1960.

[68] A. Sommerfeld, "Optics", Academic Press, pp. 245-272, 1964.

[69] E.T. Copson, "On an integral equation arising in the theory of diffraction", Quart. J. Math., Vol. 17, pp. 19-34, 1946.

[70] T.B.A. Senior, "Diffraction by a semi-infinite metallic sheet", Proc. Roy. Soc., Vol. A 213, pp. 436-458, 1952.

[71] R.A. Hurd, "Diffraction by a unidirectionally conducting half plane", Can. J. Phys., Vol. 38, pp. 168-175, 1960.

[72] S.R. Seshadri and A.K. Rajagopal, "Diffraction of a perfectly conducting semi-infinite screen in an isotropic plasma", IEEE Trans. on Antennas and Propagation, Vol. AP-11, pp. 497-502, 1963.

[73] L.A. Vainshteyn, "The theory of diffraction and the factorization method", The Golem Press, Boulder, Colorado, pp. 282-287, 1969.

[74] J.J. Taub, "The status of quasi-optical waveguide components for millimeter and submillimeter wavelengths", Microwave Journal, Vol. 13, No. 11, pp. 57-62, 1970.

[75] K.C. Kao, "The theory and practice of quasi-optical waveguide components", Proc. Symp. on Quasi-optics, Brooklyn, N.Y., Polytechnic Institute of Brooklyn Press, pp. 497-515, 1964.

[76] J. Taub, H.J. Hindin, O.F. Hinckelmann and M.L. Wright, "Submillimeter components using oversize quasi-optical waveguide", IEEE Trans. on Microwave Theory and Techniques, Vol. MTT-11, pp. 338-345, 1963.

[77] B.Z. Katzenelenbaum, "Diffraction on a broad aperture in a broad waveguide", Electromagnetic Theory and Antennas, Proc. of the Copenhagen Symp., Pergamon Press, pp. 177-184, 1963.

[78] N. Marcuvitz, "Waveguide Handbook", Dover Publications, pp. 221-257, 1965.

[79] P.M. Morse and H. Feshbach, "Methods of theoretical physics", Part I, McGraw-Hill Book Company, pp. 812-820, 1953.

[80] M.A.K. Hamid and W.A. Johnson, "Ray-optical solution for the dyadic Green's function in a rectangular cavity", Electronics Letters, Vol. 6, No. 10, pp. 317-319, 1970.

[81] L. Lewin, "Wedge diffraction functions and their use in quasi-optics", Proc. IEE, Vol. 116, No. 1, pp. 71-76, 1969.

[82] C.P. Bates and R. Mittra, "Waveguide excitation of dielectric and plasma slabs", Radio Science, Vol. 3, No. 3, pp. 251-256, 1968.